POLITECNICO DI TORINO

Corso di Laurea Magistrale in

Ingegneria Biomedica

Tesi di Laurea Magistrale

Design of theranostic nanoparticles for cancer treatment functionalised by Layer-by-Layer assembly

Supervisors

Prof. Gianluca Ciardelli
Prof. Chiara Tonda Turo
Dr. Piergiorgio Gentile
Dr. Irene Carmagnola

Candidate

Alberto Girelli
Matricola: s254524

A.A. 2019/2020

Declaration of work

I declare that this thesis is based on my own work and has not been submitted in any form for another degree at any University or any other tertiary education. Information derived from published and unpublished work of others have been acknowledged in the text and in the list of references given in the bibliography.

Abstract

Cancer is considered among the leading causes of death each year worldwide with an estimated 13.2 million deaths in 2030 for a global population of 8.3 billion people. To increase the survival rate, researchers focused on developing theranostic systems at the nanoscale, combining therapeutic compound with imaging tools in the same platform, improving drug delivery, pharmaco-kinetics, bio-distribution. In this work, we have investigated the design of an innovative theranostic nanoparticle capable to combine the SPIONs multimodal capabilities (MRI bio-imaging, magnetic targeting and hyperthermia) with more efficient and targeted drug release, exploiting Layer-by-Layer assembly (LbL) technique, using the SPION as a core. LbL technology has been studied in different contexts such as electronic, optical, biological and medical, thanks to its simplicity and versatility. It consists in the deposition of charged layers by alternating positive and negative polyelectrolytes. These layers attribute different wettability and biocompatibility characteristics to the functionalized surface. In this investigation we wanted to exploit the LbL technique as means to load the anticancer drug and to control the kinetics release through the layers degradation. The nanoparticle was designed to combine the biocompatibility standards requirements set by the Food and Drug Administration (FDA), in order to exceed the steps 1-5 provided (Discovery and Development, Preclinical Research, Clinical Research, FDA Drug Review, FDA Post-Market Drug Safety Monitoring) up to the platform marketing. It was chosen to use bottom-up strategy for this compilative study of the nanoparticle design. SPIONs, composed of Fe_3O_4 and γ-Fe_2O_3, was selected as core due to its good cytocompatibility as reported in literature. Recent works showed the SPIONs average size is approx. 20 nm by TEM images. It has been reported that the SPIONs has characterised by a surface charge (measured by of Z-potential) ranging between -4 / + 23 mV. The surface charge was assumed to be essential for the deposition of subsequent layers. A deep investigation on the potential polyelectrolytes to be used in the LbL assembly were considered: Chitosan and Alginate among the natural polymers, Poly (allylamine hydrochloride) (PAH) and Polystyrene sulfonate (PSS) among the synthetic ones. Natural polymers have been selected for their high biomimetic properties and high cytocompatibility and, also, widely approved by the FDA. PSS/PAH are the most

biocompatible and the widely used among synthetic polymers; they are available at low cost and in large quantities. Literature reports their degradation in acid environment (pH<7) can consider them as pH-responsive polyelectrolytes. The pairs of bilayers investigated showed dimensions around 200 nm and external surface charge between -50/+33 mV, suggesting to exploit passive targeting and EPR effect. Paclitaxel and Docetaxel are the most commonly used drugs in cancer therapy and those proposed in this study. Finally, it has been considered how to improve the circulation time and the target properties of this nanoparticles. “Stealth” characteristics to the immune system could be given by the external hydrophilic PEG on the shell, able to increase circulation times in blood environment. The amine groups expressed by the PEG can be exploited to graft specific antibodies (HER-2, EGFR, Biotin, HA) for the most common tumors (liver, prostate, lung, breast) by implementing active targeting.

Table of contents

Chapter 1. Introduction

1.1 Cancer overview

1.1.1 Cancer general features

Cancer is a disease that occurs when the genetic information contained in the cellular DNA is altered, causing abnormal patterns in gene expression. It is characterized by an uncontrolled growth and migration to surrounding tissues (Nenclares and Harrington, 2020).

When in physiological conditions, cells perform their metabolic functions and they divide replacing the dead ones, but in cancer this does not happen. Indeed, cells do not undergo apoptosis but they multiply forming non-functional tumor tissue. Cancer can invade other tissues, in fact when the volume of the tumoral mass grows too much, some cells can enter the blood or lymphatic system, allowing the growth of a new tumor in different areas of the body (Fig.1). This is a metastatic process and the new tumor mass is called metastatic cancer (Golub *et al.*, 1999).

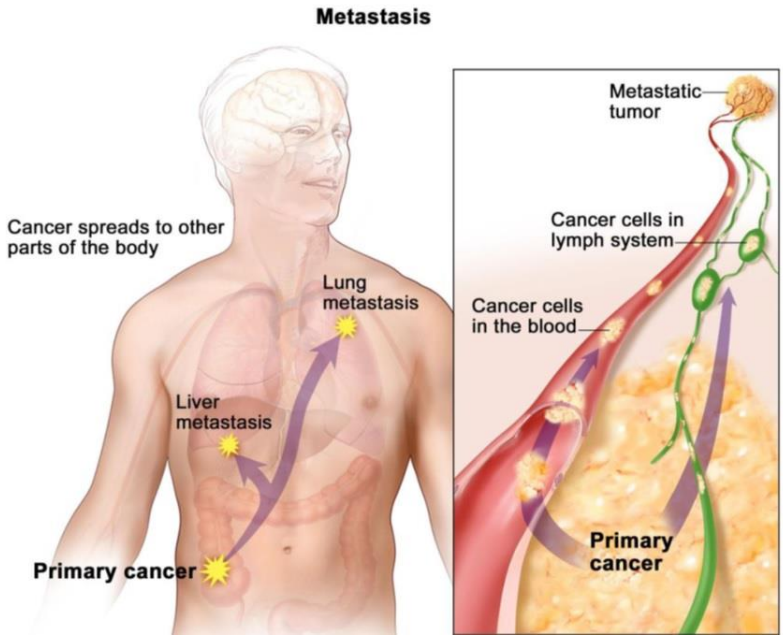

Fig. 1 Matastasis formation: cancer uses blood system and lymphatic system to spread to different areas of the body.

Metastatic cancer is, therefore, a non-functional tissue that does not perform physiological and poorly differentiated tasks, and when replacing healthy tissue, causes

its death. Early diagnosis of the tumor and its specific and synergistic treatment could increase the patient's life expectancy, reducing unwanted and harmful side effects (Chaffer and Weinberg, 2011).

1.1.2 Cancer statistics

According to estimates and demographic models, the world population will increase from 7 billion in 2012 to 8.3 billion in 2030. As a result, the number of deaths caused by cancer is estimated to increase from 7.6 million in 2008 to 13.2 million in 2030. This growth is justified, among others, by the increase in the average age of individuals, which is known to be the first factor in the onset of tumor disease (Bray *et al.*, 2012).

In the UK, between the 2015 and the 2017, were recorded $3{,}67 \times 10^5$ confirmed cases of cancer and $1{,}64 \times 10^5$ deaths in the same years, with a survival rate of approximately 50% (10 years after diagnosis)(Fig.2). It should be noted that the number of foreseeable cases concerns about 38% of the total(according to Cancer Research UK:www.cancerresearchuk.org).

Fig. 2 UK Cancer statistics (Cancerresearchuk.org)

Considering these data it will be important to reduce the number of deaths by investigating the disease in its early stages, for example the diagnosis of lung cancer has a survival rate of 54% against 4% of its metastatic form (Choi *et al.*, 2012).

1.1.2 Cancer Hallmarks

The hallmarks of cancer include six biological capacities that manifest themselves in the evolution of human tumors and they are essential for this to be defined malignant (Hanahan and Weinberg, 2011).

These are: *Sustaining proliferative signaling, Evading growth suppressor, Resisting cell death, Enabling replicative immortality, Inducing Angiogenesis, Activating invasion and metastasis* (Fig.3, (Flavahan, Gaskell and Bernstein, 2017)).

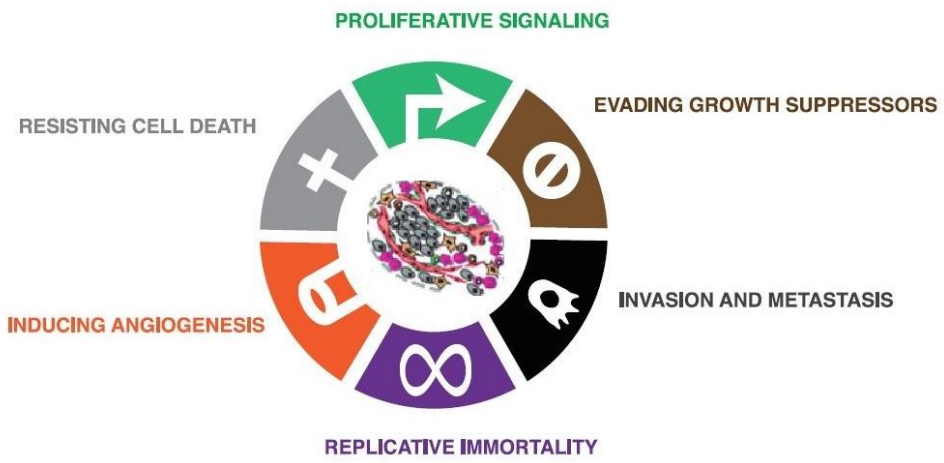

Fig. 3 The six cancer hallmarks.

First of all, the tumor produces proliferative signals in an uncontrolled way, at the same it he suppresses programmed death signals (apoptosis). Under normal conditions, cell chromosomes begin to be damaged after a finite number of mitoses, while cancer cells overcome this physiological limit and become immortalized. (Flavahan, Gaskell and Bernstein, 2017). Consequently, the increasingly large size of the tumor mass stimulates the production of angiogenetic factors, the endothelial cells produce irregular vessels, characterized by higher fenestrations diameter when compared to healthy conditions vasculature (Dai *et al.*, 2017).

Finally, immortalized cancer cells exploit these vessels to find new space starting from nearby tissues and spreading to more distant ones, giving rise to metastatic cancer. The new anticancer treatments focus on inhibiting the six characteristic processes, with the aim of first of all blocking the in situ mass growth, the spread of cancer, limiting the

patterns that lead to the formation, growth and strengthening of the pathological tissue (Hanahan and Weinberg, 2000).

1.1.3 Cancer Therapeutics

The main goals of the fight against cancer are: to cure the disease, to increase patient's life expectancy and to improve its quality. If a cure is not possible, anticancer treatments target palliative care to control symptoms and improve quality of life by prolonging the patient's life. When the tumor is limited to a specific area, a cure for many of its phenotypes is possible; however, if it is metastatic, for many types of cancer, treatment options are only palliative. Localized cancers are treated effectively with surgery and radiation while systemic chemotherapy, is used once the cancer has spread to nearby organs and tissues (Rai and Morris, 2019).

As shown in Fig.4, surgery, radiation and chemotherapy were used in 1900 as the main cancer treatment options, but the discovery and progress in understanding the molecular nature of cancer and the decoding of human genome in 2003, have brought new modalities of treatment such as molecular therapies and immunotherapy, including therapeutic vaccines (DeSantis *et al.*, 2014).

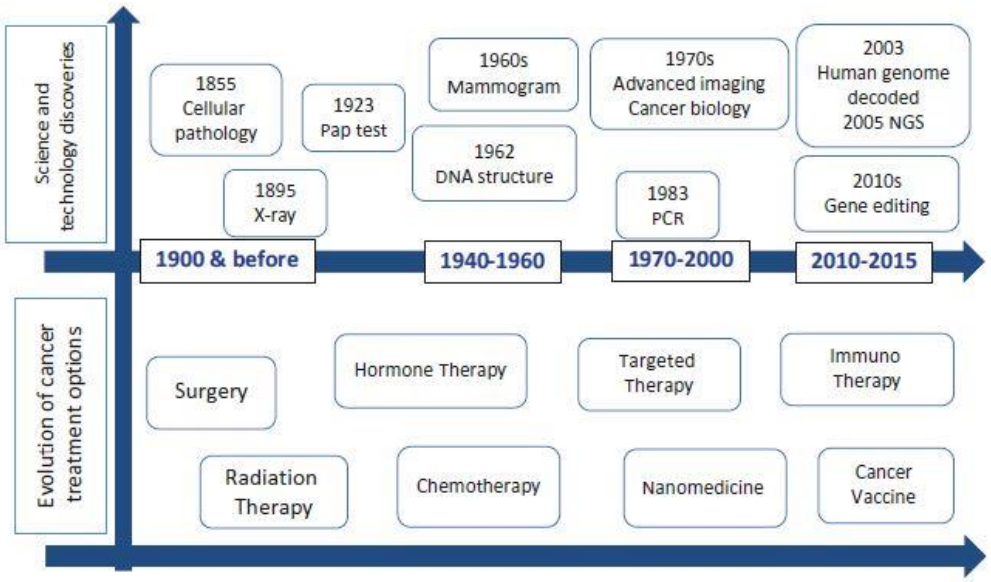

Fig. 4 Illustration of the time evolution of cancer treatment options, (Rai and Morris, 2019)

Therapeutic options for cancer, in general, largely depend on the type and stage of the cancer, possible side effects, patient preferences and general health. In the treatment of cancer, physicians with different subspecialties often work together to create a patient's overall treatment plan that combines different types of treatments (Arruebo *et al.*, 2011), the main tools commonly used for the fight against cancer are briefly described below.

Surgery

When the tumor is spatially limited, most solid tumor therapies involve surgery and are curative. Surgery for the removal of tumor masses has been used since 1700, improved over the centuries mainly thanks to the discovery of anesthetics in 1846 and cell pathology in 1900, has allowed the diagnosis of resected tissues for cancer cells (American Cancer Society, 2020).

Modern advances in surgical instruments and imaging techniques have led to less invasive and more precise surgeries. The type of surgery chosen is dependent on the goals of the treatment, such as disease prevention, diagnosis, treatment, palliative, supportive or prosthetic. If necessary, surgery is combined with radiotherapy and preoperative (neoadjuvant) or postoperative (adjuvant) chemotherapy to maximize the removal of all cancer cells and improve overall efficacy and safety outcome (Shefet-Carasso and Benhar, 2015).

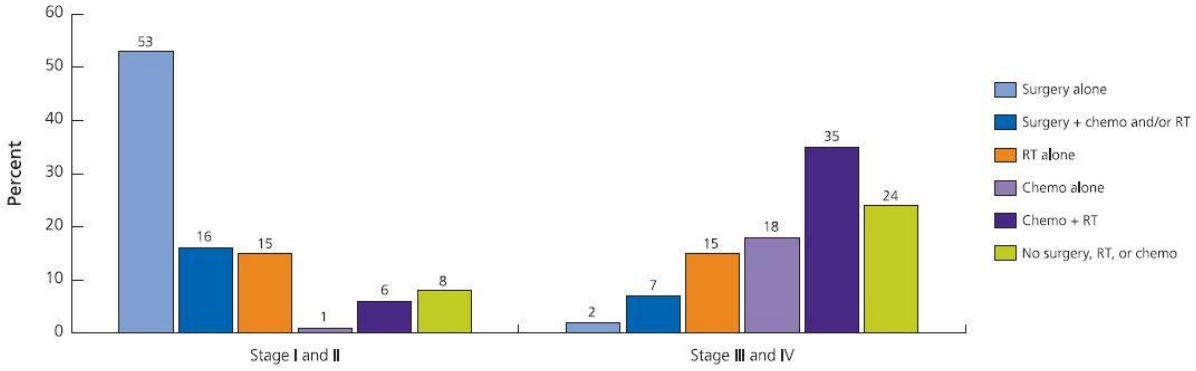

Fig. 5 Lung cancer, strategies divided by stage of the disease (Miller et al., 2016).

Radiation Therapy

Radiation was first used in 1903 to treat skin cancer, 5 years after Marie Curie's discovery of radio. It is currently used to successfully treat sarcomas, gliomas, lymphomas, thyroid, head and neck, and anal cancers, while pancreatic tumors and melanomas do not respond very well (Baskar *et al.*, 2012).

The forms of radiation most used for the treatment of cancer include ionizing radiation (X-rays and gamma rays) and non-ionizing (electrons and protons), which can be released from internal or external sources. From these sources, high doses of energy are released to the cells, which die from progressive DNA damage. These therapies cause shrinkage of the tumor, reduce its spread after removal surgery or have palliative effects for the most advanced forms of cancer. They can be used alone or in combination with chemotherapy, surgery and other drug therapies. Radiation-induced damage affects rapidly dividing cells, such as cancer cells and fast-dividing normal cells (e.g., skin, bone marrow, intestinal lining), but side effects are also seen later in the slow-growing tissues such as the nerve, bones, breasts and brain (Rai and Morris, 2019).

To maximize and concentrate the dose on the tumor by minimizing exposure to normal tissues, planning of radiation therapy is guided by simulations and imaging techniques. Treatment regimens can last several weeks and doses are split to reduce side effects (Bidram *et al.*, 2019).

Chemotherapy

One of the biggest breakthroughs in cancer treatment has been the introduction of chemotherapy. In the 1950s Sydney Farber and her colleagues studied the effects of aminopterin, a derivative of vitamin folic acid, which demonstrated remission in patients with acute lymphoblastic leukemia. Since then, more than 100 chemotherapy agents have been implemented (short example in Table 1) and continue to be used effectively in the treatment of different forms of cancer (Shapin, 2010).

Table 1 Common classes of chemotherapy agents, their mechanism of cytotoxicity (Prakash Rai Stephanie A., 2019)

Mechanism of toxicity	DNA level effects	Cell cycle
Alkylating agent	Crosslinks with DNA, interferes with replication and transcription	All phases
Antimetabolites	Substitutes for DNA/RNA building blocks causing false messages	S phase
Antitumor Antibiotics	Intercalates within DNA base pairs	All phases
Mitotic inhibitors	Interferes with micro / tubulin function during mitosis	M phase (paclitaxel, docetaxel)
Topoisomerase inhibitors	Inhibits enzymes involved in DNA cleavage and rejoining	M phase, All phases

Chemotherapy agents generally share a common mechanism of action, such as hitting DNA, causing direct toxicity or interfering with DNA synthesis (alkylating agent), replication and cell division (paclitaxel, docetaxel), resulting in cell death. Their use causes side effects as they affect rapidly dividing cells in addition to cancer cells, these include alopecia (hair loss), anemia, bone marrow depression, immune suppression, nausea and emesis (Rai and Morris, 2019).

For these reasons, numerous strategies have been implemented to maximize treatment benefits with respect to toxicity or multidrug resistance (MDR), using adjuvant and neoadjuvant therapies, combined with other drugs and treatments, and more recently, using specific targeted and selective approaches also in the drug delivery (Foo and Michor, 2014).

1.2 State of the art: New advanced approaches for cancer treatment in nanomedicine

1.2.1 Theranostic technique

Concept and strategies

Nanomedicine is defined as the application of nanotechnology in medicine. It is characterized by the use of submicrometric tools for the diagnosis, prevention and treatment of diseases, with the aim of improving the patient's quality of life. Significant efforts and investments in nanomedicine have been promoted in the recent years, demonstrating potential improvements in efficiency and less toxicity in diagnosis and therapeutic interventions. (Rizzo *et al.*, 2013). Interdisciplinary research in nanomedicine, on the diagnosis and treatment of diseases has produced considerable efforts to combine diagnosis and therapy in a single formulation: **Nanotheranostic** (Sumer and Gao, 2008),(Twan Lammers *et al.*, 2011).

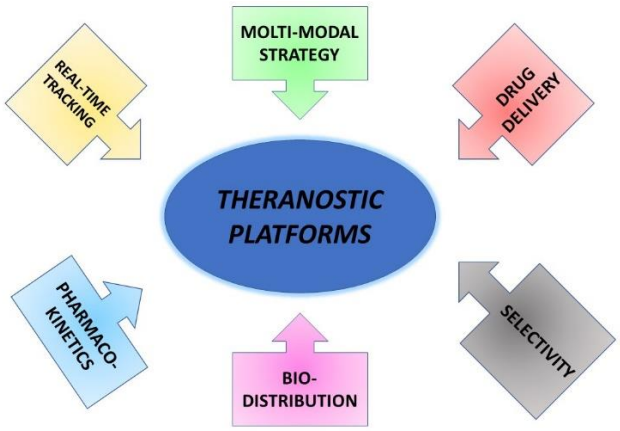

Fig. 6 Advantages of Theranostic platforms.

Theranostics are designed to facilitate different aspects of research on the delivery, pharmacokinetics, biodistribution and accumulation of the drug in the target site. They are also designed to reduce the invasiveness of visualization and allow the quantification of drugs releases (T Lammers *et al.*, 2011).

In nanotheranostics, formulations such as liposomes, polymers, micelles, solid nanoparticles and antibodies (Fig.1.2.2) are clinically relevant, due to their peculiar characteristics of biocompatibility and ability to perform their task in the different contexts in which they are used (Twan Lammers *et al.*, 2011).

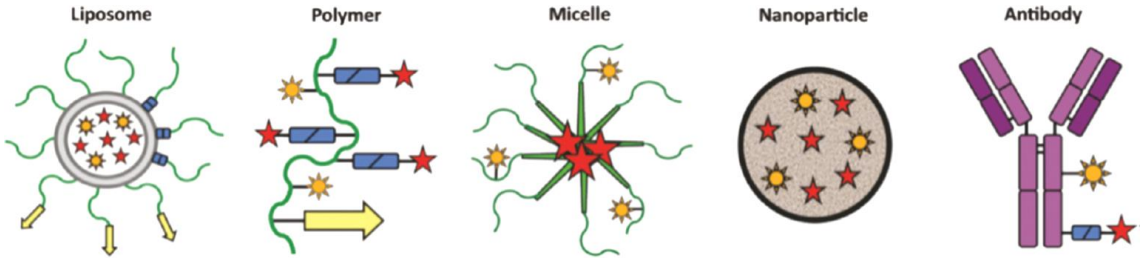

Fig. 7 Theranostic nanomedicines. Liposomes and liposomal bilayers are shown in gray; polymers and polymer-coatings in green; solid (lipid) nanoparticle components in brown; antibodies in purple. (Twan Lammers et al., 2011).

These nanocarriers, alone or more frequently combined with each other, have the ability to transport complex drugs, and respond to external stimuli such as local variations in pH, temperature, and light intensity (Liu and Picart, 2016).

Liposome

Liposome-based drug delivery systems are nano-spheres composed of one or more concentric double-lipid layers surrounding an aqueous core. Therefore, liposomes can be exploited as nano-carriers of hydrophilic drugs, which can be dissolved in the aqueous nucleus, but also for hydrophobic drugs trapped in the lipid membrane. Furthermore, the circulation times in the blood environment, *in vivo*, can be increased by modifying the external surface with hydrophilic polymers such as polyethylene glycol (PEG)(Hafner *et al.*, 2014), where hydrophilic PEG creates an aqueous layer which, in the blood environment, makes the particle more invisible to the immune system.

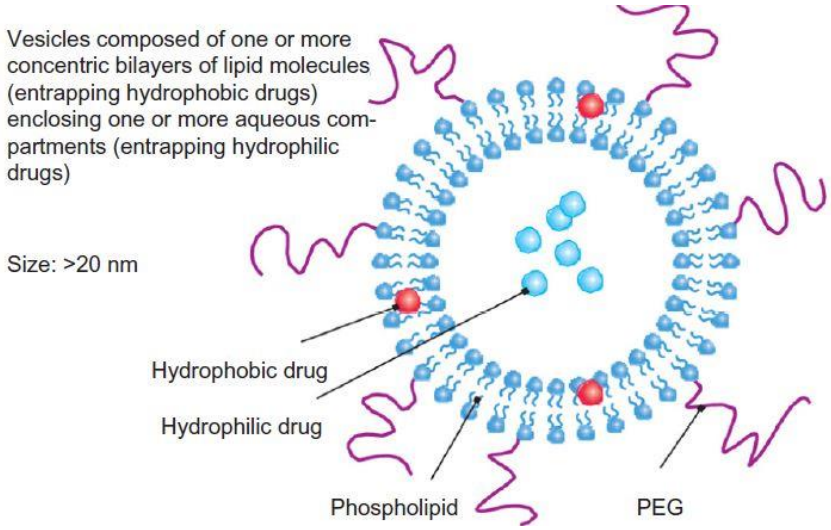

Fig. 8 Example of liposomal nanoparticle, externally functionalized with PEG, hydrophilic drug in the nucleus

Liposomes are the oldest nanotherapeutic platform for clinical use (Çağdaş, Sezer and Bucak, 2014). The first anticancer liposomal formulation involved the use of doxorubicin as a drug against ovarian and breast cancer. In the following years the improvement of this technology has widened its use to bone tumors (osteosarcoma), leukemia, and even more recently in gene therapy (Hafner *et al.*, 2014).

Polymer

Polymers in nano-polymeric fibres chain forms are widely used as biomimetic sensors. For example, Ruipeng Xue used electro-spinned core-shell nano-fibers in areas subject to severe hypoxia in the glioblastoma treatment. These intelligent platforms are able to release the drug in the regions of tissue characterized by low oxygen concentration, considered tumoral (Xue *et al.*, 2016).

Ji Hyun Choi has instead created a multi-treatment platform based on Poly(lactic-co-glycolic acid) (PLGA) nano-fibers, internally loaded with anticancer drug and gold nano-particles (GNPs), seamed externally. The system releases drug in situ, providing imaging and thermal therapy to tumor tissue, thanks to the interaction of GNPs with near-infrared stimulation, NIRS (Choi *et al.*, 2019).

Micelles

Micelles are colloidal systems with sizes ranging from 5 to 200 nm, spherical, capable of organizing themselves spontaneously in aqueous solution in an amphiphilic structure. The dimensions depend on the number of assembled molecules and therefore on the volume occupied by the hydrophilic and hydrophobic domains. In nano-medicine, the ability of micelles to trap chemical agents in different regions is useful: hydrophilic drugs and contrast agents in the hydrophilic core of the vesicles, while hydrophobic drugs in hydrophobic domains. This can redirect the biodistribution of small molecules in the body and increase the solubility of hydrophobic compounds, to allow higher dosages use (Rai and Morris, 2019).

For example, Wenjing Li created a doxorubicin-loaded and GNP-stabilized nanomicelle (Fig. 9) capable of providing tomographic imaging and drug release (Lin *et al.*, 2017).

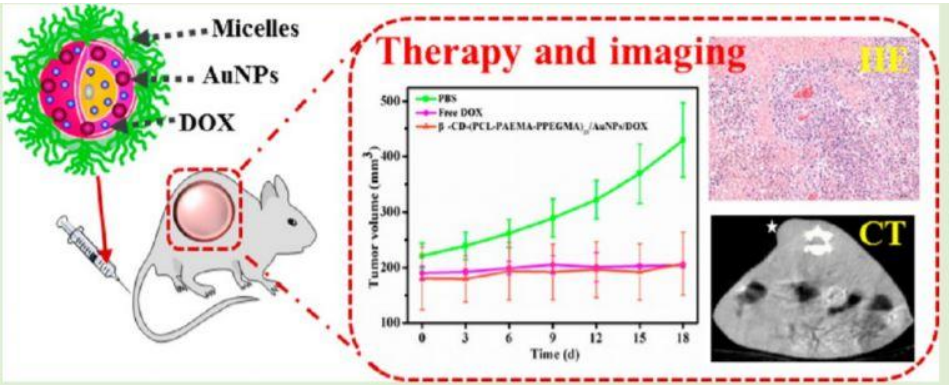

Fig. 9 Nanotheranostic platform,(Lin *et al.*, 2017).

Nanoparticles

For the nanoparticles, the outer shell can be functionalized with a variety of small molecules, polymers, polysaccharides, proteins or metal ions, while the internal core can be composed of different materials depending on the strategy. NPs are versatile and flexible, small in size, appropriately shaped, externally functionalized, with the aim of meeting the required objectives. NPs have been shown to improve pharmacokinetics by reducing drug bioabsorption in healthy tissues, instead directing it to the tumor site,

overcoming the problems of solubility and *in vivo* stability of the encapsulated drug. Organic NPs are described as being composed of organic compounds, including lipids, surfactants or polymers with the GRAS (generally considered safe) state, which offer an easy way to encapsulate the molecules. Liposomes, polymeric nanoparticles, lipid nanoparticles, polymeric micelles / micelles, protein based nanoparticles are some examples of organic NPs (Mendes *et al.*, 2018).

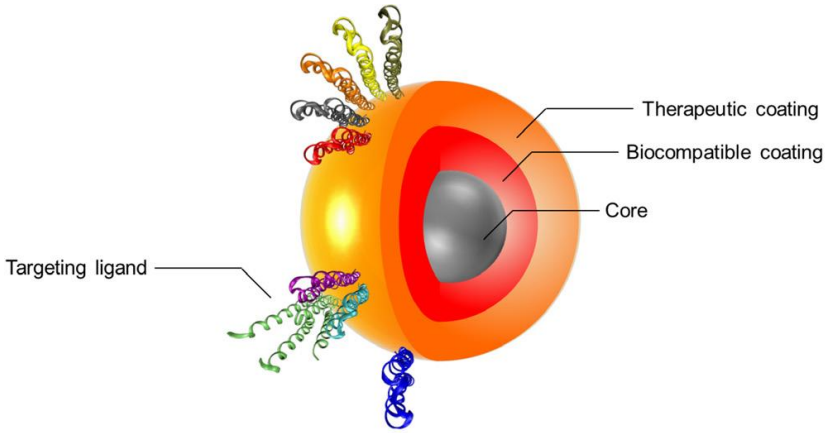

Fig. 10 Example of complex and multifunctional structure of teranostic nanoparticles

Inorganic NPs contain solid core with physico-chemical properties that can be attributed to their inorganic components, such as magnetic metal oxide or semiconductor material.(Jhaveri *et al.*, 2018). These are highly resistant to enzymatic degradation and useful for their intrinsic characteristics, such as the optical ones of Quantum Dots (QDs) and Carbon dots (CDs) capable of emitting light in the visible wavelength(Abdelhamid *et al.*, 2018); Or magnetic capacities such as SPIONs, superparamagnetic iron oxide nanoparticles, which interact with the magnetic field of magnetic resonance and offer the possibility of in situ thermotherapy (Mattu *et al.*, 2018).

Antibody

Antibodies are polypeptide sensors capable of selectively binding to their dual structure called antigen.(Scott, Wolchok and Old, 2012). In nanomedicine they are used to target a wide variety of antigens, expressed on the tumor cell membrane. The characteristics that make antigens effective targets for antibodies include the density

and coherence of molecule expression by malignant cells, limited expression of this molecule on physiologically viable benign cells.(Weiner, 2015).

The idea is to functionalize the various theranostic platforms of an antibody system which, by selectively binding to the tumor antigen, allows the selective release of the loaded drug. In fact, the antigen-antibody binding promotes the internalization of particles by cancer cells. This interaction reduces the side effects of chemotherapy drugs on healthy tissues, while increasing the effectiveness of the treatment on the tumor mass (Diamantis and Banerji, 2016).

1.2.2 Food and Drug Administration Drug-Approval Process

Most often, the development of a new drug begins when basic scientists discover a biological target (e.g. receptor, enzyme, protein, gene, etc.), involved in a biological process deemed dysfunctional in patients with a disease. When considering new drugs, analyses conducted in all therapeutic areas indicate that the development of new drugs, from target identification to approval for commercialization, takes over 12 years and often much longer (Dimasi *et al.*, 2010).

The goal of a preclinical drug discovery program is to provide one or more clinical candidate molecules, each of which has sufficient evidence of biological activity on a target relevant to a disease, as well as sufficient safety and pharmacological properties so that it can be entered in the test man (Mohs and Greig, 2017).

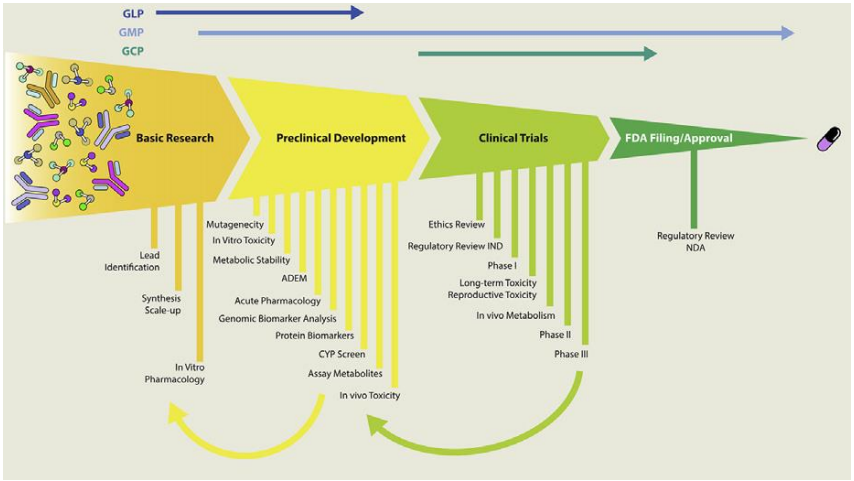

Fig. 11 A schematic of the activities involved in the drug discovery and development process (Mohs and Greig, 2017).

It is important to consider how the validation protocols affect the costs and time to market of new drugs, the process envisaged by the Food And Drug Administration (FDA) in their most recent version of 2020 is described below (https://www.fda.gov/).
This involves five stages, from discovery to marketing the platform.

Step 1: Discovery and Development

Discovery

Typically, researchers discover new drugs through:

- Insights into a pathological process that allow the design of a product to stop or reverse the effects of the disease.
- Many tests of molecular compounds to find possible beneficial effects against any of the numerous diseases.
- Existing treatments that have unexpected effects.
- New technologies, such as those that provide new ways to target medical products to specific sites within the body or to manipulate genetic material.

At this stage of the process, there may be thousands of compounds which are potential candidates for development as medical treatment. After the first tests, however, only a small number of compounds seem promising and require further study.

Development

Once a promising development compound has been identified, researchers conduct experiments to gather information on:

- Its pharmacokinetics.
- Its potential benefits and mechanisms of action.
- The best dosage and way to administer it (e.g. orally or by injection).
- Its side effects or adverse events that can often be called “toxicity”.
- How it affects different groups of people (such as by gender, race or ethnicity) differently.
- Its interaction with other drugs and treatments.
- Its effectiveness compared to similar drugs.

Figure 12 a/b shows that an average of 13 nanomedicines has been approved for specific clinical indications for a 5-year period since the mid-1990s. In the histogram, liposomal and polymeric nanoparticles predominate, which represent most of the nanomedicines approve in the 90s. Recognition in the period 2001-2005, with a significant decrease until 2008, a trend that could be related to the financing of financing associated with the global financial crisis of 2008 (Tsoulfas, 2012), (Cui *et al.*, 2014). The clinical trials data in Fig. 12 c/d shows some interesting trends in comparison to those for FDA approvals.. First, the number of nanomedicine to which IND approval is granted for undertaking clinical trials has consistently succeeded since 2007. In terms of the categories of materials under consideration, there are many more micellar, metallic and controlled particles on proteins that cross the development process than previously approved. However, this does not mean that polymeric particles and liposomes are necessarily disadvantaged. In fact, most micelle and liposome systems in development incorporate polymers such as synthetic blocks (Cui *et al.*, 2014), while the protein-based systems used also have a component of synthetic polymer.

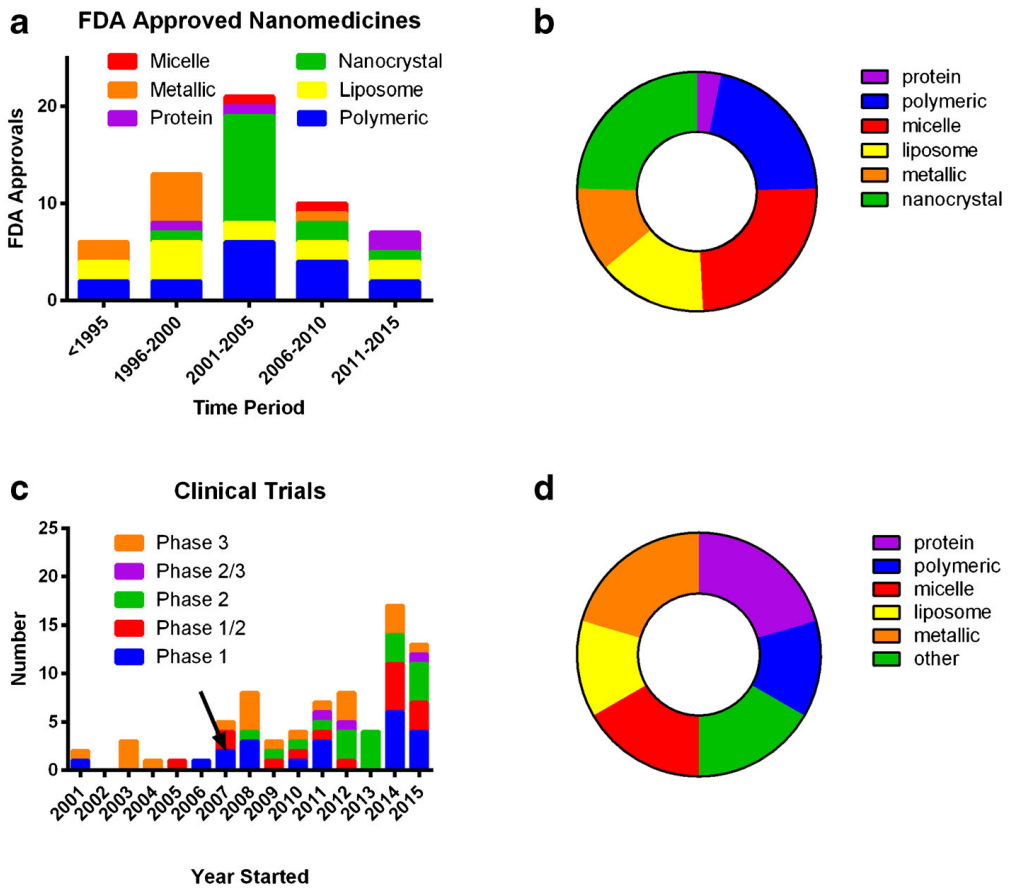

*Fig. 12 Trends in the development of nanomedicines. (**a**) FDA approved nanomedicines stratified by category; (**b**) FDA-approved nanomedicines stratified by category overall; (**c**) clinical trials identified in clinicaltrials.gov from 2001 to 2015 with arrow indicating approximate start date of US law (FDAAA 801) requiring reporting to FDA database; (**d**) nanomedicines under clinical trial investigation stratified by category overall* (Bobo *et al.*, 2016).

Step 2: Preclinical Research

Before a drug testing in people, researchers need to find out its potential harm, side effects or toxicity by *in vivo* and *in vitro* testing.

- The FDA requires researchers to use good laboratory practices (GLP), defined in medical product development regulations, for preclinical laboratory studies. These regulations establish the minimum basic requirements including: conduct study, staff, structures, written protocols, operating procedures and study reports.

Usually, preclinical studies are not very large. However, these studies need to provide detailed information on dosage and toxicity levels. After preclinical tests, the researchers review their results and decide whether the drug should be tested in people.

Step 3: Clinical Research

While preclinical research answers basic questions about the safety of a drug, it does not replace studies of how the drug will interact with the human body. "Clinical research" refers to studies conducted on people. As the developers plan the clinical study, they should consider what they want to accomplish for each of the different phases of clinical research and begin the Investigational New Drug Process (IND), a process they must follow before clinical research begins.

Design of clinical trials

Researchers design clinical trials to answer specific research questions related to a medical product. These tests follow a specific study plan, called a protocol, developed by the researcher or the manufacturer. Before a clinical trial begins, researchers review previous drug information to develop research questions and objectives. So, they decide:

- Who qualifies to participate (selection criteria).
- How many people will be part of the study.
- How long will the study last.
- Whether there will be a control group and other ways to limit the search distortion.
- How the drug will be administered to patients and at what dosage.
- What assessments will be conducted, when and what data will be collected.
- How the data will be reviewed and analysed.
- What are the phases of the clinical trial?
- Clinical research phase studies

Approval

The FDA review team has 30 days to review the original IND submission. The process protects volunteers who participate in clinical trials from unreasonable and significant risks in clinical trials. The FDA answers IND questions in two ways:

- Approval to start clinical trials.

- Clinical suspension to delay or stop the investigation. The FDA may place a clinical suspension for specific reasons, including:
    - Participants are exposed to unreasonable or significant risks.
    - Investigators are not qualified.
    - The materials for the volunteer participants are misleading.
    - The IND application does not include sufficient information on the risks of the trial.

A clinical intake is rare; instead, the FDA often provides comments aimed at improving the quality of a clinical trial. In most cases, if the FDA is convinced that the process meets federal standards, the applicant is authorized to proceed with the proposed study.

The developer is responsible for informing the review team about the new protocols, as well as the serious side effects observed during the trial. This information ensures that the team can closely monitor the evidence for any problems. At the end of the trial, researchers must submit study reports.

This process continues until the developer decides to end clinical trials or submit a marketing application. Before submitting a marketing application, a developer must have adequate data from two large controlled clinical trials.

Step 4: FDA Drug Review

If a drug developer has evidence from its early tests and preclinical and clinical research that a drug is safe and effective for its intended use, the company can file an application to market the drug. The FDA review team thoroughly examines all submitted data on the drug and makes a decision to approve or not to approve it.

New Drug Application

A New Drug Application (NDA) tells the full story of a drug. Its purpose is to demonstrate that a drug is safe and effective for its intended use in the population studied.

A drug developer must include everything about a drug—from preclinical data to Phase 3 trial data—in an NDA. Developers must include reports on all studies, data, and analyses. Along with clinical results, developers must include:

- Proposed labeling
- Safety updates
- Drug abuse information
- Patent information
- Any data from studies that may have been conducted outside the United States
- Institutional review board compliance information
- Directions for use

FDA Review

Once FDA receives an NDA, the review team decides if it is complete. If it is not complete, the review team can refuse to file the NDA. If it is complete, the review team has 6 to 10 months to make a decision on whether to approve the drug. The process includes:

- FDA inspectors travel to clinical study sites to conduct a routine inspection. The Agency looks for evidence of fabrication, manipulation, or withholding of data.
- The project manager assembles all individual reviews and other documents, such as the inspection report, into an "action package." This document becomes the record for FDA review. The review team issues a recommendation, and a senior FDA official makes a decision.

FDA Approval

In cases where FDA determines that a drug has been shown to be safe and effective for its intended use, it is then necessary to work with the applicant to develop and refine prescribing information. This is referred to as "labeling". Labeling accurately and objectively describes the basis for approval and how best to use the drug.

Step 5: FDA Post-Market Drug Safety Monitoring

Even though clinical trials provide important information on a drug's efficacy and safety, it is impossible to have complete information about the safety of a drug at the time of approval. Despite the rigorous steps in the process of drug development, limitations exist. Therefore, the true picture of a product's safety actually evolves over the months

and even years that make up a product's lifetime in the marketplace. FDA reviews reports of problems with prescription and over-the-counter drugs, and can decide to add cautions to the dosage or usage information, as well as other measures for more serious issues.

Generic Drugs

New drugs are patent protected when they are approved for marketing. This means that only the sponsor has the right to market the drug exclusively. Once the patent expires, other drug manufacturers can develop the drug, which will be known as a generic version of the drug. Generic drugs are comparable to brand name drugs and must have the same:

- Dosage form
- Strength
- Safety
- Quality
- Performance characteristics
- Intended use

Reporting Problems

FDA has several programs that allow manufacturers, health professionals, and consumers to report problems associated with approved drugs.

1.2.4 Active and Passive targeting

The main purpose of the theranostic approach is a better selectivity of the platform used towards the tumor tissue, in order to improve the release efficacy and limit side effects, and optimize the therapeutic result. The previously defined nanoparticles require some functionality to be defined "targeted"; these must circulate in the blood system for a sufficiently long period of time reaching and accumulating in the tumor area. Finally they

must be able to release the drug in a controlled period of time, without incurring the burst release. For this to happen, nanocarriers must be able to cross the endothelial barrier that makes up the blood vessels and reach the tumor through two active and / or passive targeting strategies (Uchegbu *et al.*, 2013).

Passive targeting

Nanoparticle drug carriers, with particle sizes <100-200 nm, can be delivered to tumor tissues and accumulate in the perivascular area (the area around the blood vessels) through the Enhanced Permeation and Retention (EPR) effect when going through the leaking tumor vasculature, as shown in Fig. 13.

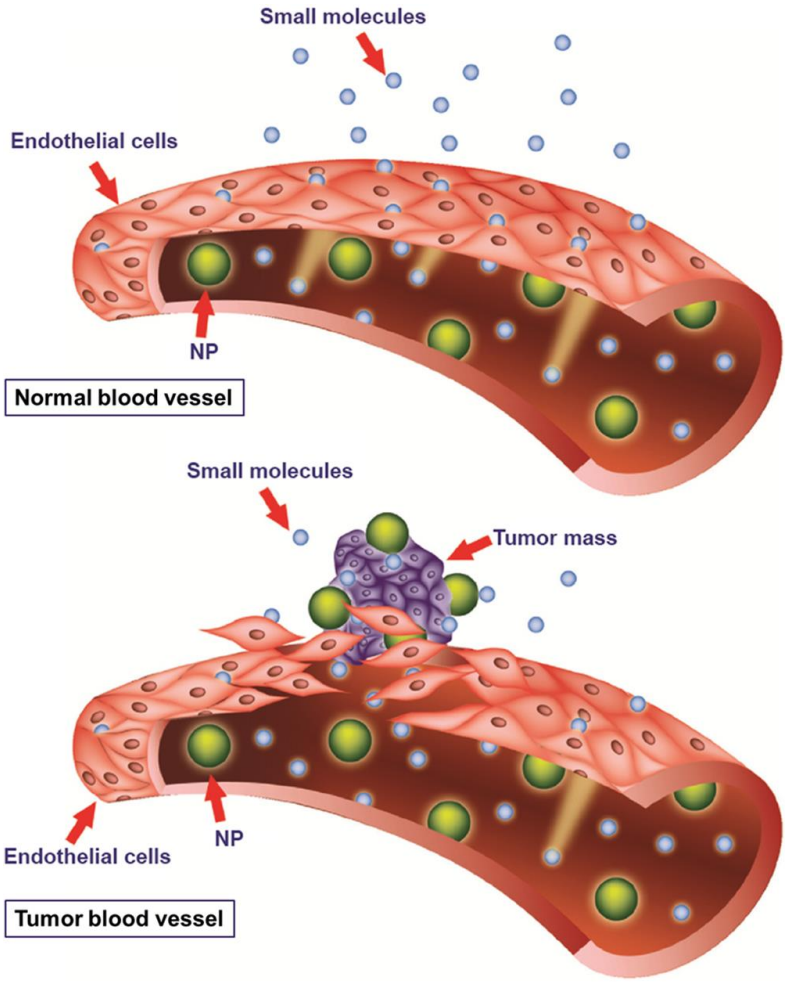

Fig. 13 Targeting of nanomedicines by the enhanced permeability and retention (EPR) effect. Tumor vessels contain large fenestrations between the endothelial cells allowing the NPs to reach the matrix and the tumor cells. Conversely, normal tissues contain tightly joined endothelial cells, preventing the diffusion of NPs from the blood vessels (T Lammers *et al.*, 2011)(Pearce and O'Reilly, 2019).

In fact, the tumor vascular tissue is characterized by a porous endothelial structure, the interstitial space from 100 nm to 800 nm, allows the accumulation of nanocarriers in the pathological environment (Maeda, Bharate and Daruwalla, 2009).

For example, Chen (Chen *et al.*, 2018) fabricated a negatively charged PEG coated magnetic nanoparticle based drug delivery system that allows for longer circulation time, avoiding clearance from the immune system and, at the same time, preventing burst release. Magnetic particles have an average diameter of 32 nm and provide the imaging component if stimulated with magnetic resonance imaging (MRI). Furthermore, the system is able to convert its surface charge in response to the more acidic pH in the extracellular environment of the tumor. It has been shown that the external charge plays an important role in order to improve the cellular absorption of the nanocarriers, being the cell membrane highly negative (about -70mv): the studies have actually concentrated to impart a positive charge to the particles.

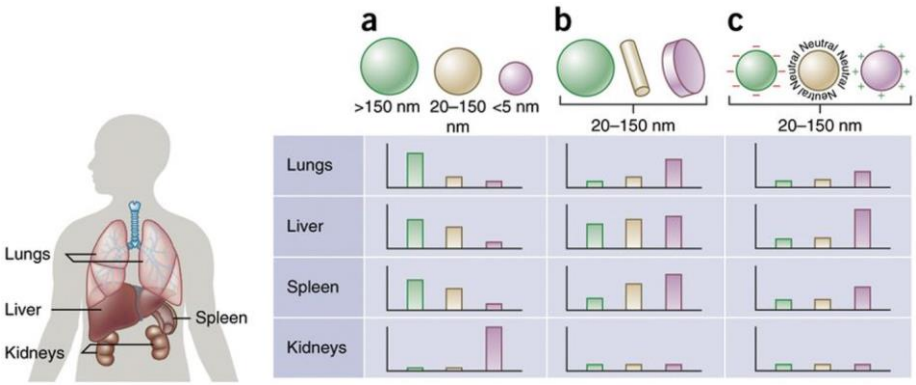

Fig. 14 Nanoparticle size, shape, and surface charge dictate biodistribution among the different organs including the lungs, liver, spleen, and kidneys (Pearce and O'Reilly, 2019).

In the Chen's study, PEG was used as an antifouling, allowing for a longer blood circulation time, without being eliminated by the immune system. It is also degradable to acid pH and useful for further functionalization thanks to its surface chemical groups.

Active targeting

The most important challenge in active targeting is the definition of the most suitable targeting agent or agents to selectively and successfully transport nanoparticle systems to cancerous tissue, thus avoiding any type of toxicity in the process. These strategies are therefore also based on the ability of the target agents or ligands to bind to the surface of the tumor cells with an extremely strong affinity to trigger the endocytosis of the receptor. With this type of interactions, therapeutic agents will then be delivered to specific regions of the tumor (Rai and Morris, 2019), (Fig.15).

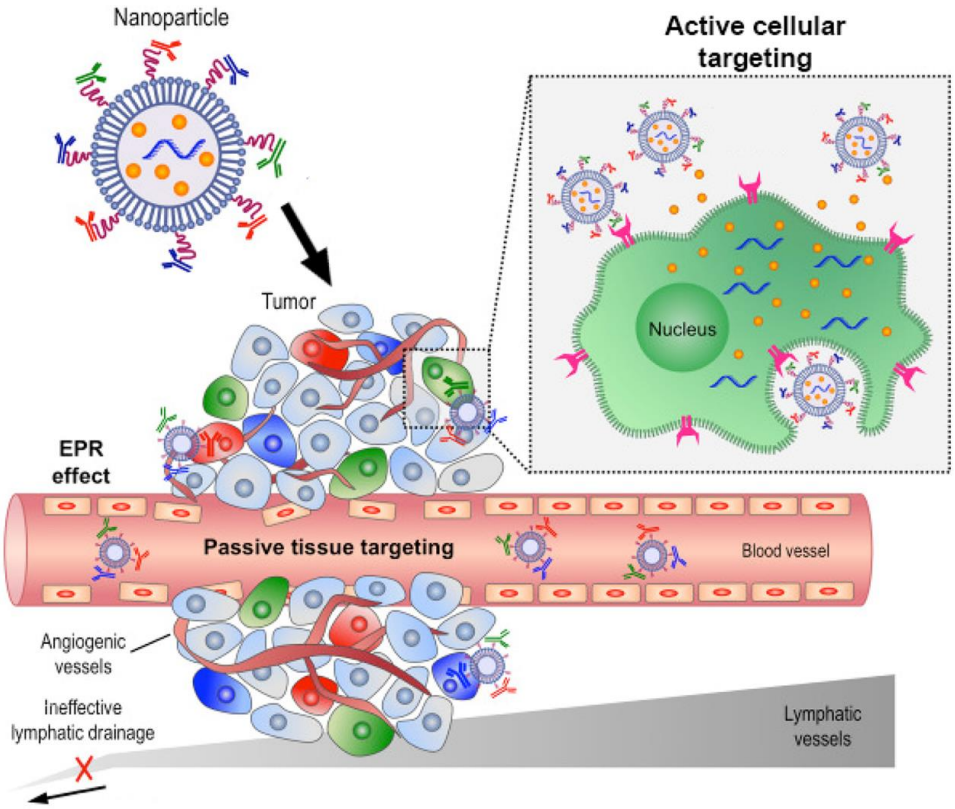

Fig. 15 Representation of the mechanism for active tumor targeting. Initially, circulating nanoparticles diffuse into the tumor mass through the EPR effect, followed by recognition by cellular receptors allowing internalization into cells(Pearce and O'Reilly, 2019).

It has been demonstrated that a ligand-conjugated nanoparticle is facilitated to reach the tumor extracellular environment and, successively, enter the cell with respect to a carrier not functionalized (Cai *et al.*, 2016).

From a general point of view, the cells express on their membrane different receptors, proteins, antibodies, peptides; this expression varies according to the type of cell and,

in particular, the tumor cells overexpress specific receptors: these peculiar characteristics can be exploited, in order to avoid non-specific bonds (Masood, 2016). Ligands can be peptides, antibodies, polysaccharides, folic acid and other biological molecules. These surface functionalization strategies improve the cellular uptake of the drug carrier (Rai and Morris, 2019).

For example, Chunhuan Shi (Shi *et al.*, 2018) has experimented a PCL-PEG-based polymer particle, loaded with Docetaxel and externally functionalized with folic acid (FA). Great affinity of FA for the folate receptor (FR) overexpressed in breast cancer has been demonstrated. The amount of drug released is more distributed over time and hemolysis is reduced by about 5 times compared to the control with only docetaxel. More importantly, the MCF-7's internalization capacity of the drug's breast cancer increases by about 20%. Furthermore, the common use in research is the exploitation of the interaction between hyaluronic acid (HA) and CD44; in this regard Al-Nahain et al (Al-Nahain *et al.*, 2013) delivered doxorubicin conjugating it with graphene QD, functionalized with hyaluronan, capable of binding to the overexpressed CD44 receptor of the tumor cell lines.

More generally, it can be said that the synergy between active targeting and improves drug release, reduces harmful effects on healthy tissues and gives specific characteristics to nanocarriers (Rai and Morris, 2019).

Therefore, there are different strategies to obtain nanotheranostic platforms. Among them, nanoparticles have shown considerable versatility. For example (Chai *et al.*, 2017)created Cadmium selenide / zinc sulphide (CdSe / ZnS) QDs pH-responsive microcapsules, bounded with DNA microcapsules composed of nucleic acid layers C-G * C (Cytosine - Guanine) and T-A * T (Thymine – Adenine), whose layers started to degrade in the acidic tumor environment (pH<7) releasing QDs. When stimulated at a wavelength between 620 nm and 560 nm provide, these metallic based QDs were fluorescent. Fluorescence emission is used in vitro to monitor the actual release of QD at pH 5.0 and 7.2. However, although these QDs based were compatible, their micrometric dimensions did not allow to exploit the EPR effect, and moreover their fluorescence emission scarcely penetrates the thickness of human tissues (Rai and Jamil, 2019).

Similar strategy is based on the use of Carbon Dots as imaging probes. Du et al reported the low *in vitro* cytotoxicity and easily functionalisation with PEG and Aspartic acid (ASP), thanks to the presence of carboxylic (-COOH) groups. The figure 16 shows the ability of these nanoparticles to overcome the blood brain barrier (BBB) and to be visible in anatomical structures of reduced dimensions under confocal microscopy (Du *et al.*, 2019).

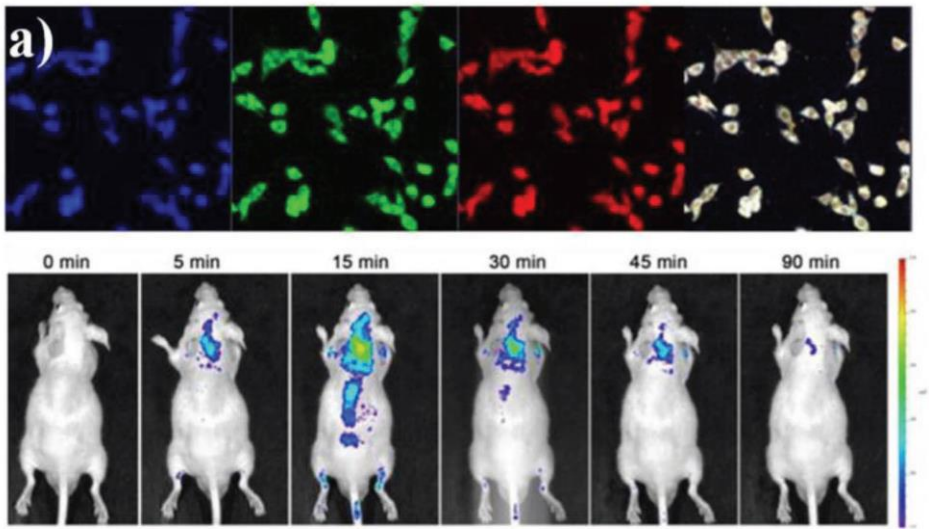

Fig. 16 Laser confocal scanning microscopy (LCSM) images of C6 cell lines pre-treated with Asp–CDs under excitation of 405, 488, and 555 nm(up) and whole body distribution of Asp–CDs as a function of time after injection (down), (Du *et al.*, 2019).

In a recent work Wang et al proposed magnetic particles functionalised with Poly(lactic-co-glycolic acid) - Polyethylenimine (PLGA-PEI), loaded with Paclitaxel, to treat brain cancer (Wang *et al.*, 2018). Fluorescence imaging of magnetic nanoparticles has been shown to be effective *in vitro* but strong limitations *in vivo*. It should be noted that all *in vivo* applications of QDs have been limited to animals. However, this is a general limitation for fluorescence imaging and is mainly related to the limited tissue penetration depth of light and the very few imaging agents that have been approved for humans. Therefore only NIR-fluorescence based proof-of-concept studies, imaging of body parts, and endoscopic investigations have been performed so far (Wegner and Hildebrandt, 2015).

A promising technique for the NPs manufacturing is the Layer by Layer (Poon *et al.*, 2011) (more details on this technique will be provided in the next chapter). In the same

work QDs, Poly-lysine and PEG have been alternated in a trilayered structure, forming a pH-responsive nanoparticle for being triggered into the tumor environment. Also, the average circulation time of the particles in the blood vessels increased thanks to the presence of hydrophilic PEG, Fig.17.

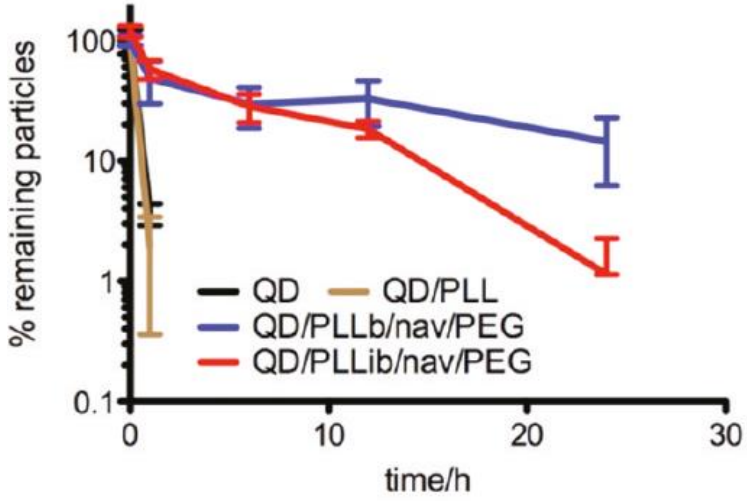

Fig. 17 Log linear blood circulation profiles of QD, QD/PLL, QD/PLLib/nav/PEG, and QD/PLLb/nav/PEG.

Gold nanoparticles (AuNP) have been studied recently to overcome the toxicity of heavy metals used in diagnostics. These showed stability in a biological environment without being subject to oxidation and also could be easily synthesised in dimensions of about 20 nm. AuNP have excellent optical properties: diameters of 13 nm emit in the blue field (wavelength of 520 nm), while an increase in the particles' size leads to a shift in the red field. The intracellular location of the AuNPs may also be traced using fluorescent microscopy (Matea et al. 2017).

Depending on the shape and functionalities, AuNP could interact with the biological system in different ways based on the type of cell, specific absorption or targeting pathways. Also, their marked surface plasmon resonance-enhanced absorption in the NIR range allows obtaining images by different methods: optical coherence tomography (OCT), X-ray computed tomography (CT), two-photon luminescence (TPL), or photoacoustic imaging (PA). All these characteristics are influenced by the particles size, shape, and aggregation state (Rai and Morris, 2019).

Table 2 Different types of AuNPs, categorized upon particle shape and tuneable optical and electronic properties.

AuNPs	Particle size	Plasmon characteristics	Applications
Nanospheres (AuSs)	2–100 nm	522–539 nm	Cell imaging Photothermal therapy Delivery of therapeutic molecules
Nanorods (AuNRs)	Length: 50–250 Diameter: 5–50 nm	Transversal band 520 Longitudinal band infrared region dependent of the aspect ratio: 800 nm or >1200 nm	Tumour imaging Photothermal therapy Delivery of therapeutic molecules
Nanoshells (AuSLs)	10–150 nm	510–575 nm	Tumour imaging Photothermal therapy Photodynamic therapy Delivery of therapeutic molecules
Nanocages (AuCs)	Length: 30–70 nm	532–575 nm	Tumour imaging Photothermal therapy Photodynamic therapy Delivery of therapeutic molecules
Nanostars (AuNSs)	18–90 nm	590–1000 nm	Photothermal therapy Photodynamic therapy

The use of gold nanoparticles for brain tumor treatment is still in the clinical and preclinical phase. Besides many promising studies have been found in the literature, AuNPs have toxicity with a strong dependence on concentrations and particle sizes (Xiaomin Li *et al.*, 2018).

For example Jia et al. showed an increase in cell's death (mouse fibroblasts) by injecting 5 nm diameter AuNPs at a concentration of 300 mmol/L(Jia *et al.*, 2017). Despite the presence of biocompatible polyelectrolytes (PSS) or hydrophilic polymers (PEG) which could increase the circulation time *in vivo*, damages to cells membrane and their consequent death were found.

In the same study, the authors related the biodistribution of gold nanoparticles in different organs for a total of 24 hours. AuNPs were injected *in situ* (figure a) and systemically (figure b). A clear great topological disparity was found in the two cases.

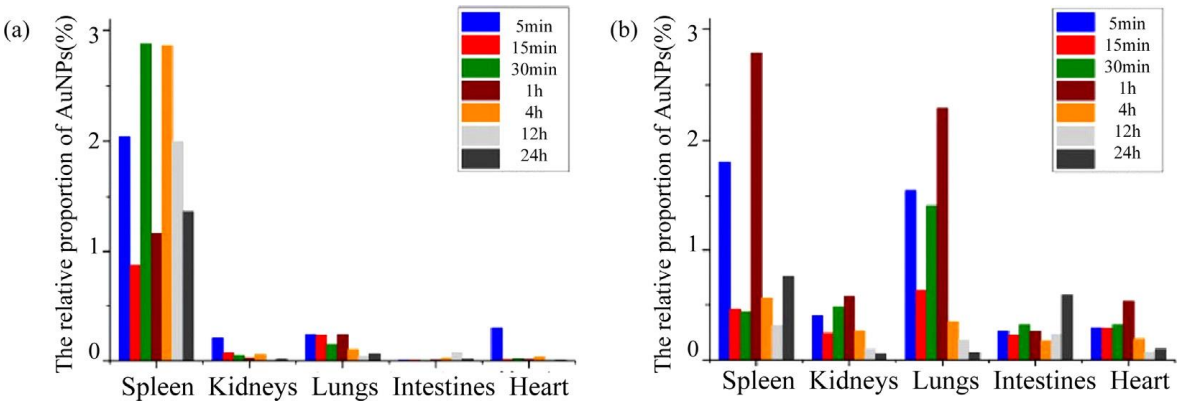

Fig. 18 The relative distribution proportion of the Gold nanoparticles in the spleen, kidneys, lungs, intestines, and heart of SD rats at 5 min, 15 min, 30 min, 1 h, 4 h, 12 h, and 24 h after IVI (a), and after ISI in the tarsal tunnel (b), (Jia *et al.*, 2017).

For these reasons the AuNPs biodistribution and pharmacokinetics must be investigated more in order to know their course *in vivo*.

Despite the significant increase in AuNPs in biomedical research, only a few types of nanoparticles have been approved in clinical practice for simultaneous therapeutics and diagnostics application (Rai and Jamil, 2019).

As has just been described, there are multiple strategies which, using different materials, give rise to theranostic platforms. The aim of this work is to propose the preliminary implementation of a theranostic nanoparticle, capable of meeting the specificity and efficacy requirements of the treatment. This platform was designed to comply, as far as possible, with the five steps of the Food and Drug Administration Drug-Approval Process. There are often references in the literature on the effectiveness of contrast media of magnetic resonance images created with magnetic nanoparticles (Rai and Jamil, 2019). Indeed, MRI has become a popular and non-invasive method for diagnosis, especially for soft tissues, due to the different relaxation times of the hydrogen atoms (contained in the water) when they are exposed to a suitably sized magnetic field. (Tanimoto *et al.*, 1994). Subsequently, Superparamagnetic iron oxide nanoparticles (SPIONs) were developed as contrast agents for MRI and increasing the diagnostic sensitivity and specificity due to modifications of the protons relaxation time (Scientific and Clinical Applications of Magnetic Carriers, 1997), (Bordat et al., 2000), (Urhahn et al., 1996).

The effectiveness of SPIONs as a contrast agent in the various tissues depends on its physiochemical properties, such as size, charge and coating, and can be increased through surface modifications by active biological substances (antibodies, receptor ligands, polysaccharides, proteins) (Rai and Morris, 2019).

The hydrodynamic diameter of the SPION used with MRI varies between 20 and 3500 nm, although intravenously applied particles are relatively small and range between 20 and 150 nm with, or 5–15 nm without coating (Wan *et al.*, 2016). Coatings are usually made from derivates of dextran and Poly(ethyleneglycol) (Jeon *et al.*, 2016), but also starch, albumin, silica, etc. (Singh *et al.*, 2010). Since most of the particles are ingested by the cells of the reticuloendothelial system (RES), their distribution is made more easily visible in the liver, spleen, bone marrow and lymph nodes. Renal flow can also be visualized by means of SPIONs (Beckmann *et al.*, 2003), (Qing *et al.*, 2002). For these reasons, the SPIONs will be exploited below to create the structural core of the theranostic nanoparticle.

AIM and OBJECTIVES

Aim: The main purpose of this project is to show a new theranostic nanoparticle architecture treatment cancer. The platform has an internal core made up of single superparamagnetic iron oxide nanoparticles (SPIONs) covered with polyelectrolytes loaded with anticancer drugs, deposited using the Layer by Layer (LbL) technique, for double therapy: pharmacological and thermal. We also want to optimize the platform versatility increasing the average circulation times *in vivo* through hydrophilic PEG-based polymer deposition, on which to set specific targeting molecules for the most common tumor phenotypes (breast, prostate, lung cancer) by implementing active targeting.

Objective 1: To discuss the manufacturing process and the therapeutic requirement in order to build-up the nanoparticles. Polyelectrolytes, drugs and SPIONs must operate in the tumor therapeutic window, be pH responsive and satisfy the active and passive targeting requirements mentioned in the previous chapter. Therapeutic efficacy is assessed through characterization tools and instrumental tests (SEM, TEM, Confocal Microscopy, Live / Dead Cell Viability Assays, MRI, drug release profiles). Finally, macroscopic evaluation of tumor volume *in vivo* during and after nanoparticle therapy is of fundamental importance.

Objective 2: To select the components for the build-up of the functionalised nanoparticle. We intend to encapsulate SPIONs with highly biocompatible and biomimetic natural polymers, such as Chitosan and Alginate or synthetic, Poly (allylamine hydrochloride) (PAH) and Polystyrene sulfonate (PSS). Paclitaxel, Docetaxel, DOX are intended as reference anticancer drugs deposited between the layers. Presence of PEG as the last layer for hydrophilic characteristics in a blood environment. HER-2 antibody, EGFR, Biotin, HA sequences expressed by active targeting.

Objective 3: To investigate how to increase the nanoparticles stability, SPION core (diameter <20 nm) must be characterized by a charge that allows the subsequent layers deposition, evaluation of Zeta potential -4 / + 23 mV. After the the layers deposition, the diameter is considered to be about 200 nm and with Zeta-potential -50 / +33 mV. The anchoring of the targeting molecules is estimated through the FTIR-ATR study,

treatment efficacy estimated with the use of Live and Dead cell, tumor volume, Immunohistochemical images.

Table 3 Summary table of the theranostic and design characteristics of the nanoparticle.

	Core	Layer by Layer	External coating	External surface functionalization
Challenges	Biocompatibility Magnetic targeting Imaging (MRI) Hyperthermia	Biocompatibility pH-responsive Passive targeting & EPR Effect Drug release	Biocompatibility Immune System Stealth strategy Increase circulation time	External probes Active Targeting Tumor specificity
Specifications	SPIONs	Polyelectrolytes (polycation/polyanion): Chitosan/Alginate PAH/PSS Drugs: Paclitaxel and Docetaxel	Hydrophilic polymer grafting: PEG	HER-2 antibody EGFR Biotin HA
Value/Details	Size: < 20 nm Surface charge: -4 /+23 mV	Strong interactions between the polyelectrolytes: -30 /+30 mV Particle size: < 150-200 nm Drug efficiency loading: > 70% pH operativity: acidic conditions Drug release kinetics: controlled and constant up to 24 hours	Avoided Immune system activation High circulation time: up to 24 hours	Demonstration of active targeting and tumour specificity by cellular uptake analysis and

Figure 19 schematically shows the nanoparticle design, materials and strategies, chosen to meet the objectives mentioned above 1-3. We want to underline that the composition of the nanoparticle has followed a bottom-up logic starting from the core up to the external functionalization for active targeting. The possible alternatives (natural and synthetic polymers) have been proposed because they are considered valid in a comparable way and will be subsequently evaluated in their specifications.

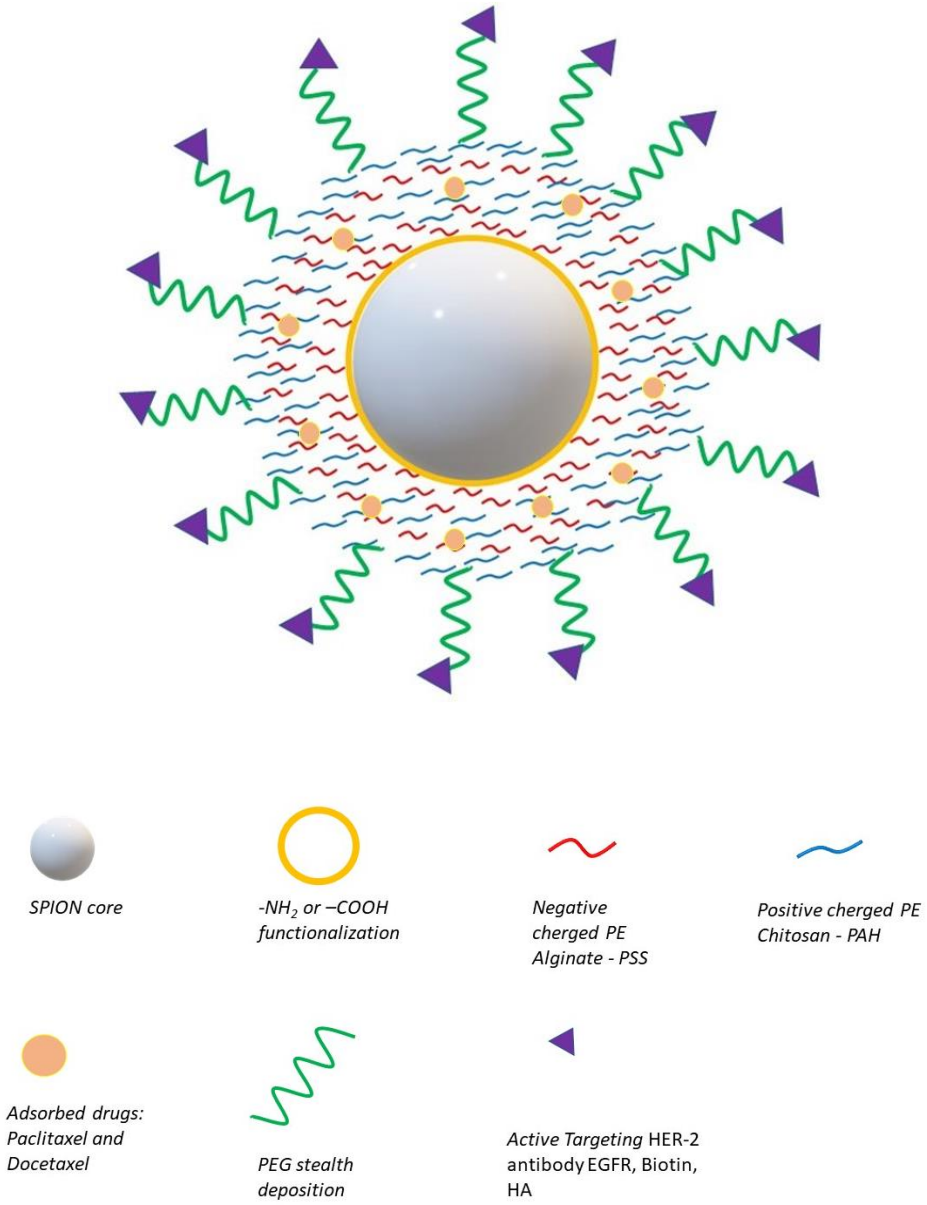

Fig. 19 Schematic representation of the nanoparticle

2.1 Core of the functionalised nanoparticle

In literature there are many solutions for the formation of nanoparticles templates. Volodkin *et al.* created Calcium Carbonate (CaCO3) microparticles as a sacrificial template using $CaCl_2$ and Na_2CO_3 as precursors, then the particles were functionalized with PAH and PSS. The anticancer drug was encapsulated replacing the $CaCO_3$ core. Polymer nanocores are also used to encapsulate drug in the nanoparticles, for example (mRNA delivery using non-viral PCL nanoparticles) used biodegradable polymer of PCL for mRNA using w / o emulsion. Although there are valid solutions, the proposed idea is to maximize the efficiency of the template that allows to simplify the chemistry of the nanoparticle and the use of additional imaging means.

As mentioned in the previous paragraph, it was decided to exploit the biocompatibility characteristics of the SPIONs to implement the theranostic nanoparticle. SPIONs can be used either as a single core or as agglomeration. The substantial differences are found in the intensity of the drawing in MRI and in the dimensions. It is important to note that the single superparamagnetic particles need surfactants during their formation process, therefore it is necessary to avoid the presence of residual cytotoxic agents. Although, dimensions are comparable, it is still difficult to obtain multicore nanoparticles containing (Fig.20) a number of single comparable units. Furthermore, the small size of the individual SPIONs allows to better respect the passive targeting parameters (EPR-effect) (Gutiérrez *et al.*, 2015). It is assumed that the nanoparticles synthesized for biomedical use are further washed by surfactants and made biocompatible. For these reasons, the design of the proposed particle is chosen by using single core particles.

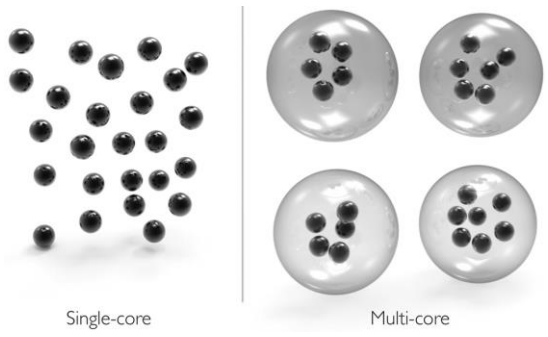

Fig. 20 Schematic representation of single-core and multi-core particles. Single-core particles contain only one magnetic core (single domain nanocrystal) per particle (Gutiérrez *et al.*, 2015).

2.1.1 Description of the Superparamagnetic iron oxide nanoparticles (SPIONs)

Superparamagnetic iron oxide nanoparticles (SPIONs) are among the most widely used magnetic nanoparticles and are widely investigated for biomedical applications including drug release, magnetic fluid hyperthermia (MFH), magnetic resonance imaging (MRI), gene delivery, and tissue engineering, due to their peculiar magnetic characteristics, excellent chemical stability, biodegradability and low toxicity (Ali *et al.*, 2019), (Danhier, Feron and Préat, 2010), (Merbach, Helm and Tóth, 2013). SPIONs are commonly formed by magnetite (Fe_3O_4) and maghemit (γ-Fe_2O_3) and their poor cytotoxicity is due to their degradation in cells and their products (Fe + O_2 ions) are used for cellular metabolism (Shen *et al.*, 2015), (Ho, Sun and Sun, 2011).

Magnetic nanoparticles based on iron oxides are synthesized with a nanodimensional diameter between 1 and 100 nm. In general, the larger magnetic particles show coercivity (Hc) and residual magnetization (Mr) values due to their multi-domain structure attributed to different orientations of the crystalline grains (as shown in the figure 21). However, when the particle size changes to the submicron (nanometric) regime, the multidomain structure changes to a single domain structure and the coercivity value is maximized. The single domain characteristic of these nanoparticles is maintained if the particle radius is below its critical value (r_c), For example, the r_c values of the single domain Fe_3O_4 and γ-Fe_2O_3 nanoparticles are calculated as 30 nm and 60 nm respectively (Turcheniuk *et al.*, 2013), (Li *et al.*, 2017).

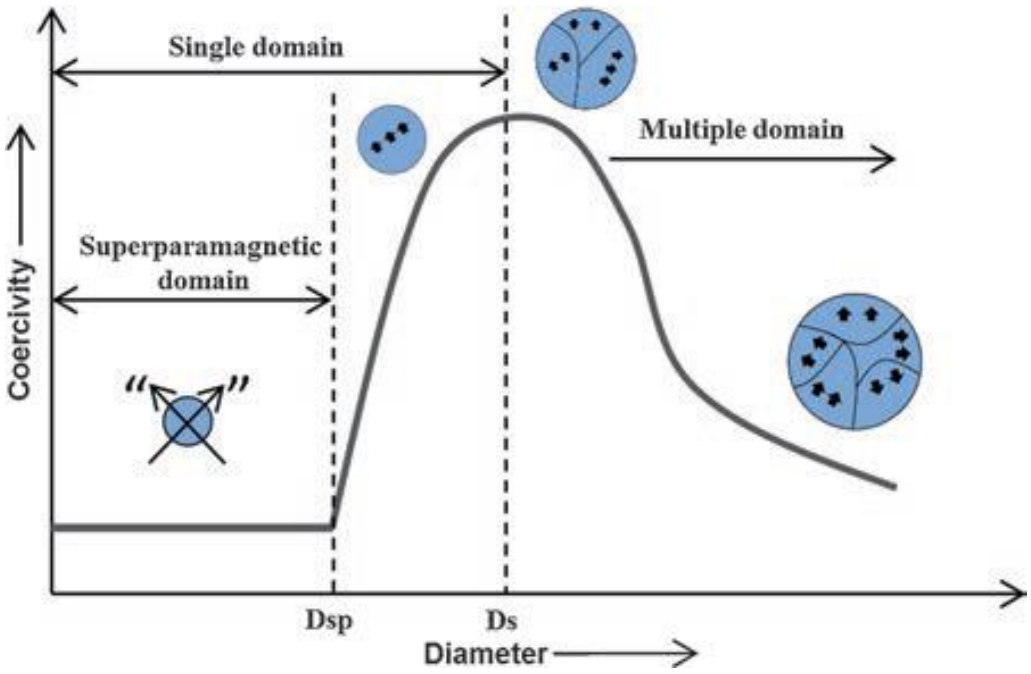

Fig. 21 Schematic representation of coercivity change depending on the magnetic nanoparticle size (Rai and Jamil, 2019)

Furthermore, when the size of the magnetic particles is further reduced, these particles may have a "Superparamagnetism" and this reduced size is called the superparamagnetic size, generally in the range 4–20 nm for the Fe_3O_4 / γ-Fe_2O_3 nanoparticles at room temperature (Ortega and Giorgio, 2012). With the aim of studying the magnetism of these particles, the hysteresis cycle refers to the relationship between the magnetic field (H) and the magnetization (M) of the particles (Fig. 22). The loop is generated by measuring the magnetic flux of a ferromagnetic material while the magnetizing force changes.

Saturation magnetization (Ms) is obtained when all the orientation of the magnetic dipoles of nanoparticles' domains is aligned with the applied magnetic field. In the case of SPOIN, as ferromagnetic nanoparticles, by decreasing or removing the magnetic field, the orientation of some domains changes, therefore the magnetization is reduced but does not reach zero. Retention magnetization (Mr) is the density of the magnetic flux that remains in the nanoparticles when the magnetization force is removed.

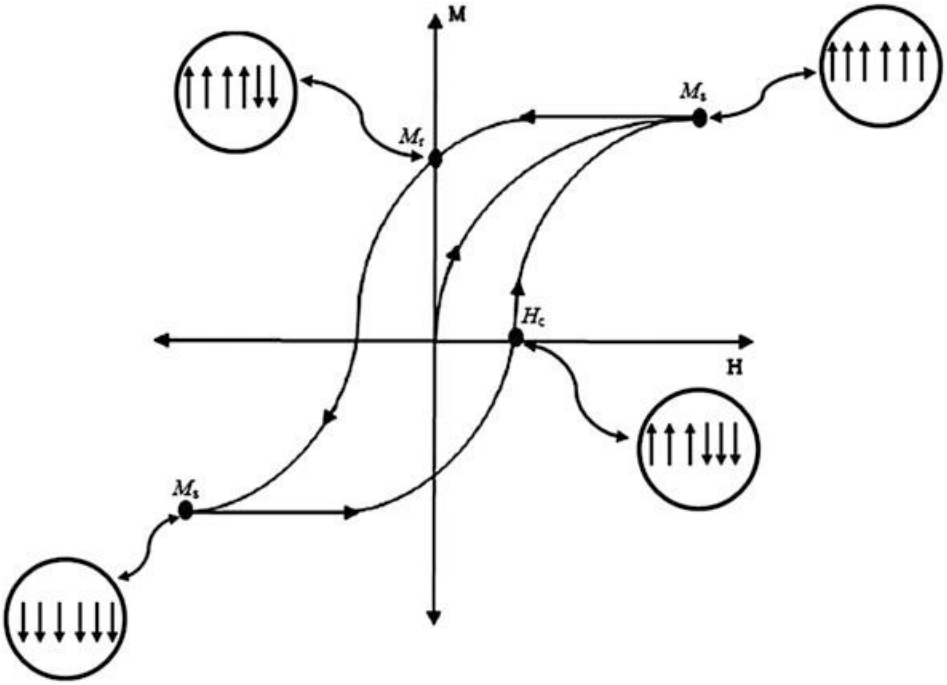

Fig. 22 Magnetization hysteresis loop (Zarepour, Zarrabi and Khosravi, 2017)

By changing the direction of the magnetic field in the opposite direction, the orientation of the dipoles changes. The magnetization flow returns to zero (Hc) when the number of domains with opposite orientations is equal. Subsequently, by increasing the magnetic field, the magnetization is saturated again and this process will be repeated several times in the presence of an alternating current (AC) magnetic field. The nanometric dimensions of the SPIONs therefore characterize superparamagnetic phenomena that radically change some magnetic properties. Indeed, in the presence of an external magnetic field, their magnetization can be as saturated as other ferromagnetic materials, while their net magnetic moments are brought to zero when the magnetic force is removed. Furthermore, the points Mr and Hc are eliminated from the hysteresis cycle of the SPIONs due to their molecular structure which consists of a single magnetic domain (Rui *et al.*, 2010), (Tartaj *et al.*, 2003), (Sun *et al.*, 2007), (Wei *et al.*, 2012).

2.1.2 SPIONs features: size and charge

The size of the nanoparticles is one of the most important characteristics in biomedical applications (Leung, Xuan and Wang, 2010), (Soares *et al.*, 2015). As previously mentioned, the nanometric dimensions are fundamental to exploit the EPR effect of the blood vessels to the tumor microenvironment, also the large particles are easily detectable by the reticuloendothelial system (RES) and excluded from the circulatory system (Aillon *et al.*, 2009), (Berry *et al.*, 2003).

Revia and Zhang (Revia and Zhang, 2016) verified Signal to Noise Ratio (SNR) of SPIONs with a diameter between 4 - 20 nm, injected into the vessels surrounding the mouse liver. After accumulation the SNR increases by about five times when compared with the particle-free control (fig.23). The overall size of the theranostic nanoparticle is therefore fundamental to guarantee the accumulation of SPIONs in the tumor.

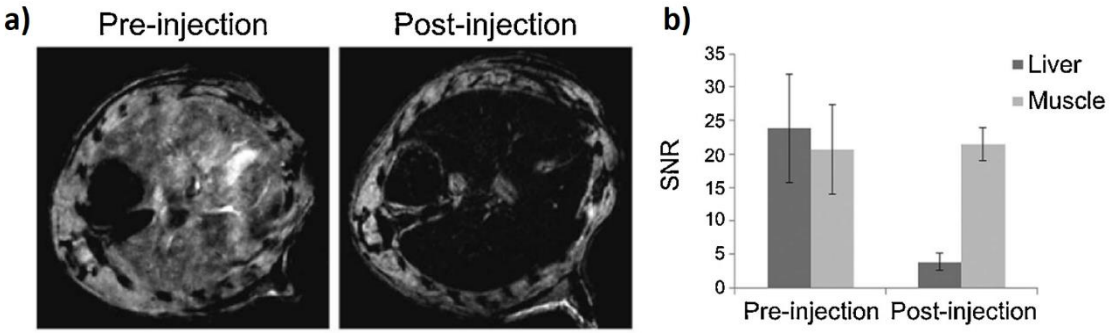

Fig. 23 a) In vivo MRI of the mouse liver before and 2 h after injection. b) Quantitation of the MRI signal intensity in the liver compared for pre and postinjection images (Revia and Zhang, 2016).

Surface charge has an important role in the biodistribution and cytotoxicity of nanoparticles. Neutral-charged particles have low interactions with plasma proteins, this leads to a prolonged circulation time, while a high surface charge (positive or negative) induces the process of phagocytosis and therefore less circulation time(Corot *et al.*, 2006).

The positively charged particles attract proteins and agents of the immune system, therefore they are quickly eliminated (within a few minutes) from the systemic

circulation, the strong negatively charged particles are absorbed by the hepatic clearance system (Reddy *et al.*, 2012), (Li *et al.*, 2015).

Naked SPIONs are generally negatively charged due to the presence of a limited number of hydroxyl groups on their surface. In the aqueous electrolyte solution, solid particles usually have a surface charge. This surface charge is usually used to improve their stability and prevent their aggregation in aqueous solution through electrostatic repulsion (Xiao *et al.*, 2011).

The functionalization of SPIONs by different polymers could introduce these groups loaded on the surface to increase their solubility in water. For example Mirsadeghi *et al.*, compared the net charge, zeta potential, of SPIONs coated with PEG and functionalized with amino (-NH2) and carboxylic (-COOH) groups. It is interesting to note that the particle has a negative charge if covered with only PEG (−4 ± 0.3 mV) or with carboxylic groups (−15.1 ± 1.4 mV), positive if it has exposed amino groups (23 ± 0.65 mV) (Fig.24 and Table 4).

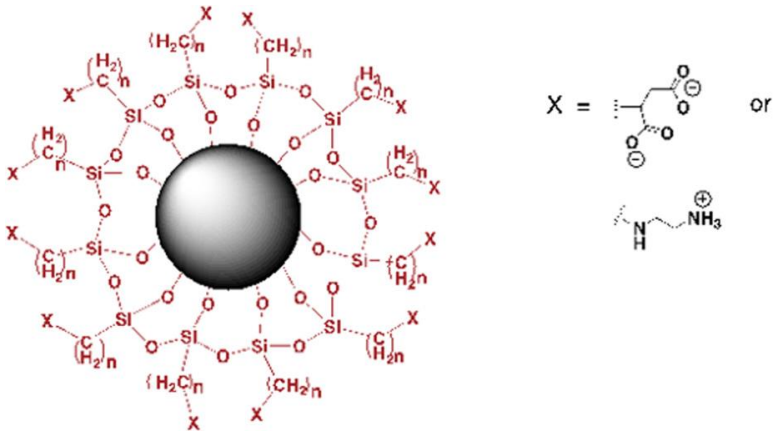

Fig. 24 Structure of the charged SPIONs. The amine and carboxyl functional groups are attached to the silica shell on the surface of the SPIONs (Javanbakht *et al.*, 2016).

Table 4 Description of the Various SPIONs in DI (deionized) Water.

Sample	Functional group	TEM size (nm)	D_H (nm)	ζ potential (mV)
SPIONs-PEG	plain	20	68.1 ± 0.2	−4 ± 0.3
SPIONs-PEG	COOH	20	49.5 ± 1.0	−15.1 ± 1.4
SPIONs-PEG	NH_2	20	88.0 ± 5.1	23 ± 0.65
Magnetic field-SPIONs-PEG	Plain	-	75.1 ± 3.6	−2.5 ± 0.5
Magnetic field-SPIONs-PEG	COOH	-	65.1 ± 0.5	−11.6 ± 2.4
Magnetic field-SPIONs-PEG	NH_2	-	111 ± 4.1	17.4 ± 2.5

The presence of a static magnetic field influences the charge of the particles respectively, reducing their absolute value.

The presence of charge on the SPIONs makes possible further functionalisations such as the Layer by Layer technique, thanks to the interactions with alternatively positively and negatively charged polyelectrolytes. In the next chapter we will investigate materials that can satisfy this stability, from polymers to coating polyelectrolytes.

2.1.3 Synthesis methods of SPIONs

Preparation methods have a direct effect on the properties of the magnetic particles: size, shape, crystallinity and magnetism confer specific characteristics for the functions the SPIONs must fulfil. Parameters such as temperature, pressure, pH and molar ratio play a major role in the development and production of MNP (Zarepour, Zarrabi and Khosravi, 2017). Some of the most common preparation methods with their advantages are briefly described below. It is appropriate to specify how common it is to find on the

market various types of monodisperse SPIONs useful for the development of nanotheranostic particles, therefore their production in the laboratory is not essential.

Copercipitation

SPIONs of Fe_3O_4 are synthesized from ferric chloride hexahydrate ($FeCl_3–6H_2O$) and ferrous chloride tetrahydrate ($FeCl_2–4H_2O$) as sources of iron and ammonia as a precipitator. It is a simple and common synthesis method. It has a high production yield and is used to produce nanoparticles with different sizes and shapes by regulating pH, ionic strength, temperature and other reaction conditions. However, it does have a limitation on controlling the particle size distribution (Laurent *et al.*, 2008), (Mornet, Portier and Duguet, 2005), (Laconte, Nitin and Bao, 2005).

Sol-Gel

This method is based on hydration and subsequent condensation of metal precursors, forming a colloidal solution of nanoparticles. Mulberry is obtained through further condensation and inorganic polymerization. Subsequently, through thermal treatments, the final crystalline structure is obtained. The main properties of the gel depend mainly on the reaction conditions and the structure of the sol phase. The magnetic particles thus formed have particularly homogeneous dimensions (Rahman and Padavettan, 2012), (Teja and Koh, 2009).

Microemulsion method

SPIONs are formed by two impermeable phases of oil and water in the presence of stabilizing agents, thus forming a monolayer at the interface between the immiscible phases. Water-in-Oil (W / O) and Oil-in-Water (O / W) are the two types of microemulsions formed to synthesize different types of nanoparticles. The hydrophilic

and hydrophobic coatings stabilize the particles, provide the necessary chemical reactions and control the chemical-physical parameters. The W / O microemulsion method is often used to form SPION, wherein the continuous oil phase stabilizing agents initially protect the droplets formed by iron oxide reagents, which then react to form SPION. The dimensions and shapes are controlled by changing the concentrations of the iron oxide precursor, surfactant and / or solvents. In literature, cetyltrimethylammonium bromide (CTAB) (Okoli *et al.*, 2011) has been used to customize the size of the SPION. Similarly, SPION with different sizes (6.5, 4.2 and 8.7 nm) were synthesized by varying the ratio between the concentrations of the iron oxide precursor and the base (1: 1 and 2: 1) (Chin and Yaacob, 2007). However, the removal of unreacted precursors, base and surfactants remains complex in this method.

Sonochemical method

Ultrasound can be used to produce SPIONs, the cavitation effect of the bubbles produced by ultrasound transforms the reagents into desired products at room temperature. Particle sizes and shapes can be controlled by varying reflux time, irradiation time and power. In 2015 Dolores *et al*. reported that the production of Fe3 + ions for the manufacture of iron oxide nanoparticles (using ethylene glycol as surfactant) it increased linearly with increasing reaction time at a particular ultrasonic frequency (581 kHz) compared to other frequencies (861 and 1141 kHz).

Microwave-assisted synthesis

The energy of microwave waves can be used in the synthesis of SPIONs in a short time and with low energy costs. Uniform heat is provided by microwaves inside the reaction vessels homogeneously in space. Thus stable crystalline iron oxide nanoparticles are synthesized. But these nanoparticles have a reduced surface reactivity (due to the low energy surface crystalline facets), which is evaluated on the basis of the interaction with the water and aggregate formation process (Pascu *et al.*, 2012). Interestingly, low surface reactive nanoparticles can improve the stability of SPION (Carenza *et al.*, 2014),

which is an advantage of this method. The magnetic properties of SPION can be controlled by changing the concentration of surfactants, the power of the microwaves and the reaction time.

Through these methods it is possible to synthesize SPIONs nanoparticles with comparable characteristics. Their characterization shows substantially (Fig.25-a) homogeneous dimensions <20 nm (Baykal *et al.*, 2015) and analysis by the Transmission Electron Microscope (TEM) (Fig.25-b). Specifically, it has been shown that the positive, negative or neutral surface charge of the particles does not influence its size.

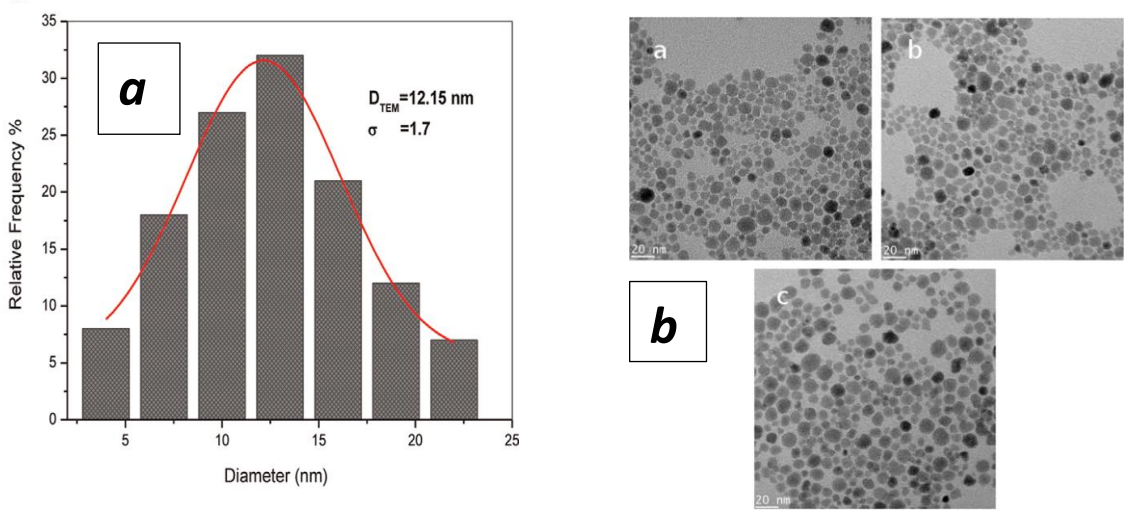

Fig. 25 Particle size distribution diagram of SPION-CFA and TEM images (Baykal *et al.*, 2015).

Ultimately, the presence of charged SPIONs, through Fourier transform infrared spectroscopy - Attenuated total reflectance (FTIR-ATR) technique, where Peaks at 635 cm^{-1}, 1000 cm^{-1} and the strong band at 1330 cm^{-1} are attributed to Fe-O stretching (Javanbakht *et al.*, 2016).

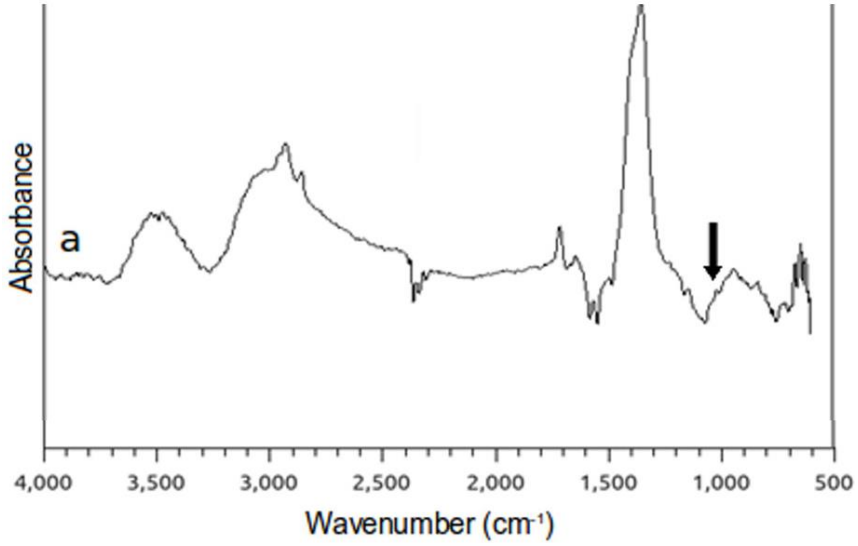

Fig. 26 FTIR spectra of bare SPIONs (Javanbakht *et al.*, 2016).

2.1.4 SPIONs Hyperthermia

Hyperthermia is defined as the treatment of the lesion through the use of localized heat. The choice of SPIONs has been weighted to allow cancer treatment by exploiting two deeply related strategies: drug release and heat therapy. Magnetic particles allow to control the heat exchange with the target tissue by reducing the side effects of heating on the surrounding healthy tissues, as the cancer cells show more sensitivity to damage from thermal induction than healthy ones (Jordan *et al.*, 2001), (Fig. 27).

Based on the amount of heat generated, there are two types of treatments: induction heating of cells between 41 and 46 ° C, which (hyperthermia) leading to DNA damage, protein denaturation and cell apoptosis, and thermal ablation (also called hyperthermia) which is performed at higher temperatures, up to 56 ° C, and results in necrosis, carbonization or coagulation of the target tissue (Deatsch and Evans, 2014), (Kumar and Mohammad, 2011). The heat produced is due to the relaxation processes and hysteresis losses of the magnetic particles when they are crossed by an external magnetic field. Specifically, single domain SPIONs transfer the energy acquired to align their magnetic moment with the external field applied when it is removed. In the relaxation phase the trapped energy is released in the form of heat (Kita *et al.*, 2010), (Kalber *et al.*, 2016).

The idea is therefore to accumulate particles in the tumor mass by exploiting active and passive targeting techniques, activating hyperthermia in the only area to be treated. (Fig.27).

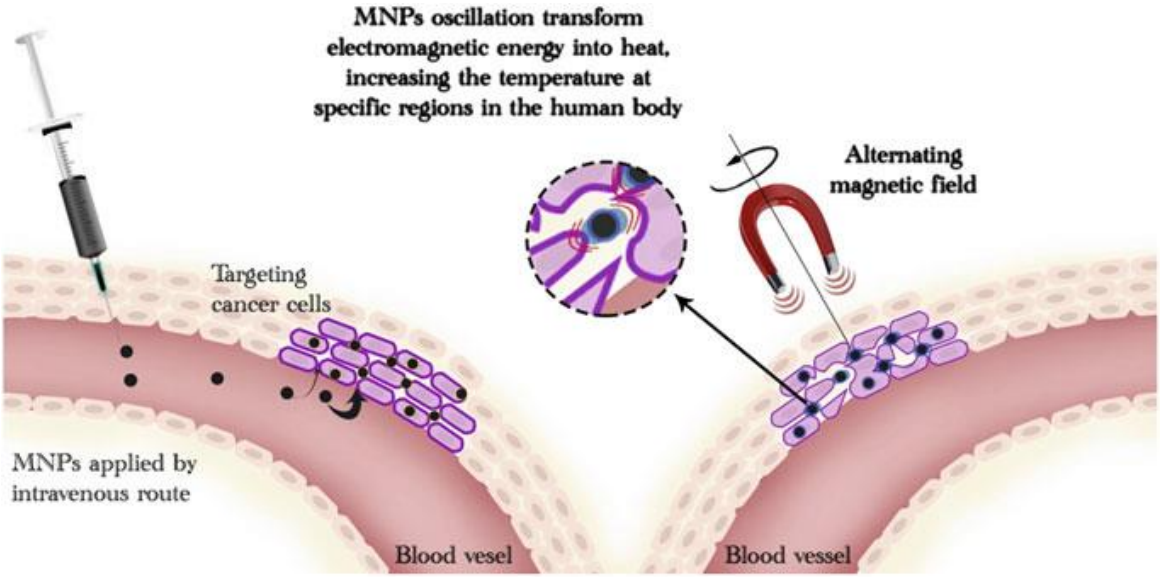

Fig. 27 Destruction of tumor tissue with magnetic hyperthermia (Rai and Jamil, 2019).

Although other thermal therapies are largely to be investigated, it is important to note how the net reduction of tumor volume *in vivo*, when this is treated with multiple instruments (Espinosa *et al.*, 2016).For example, in the figure 28 is shown a temperature difference of about 8°C compared to the physiological temperature, when hyperthermia is applied using only SPIONs, but duplicates (16 °C) if laser stimulation is also associated.

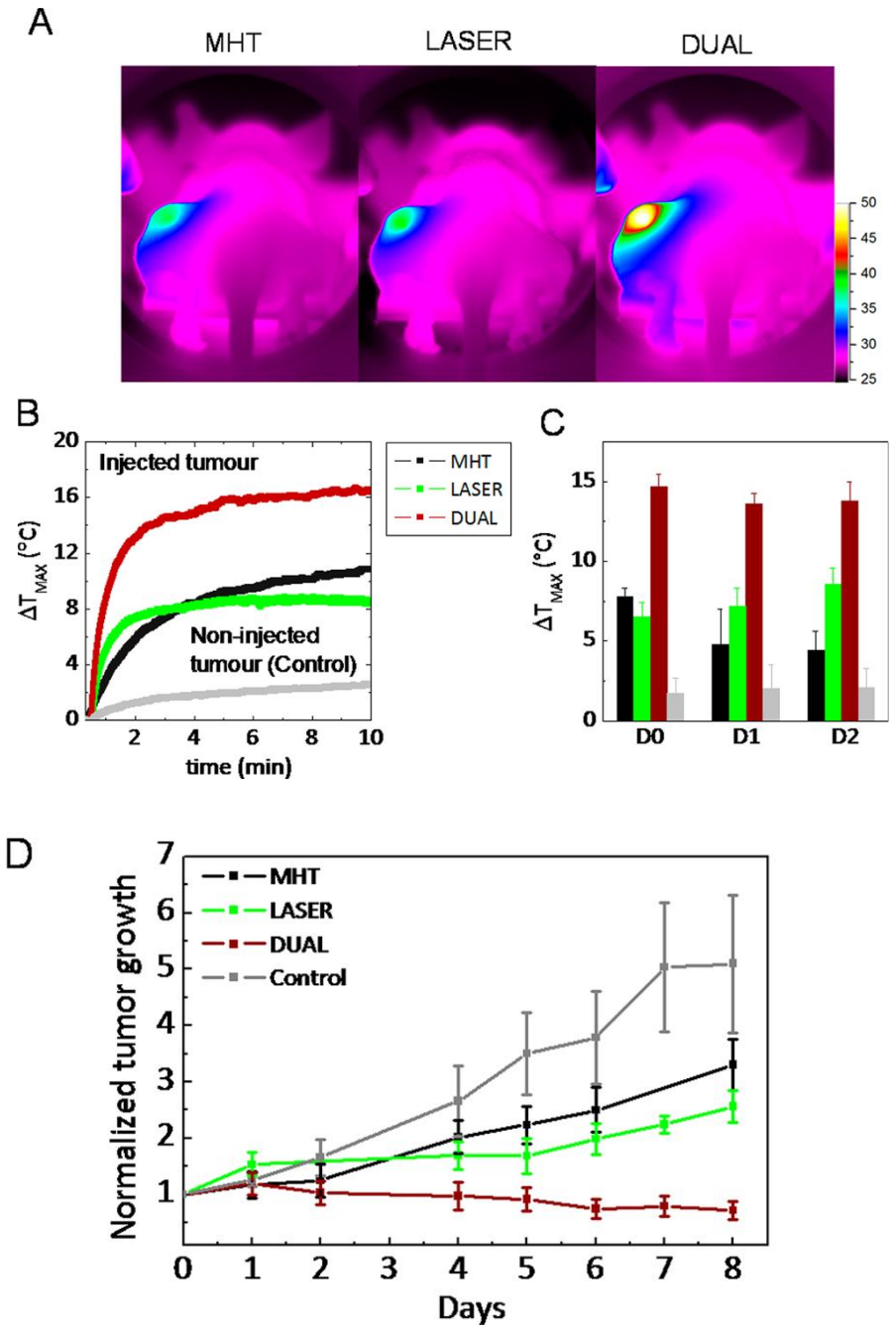

Fig. 28 In vivo heat therapy. (A) Thermal images obtained with the IR camera in mice, after intratumoral injection, after 10 min application of magnetic hyperthermia, NIR-laser irradiation or DUAL (both effects). (B) Corresponding thermal elevation curves for all treatments and for the noninjected tumor in the DUAL condition. (C) Average final temperature increase obtained after 10 min (MHT, LASER, and DUAL) on day 0 (1 h after injection) and 1 and 2 days after injection and for noninjected tumors. (D) Average tumor growth (groups of six tumors each in noninjected mice submitted to no treatment (Control) and in nanocube-injected mice exposed to MHT, LASER, and DUAL during the 8 days following the 3 days of treatment (Di Corato *et al.*, 2015).

Furthermore, the graph in figure 28-D shows the relative tumor growth in the different thermal applications. Although the performance of the best therapy is associated with the higher temperature gap, is important to note the reduced growth rate compared to the control using SPIONs in the hyperthermia production. On the other hand, high

temperature difference leads to indiscriminate tissue necrosis, while the purpose of this theranostic particle is to preserve healthy tissues. Sanz *et al.*, compared tumor cell death with hyperthermia produced by magnetic particles and exogenous instruments: an increase of 6 °C with MNPs obtains the same results as an increase of 15 °C with exogenous hyperthermia.

In a similar study (Di Corato *et al.*, 2015) treatment efficacy of hyperthermia induced by magnetic nanoparticles and photodynamic therapy (PDT) was evaluated . The temperature was monitored with an infrared thermocamera. (fig 29-b). The mouse tumor mass is heated from 31 °C to 40 °C for 30 minutes (D0), then the size of the tumor was assessed in the following days (fig 29-c).

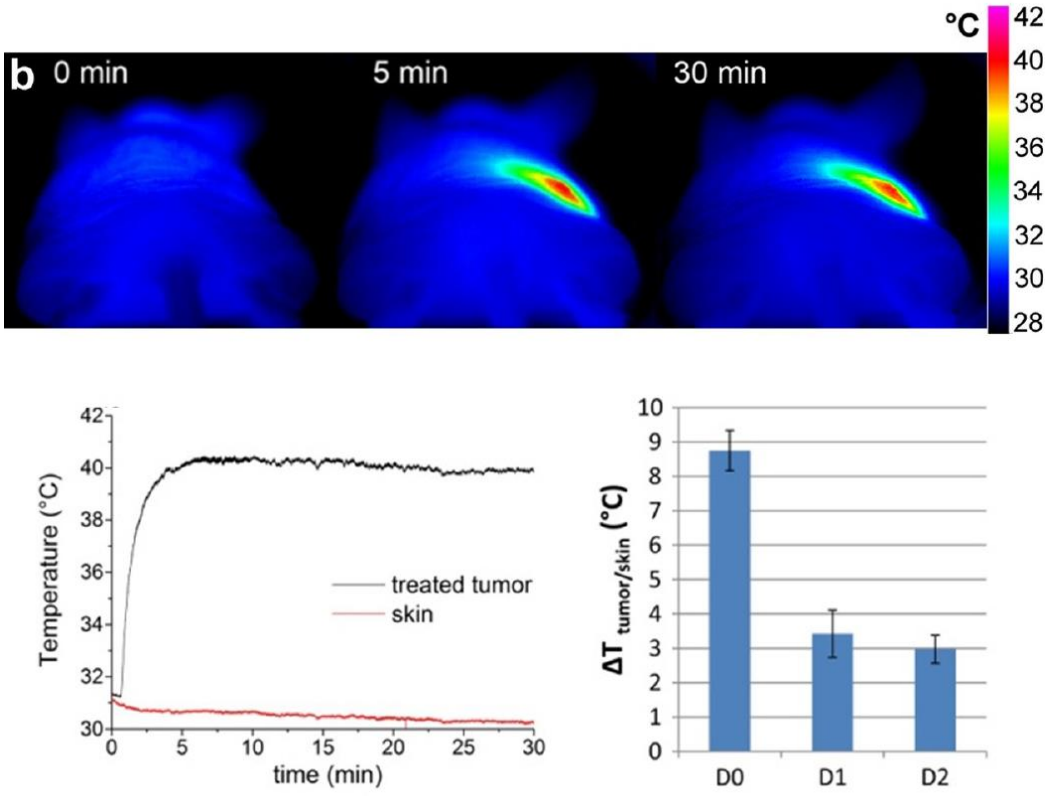

Fig. 29 (b) Increase in local temperature during magnetic hyperthermia treatment was monitored with an infrared thermocamera. The maximum temperature was reached about 5 min after field application and maintained for the entire treatment cycle (30 min) (Di Corato *et al.*, 2015).

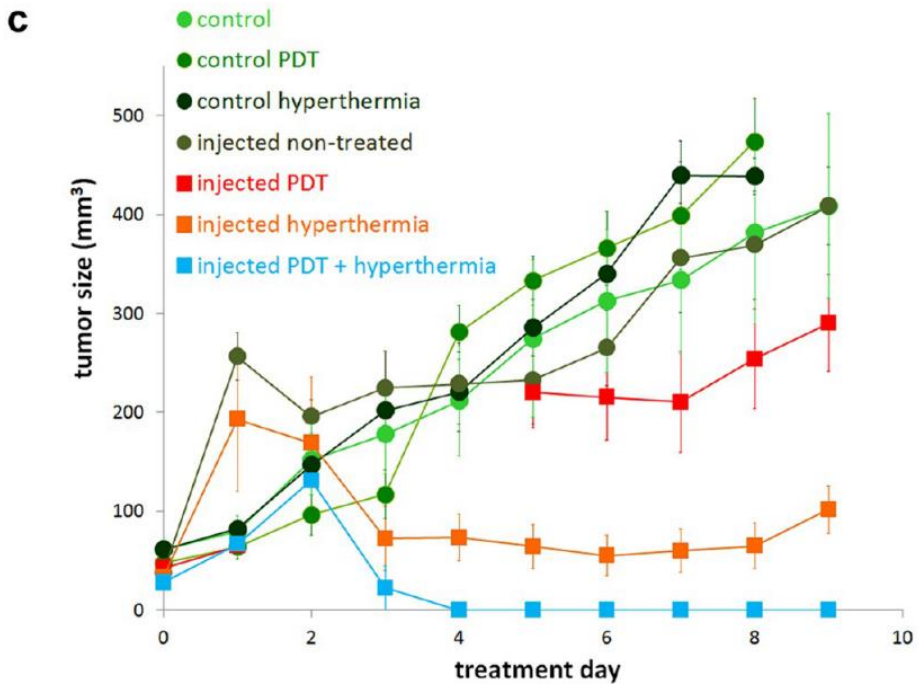

Fig. 30 (c) Tumor growth curves of different control groups and treatment groups. D0 on the graph corresponds to the day of liposome injection, which also corresponds to the first day of treatment (Di Corato *et al.*, 2015).

In this case, an increase in tumor size is noted, from 40-50 mm^3 on day zero to about 200 mm^3 on day one. Unlike the control that up to day eight quadruples the size, the mass treated with hyperthermia by MNPs return to the initial values of day zero. Compared to the previous case the absolute temperature is lower, it is therefore likely to think that the damage less induced.
For a greater therapeutic effect, it was therefore decided to associate the pharmacological one with the thermal therapy (Grillone *et al.*, 2015), proposing in the following chapter the strategies of encapsulation and release intended for the theranostic particle.

2.2 Multilayer nanocoating on the SPION-based core

2.2.1 Layer-by-Layer: definition and methods

Surface chemical modification is a very important element in order to improve the substrate optical, electrical and mechanical properties, as well as interactions with biomaterials, medical devices and the surrounding environment. The aim is to improve the performance of the device while preserving the integrity and health of the surrounding tissues (Richardson *et al.*, 2016). These materials actually have an electrolytic group which, following its dissociation in water, gives them a charge, positive or negative. In general, LbL uses a pre-charged substrate immersed in an opposite charge PE which is adsorbed on its surface forming a first layer. Subsequently washing is carried out in water to remove polymers or unwanted substances which can contaminate the subsequent phases. The material is then immersed in the solution of the second PE, creating the first double layer. The alternate washing and deposition procedure is repeated until it forms a construct consistent with the specific requests.

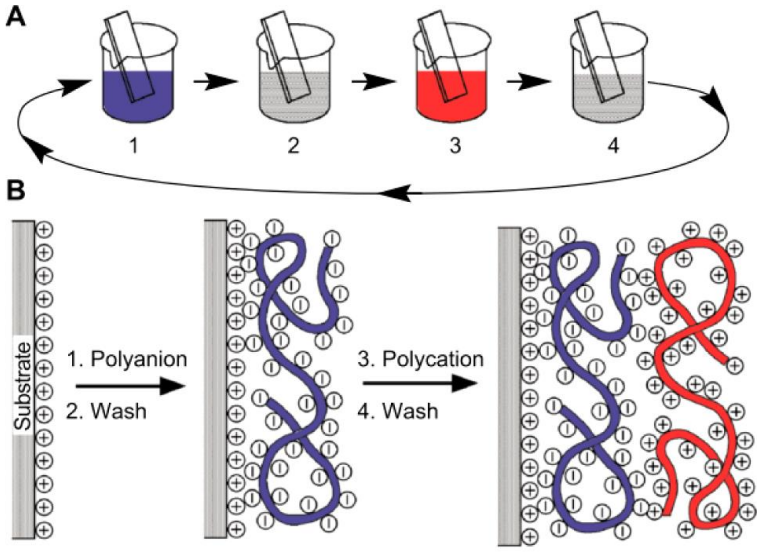

Fig. 31 Alternative deposition of oppositely charged polyelectrolytes on a pre charged substrate

Simplicity and versatility of this technique make it particularly exploited in sectors such as catalysis, optics, energy, membranes and biomedicine (Richardson, Björnmalm and

Caruso, 2015). The deposited layers have a nanometric scale controlled thickness, which guarantees the effectiveness of functionalization without significantly affecting the size of the substrate. Planar surfaces, curves, micro and nano-particles and fibers, are the substrates that can be coated with electrostatic LbL using various techniques. For example, Xiankai Li et al (Xiankai Li *et al.*, 2018) implemented elongated spider silk fibers, alternating deposition of positive Bovine Serum Albumin (BSA) and negative graphene sheets. A biomimetic study to create a movement and humidity sensor sensitive to small vibrations, capable of translating those mechanical stimuli into electrical signals. In another experiment Gai et al (Gai *et al.*, 2018) used a polystyrene substrate, modelled on a PDMS master as a sacrificial template on which to deposit polyelectrolytes with opposite charges forming a free-standing self-assembled polyelectrolyte multilayer (PEM) thin films.

There are several factors that influence the LbL deposition and therefore the final multilayer. For example Chai et al (Chai *et al.*, 2017) coated PLGA nanoparticles with alternating layers of chitosan and alginate, deposited by dissolving the sphere in PE solutions and washing through centrifugation cycles. They verified the amount of PE bound as a function of the adsorption time, showing that after 20 minutes the remaining alginate in the supernatant is less. They also studied the weight of the coating by varying the PE concentrations, the NaCl molarity and temperature, reporting that the multilayer growth increases with the polyelectrolytes and NaCl concentrations and that at physiological temperature the deposition is better than the lower temperature. The pH of the solution is an important parameter that influences the thickness of the layer, an increase or a decrease in the pH depending on the charge density of the polyelectrolytes, changes the ionization state of the polymers (Saqib and Aljundi, 2016).The versatility also extends to the type of materials deposited, with respect to the application: polymers, proteins, lipids, nucleic acids, nanoparticles can all be used as surface coatings.

Deng et al (Deng *et al.*, 2013) and his team implemented nanoparticles for cancer treatment with polystyrene cores and alternating the deposition of negatively charged siRNA and different polycations. Many combinations have been studied, in order to exploit the release of genes and drugs: polyethylenimine (PEI), chitosan, poly-β-amino-ester and poly-arginine have all been evaluated, finding with them the best charge

alternation (z-potential) with siRNA. The disadvantages of this classic method of repeated diving are long times and dependence on the operator: scaling the process and moving towards automated systems has been an important research topic in this decade (Richardson, Björnmalm and Caruso, 2015).These limitations have led research groups to find new tools that aim to produce multilayer nanofilms on surfaces of different shapes, but in a faster and more reproducible process. These methods can be summarized in four categories: Spin, Spray, Electromagnetic and Microfluidic layer by layer.

Spin LbL is a more recent approach that uses a complex rotating base and substrate, on which the polyelectrolyte sequence is injected (Fig.31), this allows a very rapid deposition of the film (Vozar *et al.*, 2009). The structure that the LbL spin allows to obtain is more organized than the traditional immersion coating process. This is explained by analyzing the different forces that determine the deposition of the layers: centrifugal, viscous and electrostatic. Indeed, the rapid removal of water from polyelectrolyte solutions allows for better chain organization and a smoother interface. Furthermore, the high speed allows a control of the thickness and the final surface morphology.

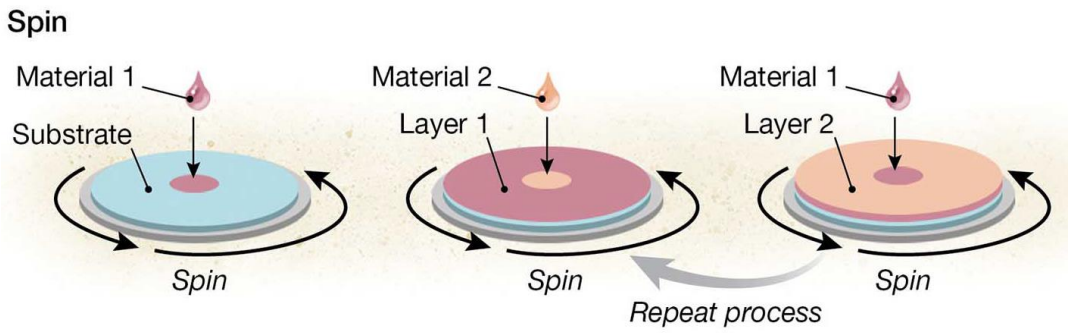

Fig. 32 Schematic illustration of Spin LbL technique (Richardson, Björnmalm and Caruso, 2015).

A new strategy for depositing oppositely charged PE on the substrate involves spraying the polyelectrolytes directly onto the surface, the washing phase is also carried out by spraying with deionized water (Fig.33). This technique is much faster than the first immersion method, it allows the deposition in few seconds compared to the necessary minutes of the immersion method (Dierendonck *et al.*, 2014), (Richardson, Björnmalm and Caruso, 2015).

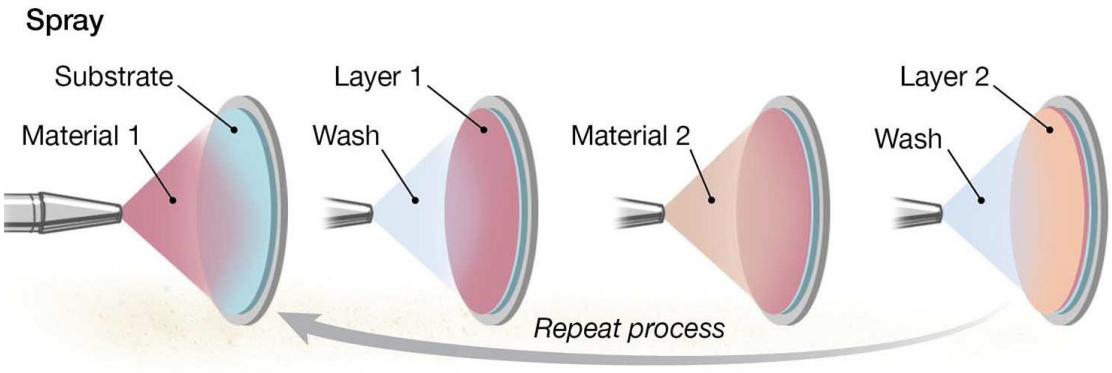

Fig. 33 Representation of spay LbL deposition (Richardson, Björnmalm and Caruso, 2015)

The results are very similar to those obtained with the most used classic LbL, which covers the surface homogeneously and it has been shown that even without washing it is possible to obtain well organized and regular multilayers, although the rinsing phase makes them thicker, probably due to of recombination of the polymer chains at the interface between the layers (Dierendonck *et al.*, 2014),(Richardson, Björnmalm and Caruso, 2015). Again Deng *et al.*, for example, used the spray technique to coat PLGA nanoparticles fixed on a planar polyester support film, depositing Hyaluronan and PLL. Each deposition step took 3 seconds, with 3 seconds of washing. The deposition of the film was confirmed thanks to the characterization tools, Atomic Force Microscopy (AFM) and Dynamic Light Scattering (DLS). These highlighted the maintenance of the spherical shapes of the particles with an increase in height of 5 nm. In addition, they observed that a conformal coating was made around the entire NP, even if one side of the particles was not accessible.

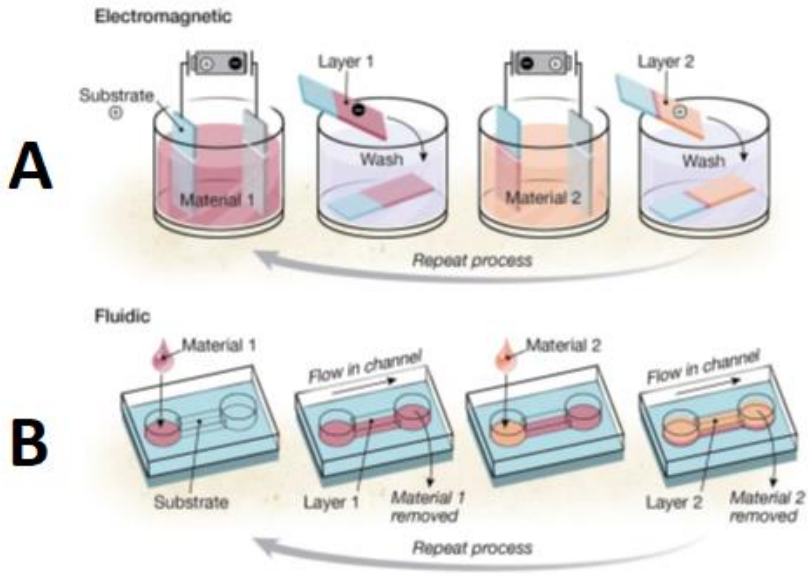

Fig. 34 Representation of the electrodeposition and microfluidic LbL (Xiao *et al.*, 2016).

Electromagnetic and fluidic LbL are two interesting techniques with regards to technologies and applications.

The coating mechanism adopted by the former is based on the application of an electric or magnetic field in an electrolytic cell, the force produced supports a charged polyelectrolyte which is deposited on the inversely charged electrode. This is known as electrodeposition (Xiao *et al.*, 2016), (Fig-33-A). As an immersive LbL, the electrodes are subsequently washed and introduced subsequent polyelectrolyte solution. Magnetic particles can also be used as building blocks (Richardson *et al.*, 2016).This feature may prove useful for the implementation of the existing particle. The fluid LbL complex on the other hand (Fig-33-B), is a method for coating different substrates with layers of nanometric dimensions and high productivity, but the equipment is expensive and difficult to manufacture. Vacuum or pressure are the two main methods of moving fluids into microfluidic tubes or devices, often produced "on chip".

Capillary forces are also used to move solutions, which are easy to implement given the absence of active devices (pumps), but does not allow dynamic control over deposition. It is an interesting method for coating surfaces placed in fluidic channels or for depositing multilayers on the walls of capillaries (Xiao *et al.*, 2016), (Richardson *et al.*,

2016). In addition to the applications just mentioned, microfluidic assembly has also been used in the manufacture of artificial cells, coating droplets containing biomolecules with lipids that should form the membrane (Elani, 2016).

2.2.2 LbL application in nanotheranostics

The LbL technique has been extensively studied in the biomedical field, but only recently has been developed in nanotheranostics, improving the stability of nanomaterials and the interaction with the organism at the nanometric scale. LbL is also exploited to provide active targeting and specific drug release to nanoparticles in a controlled manner (Poon *et al.*, 2011). These nano-platforms must be hidden from the immune system, which by recognizing them as foreign bodies, can trigger inflammatory or phagocytotic responses that would render therapy ineffective. Theranostic applications are diversified: Dreaden *et al.* have deposited poly-L-lysine (PLL) and hyaluronic acid (HA) on polystyrene nanoparticles, giving them targeting skills; in fact, hyaluronan and other GAGs selectively bind to cell-surface receptor CD44 overexpressed by cancer cells. By controlling the number of layers deposited, it is possible to modulate the amount of encapsulated drug and its subsequent release.

Research is focusing on the creation of controlled drug delivery systems, which allow a more specific therapeutic effect by avoiding the premature drugs release that can damage healthy tissues and, of course, decrease the amount of drug that reaches the tumor (Liu and Picart, 2016).

Literature reports also the use of LbL to incorporate growth factors (GF) on scaffolds, such as Bone Morphogenetic Protein 2 (BMP-2) with the aim of directing progenitor cells to create bone (Macdonald *et al.*, 2011). In fact, LbL allows to trap a greater quantity of biomolecules, prolonging release and therapeutic effect.

Thanks to the versatility of LbL technology, the substrates have different shapes and materials, and can be coated with various polyelectrolytes and blocks. Jia *et al.*, functionalized multiple-walled carbon nanotubes (MWCNT) via electrostatic LbL, with antisense oligodeoxynucleotides, in order to regulate the expression of some genes downwards. The cells internalization of system was examined under a confocal microscope: the device was found in the cytoplasm (without nucleic acid) and in the

nucleus (with nucleic acid). The suitability of LbL to release biomolecules for gene therapy has therefore been demonstrated in order to inhibit the proteins expression. LbL allows the creation of a shell sensitive to different stimuli: chemical, such as PH, solvents and electrochemical and physical, such as temperature, light and others. In fact, it is well known that the tumor environment has a slightly acidic pH (6.5), Dreaden *et al.*, compared to the rest of the body (7.4), therefore it is possible to exploit this variation by giving the drug release systems the ability to degrade when the pH drops, as mentioned in the previous chapter.

Similarly, this study proposes the use of different polyelectrolytes for the nanoparticle formulation. Various solutions have been found in the literature, many of which are redundant or complementary: Z-potential, Size, Cellular Uptake, Drug Encapsulation Efficiency (%), Drug Release and Treatment Specificity are among the values most considered for the choice of polycations and polyanions used in the LbL technique. Below (Table 5) the table summarizing the polyelectrolytes used in nanotheranostics, coupled with the anticancer drug (Santos *et al.*, 2018).

It should be specified that the drugs in the following table have been encapsulated by polyelectrolytes and actually form the nanoparticle core. In this case, instead, the choice was made to simplify the chemistry of the particle in order to make it more repeatable, also limiting the final size. For these reasons, the drugs are simply adsorbed between the polyelectrolytes layers.

Table 5 LbL-Coated Drug Nanocore-Based Nanoparticles and their main characteristics.

Polycation	Polyanion	Number of Bilayers	LbL-Coated Nanoparticles Particle Size (nm)	LbL-Coated Nanoparticles Zeta-Potential (mV)	Drug-Based Nanocore	Encapsulation Efficiency (%)	References
PAH, PS	PSS	2	107	-40	Curcumin	N/A	(Lvov *et al.*, 2011)
PAH	PSS	2	80	-50	Curcumin	80-90	(Zheng *et al.*, 2010)
PAH	PSS	3	150	+5	Dexamethasone	N/A	(Zahr, De Villiers and Pishko, 2005)
Chitosan	Alginate	2	336-354	-32/+36	Docetaxel	94-97	(Singh *et al.*, 2015)
Gelatin-A	PSS	2	265	+2	Lornoxicam	57	(Pandey *et al.*, 2015)
PAH, Chitosan	PSS, Alginate	2	211	-40	Paclitaxel	N/A	(Lvov *et al.*, 2011)
PAH	PSS	2	120	-40	Paclitaxel	N/A	(Agarwal *et al.*, 2008)
Chitosan	Dextran	2,5	110	-28	Paclitaxel	98	(Yu and Pishko, 2011)
PLL	PLA	1	127	26	Doxorubicin	18.7	(Lim *et al.*, 2017)

PLL	HA	1	135	-33	Not specified	N/A	(Dreaden *et al.*, 2014)
PEI, Chitosan, PLA	siRNA	2	142	-37	Not specified	N/A	(Deng *et al.*, 2013)
PAH	PSS	7,5	128	+33	Ibuprofen	72	(Santos *et al.*, 2015)

The necessary condition for the success of the surface coating of LbL is the existence of the surface charge, as shown in the previous section. Both bare and functionalized SPIONs with amino and carboxylic groups possess the surface charge which allows the deposition of polyelectrolytes. Furthermore, the presence of alternating layers has been shown to stabilize the loaded drug by preventing the formation of nanocrystals in a biological environment (Lvov *et al.*, 2011). In this way, the LbL shell performs a dual task in stabilizing the nanoparticles. The inner layers prevent recrystallization into larger particles, while the outer layers improve the colloidal stability attributed to the high hydrophilicity of polyelectrolytes (Shutava *et al.*, 2012). These multilayers of polyelectrolytes together provide a long colloidal stability to the nanoparticle system and chemical stability of the encapsulated drug, preventing its degradation.
As shown in the Table 4 polyelectrolyte pairs have been studied for different therapies, from anti-inflammatory ones (Ibuprofen and Dexamethasone), to anticancer ones (Paclitaxel and Doxorubicin). It is important to note that most of the particles have a limited number of layers and this aspect should be deeply analyzed, especially in the evaluation of pharmacokinetics. On the other hand, a high number of layers leads to final dimensions of the particle that are not suitable for the passive targeting conditions (EPR effect). All nano-platforms have diameters under 200 nm, except for the Chitosan / Alginate combination (Singh *et al.*, 2015). Among the most used synthetic polymers in literature we find Poly (allylamine hydrochloride) (PAH) and Poly (styrenesulfonate) (PSS), but also couplings between Poly-L-lysine (PLL), Polylactic Acid (PLA), Hyaluronan (HA) find space in many applications.

Again in this summary it is noted that the polyelectrolytes with the greatest encapsulation capacity of the drug are those composed of PAH and PSS (72 - 90%) (Santos *et al.*, 2015), (Zheng *et al.*, 2010) and Chitosan and Alginate (94-97%) (Pandey *et al.*, 2015).

The worst result sees the use of Polylysine (PLL) and Polylactic acid (PLA) (18%). This value could be increased by adopting different encapsulation strategies or by changing the drug. Nevertheless, for the proposed study, a drug loading value of around 50-55% or higher can be considered acceptable. Values that should be deeply evaluated in an experimental study.

These polyelectrolytes also show both a positive and negative surface charge described by zeta-potential, the possibility of expressing a positive charge as the last layer allows to better internalize the particles by exploiting the interaction with the negative charge expressed by the cells (Wang *et al.*, 2020). Finally, it was considered that the natural polymers, Chitosan and Alginate, could provide excellent biomimetic abilities, while PAH and PSS (synthetic polymers) highly biocompatible, are easily produced on a large scale. Therefore, PAH and PSS, Chitosan and Alginate have been conceived as potentially suitable for forming the layers of the proposed theranostic particle.

2.2.3 Natural and synthetic Polyelectrolytes

Inorganic particles can be superficially engineered to increase their physical, chemical and colloidal properties, reducing toxicity, as well as improving therapeutic efficacy .It is common practice in literature to encapsulate cores or drugs through functional deposition techniques, protecting the load from enzymatic degradation making the system more stable (Carregal-Romero *et al.*, 2015).

As mentioned previously, it was decided to investigate two pairs of polyelectrolytes: Chitosan and Alginate among natural polymers and PAH and PSS among biocompatible synthetic polymers. Here are some studies that are reflected in the choice of these PEs.

Natural polymers: Chitosan and Alginate

Chitosan, highly soluble and biocompatible agent, is applied for the surface coating. Furthermore, due to the presence of amino groups of β-(1-4)-linked D-glucosamine and N-acetyl D-glucosamine, it carries a slightly positive charge.

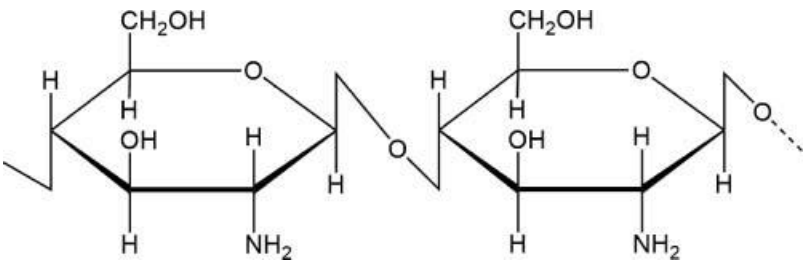

Fig. 35 Structure of Chitosan.

Chitosan together with Alginate showed to be a simple but effective solution for covering the surface of NPs. They reduce non-specific interactions but allow the grafting of targeting and functionalization molecules (PEG, FA) promoting specific targeting properties. For example Zhou *et al.*, created Polyelectrolyte multilayers (PEMs) composed of growing layers of Chitosan and Alginate deposited on poly(lactide-co-glycolide) (PLGA) nanoparticles. The alternating charge was verified (Fig.36) showing the effective stratification.

The charge values show a range between about -45 / + 5 mV between the first and third layers of Chitosan. Furthermore, the presence of folic acid (FA) and external PEG-FA did not particularly alter the overall NP charge, which settles at -5 mV.

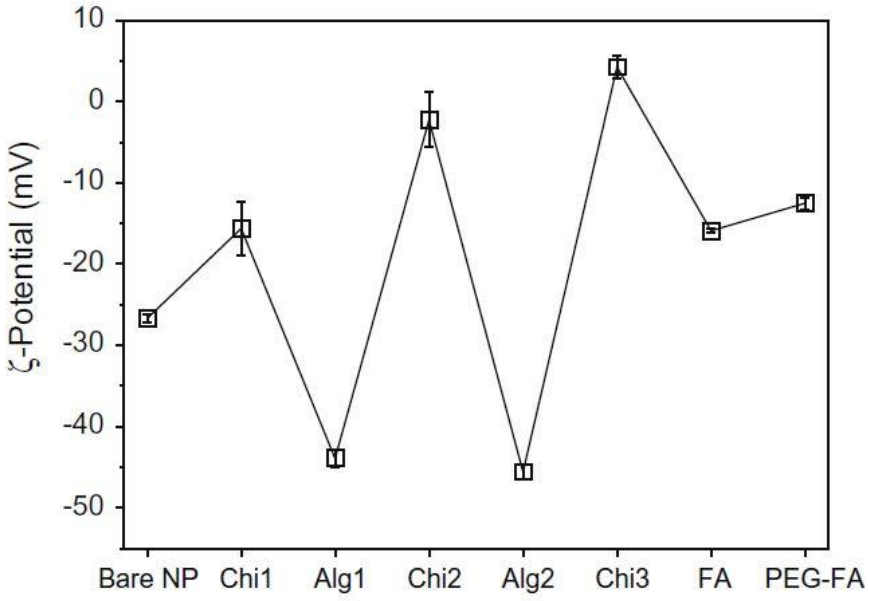

Fig. 36 Changes in f-potential during the assembly of alginate and chitosan on PLGA NPs (Zhou *et al.*, 2010).

Furthermore, the TEM image showed that the coating of NP PLGA with polyelectrolyte multilayers did not induce changes in the nanoparticles morphology and did not induce their aggregation. Cell uptake ratio was subsequently studied for the different combinations of layers. Fig.36 shows two types of absorption profiles; the first profile is highlighted by naked NPs, whose absorption value has increased rapidly in the first 1–2 hours reaching the highest value, 90%. For all engineered NPs, the cell uptake ratio increased continuously during the first 8 to remain constant subsequently.

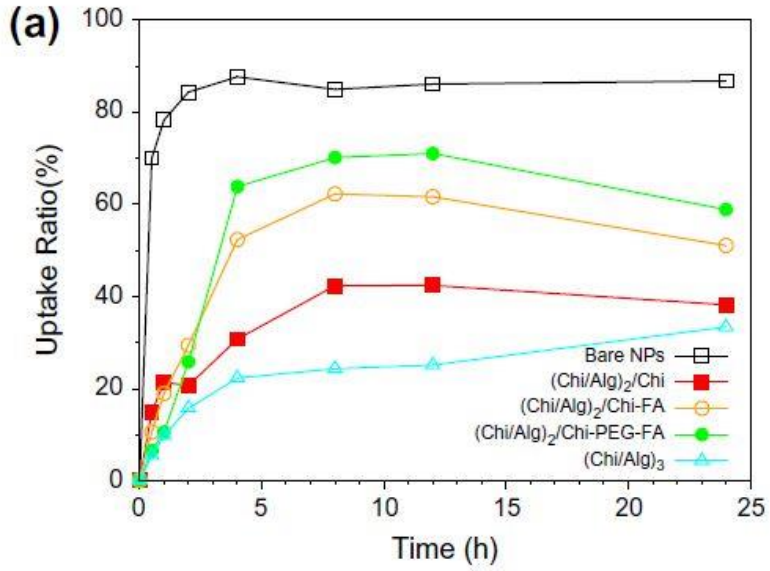

Fig. 37 Cell uptake ratio (Zhou *et al.*, 2010).

However, the absorption ratio has changed significantly with the nature of surface functionalization. The absorption ratios of $(Chi/Alg)_2$/Chi-FA $(Chi/Alg)_2$/Chi-PEG - FA were 10-20% higher than those of $(Chi/Alg)_2$/Chi and $(Chi/Alg)_3$ NP coated. This very important feature is presumed to be applied to the proposed particle design. Indeed, the deposition of Chitosan and Alginate does not seem to interact significantly with cells in vivo, and absorption can be promoted through the adhesion of specific targeting molecules.

Synthetic polymers: PSS – PAH

Synthetic polymers have obtained great consideration in the formulation for the therapeutic molecules, proteins and peptides delivery. These polymers have been shown to increase the pharmacokinetics and *in vivo* circulation times of incorporated therapeutic substances. Synthetic polymers often perform a passive function as drug carriers, but also be similarly functionalized as previously expressed for natural polymers (Hamid Akash, Rehman and Chen, 2015).

A preliminary study similar to our prerogatives has been found in the literature, on the encapsulation of ferromagnetic particles covered by layers of PSS and PAH (Choi *et al.*,

2015). The iron oxide particles were dispersed using charged polyelectrolytes by electrostatic interaction. The surface modified iron oxide particles coated with charged surfactants showed good stability in 24 hours compared to the oxide particles of bare NPs in aqueous solution. The NPs showed large distributions when coated with hydrophobic surfactants such as Sodium dodecyl sulfate (SDS) and PAH, while the Poly(acrylic acid) (PAA) and PSS coated particles showed a narrower distribution of particles. The surface deposition was promoted by exposing carboxylated groups and amino acids on magnetic particles, confirming the thesis of good versatility of the theranostic particle under study.

The surface charge (Fig.38) was also evaluated as a function of the stratified PEs, Habibi *et al.*, showed the possibility of creating alternation of PSS and PAH with charge electrostatic in line with the values shown in Table 5.

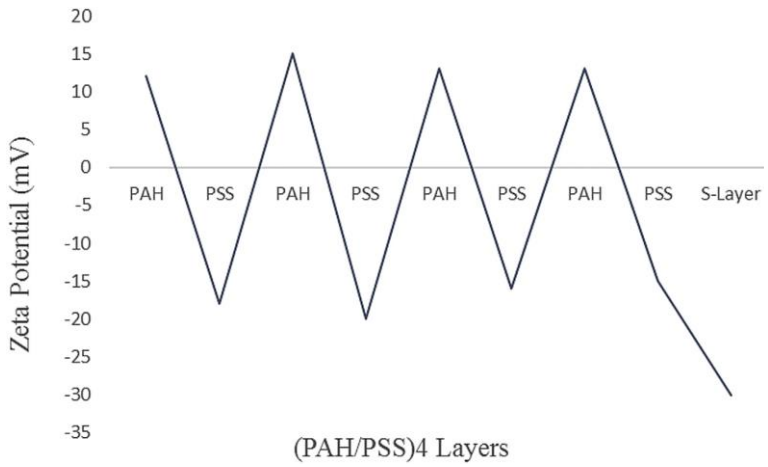

Fig. 38 Zeta potential analysis of LbL capsules fabrication (Habibi *et al.*, 2017).

Subsequently, it was decided to investigate the effects of these PEs at different concentrations, in terms of cytotoxicity by comparing two different cell lines. Naumov *et al.*, showed that the presence of $(PAH/PSS)_3PAH$ and $(PAH/PSS)_3$ did not lead to significant cell death of the Ehrlich carcinoma (derived from breast cancer) when compared to the control (Fig.39). Comparable values were obtained in the *in vitro* study in the Macrophages culture, in fact the presence of PEs does not induce significant fluctuations in the number of cells. PSS and PAH were therefore evaluated as largely

biocompatible and non-cytotoxic, exploitable for the LbL technique in the creation of the nanoparticle.

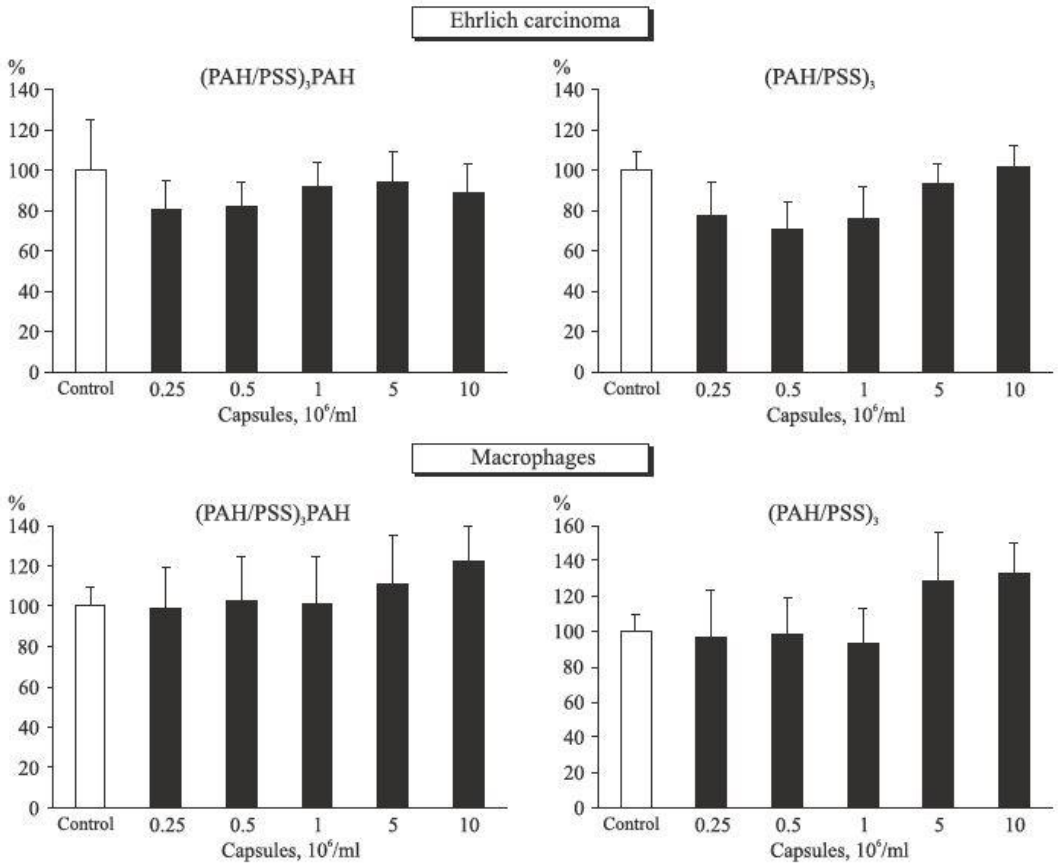

*Fig. 39 Effect of different concentrations of PAH and PSS on viability of Ehrlich ascites carcinoma cells and peritoneal macrophages. *p<0.05 in comparison with the control (pure cells)* (Naumov *et al.*, 2018).

2.2.4 Stealth strategy: PEG to avoid opsonization

Poly (ethylene glycol) (PEG) was first introduced in the 1990s to modify the surface of liposomes to improve their pharmacokinetics after intravenous administration. Hydrophilic and inert PEG provides a steric barrier on the particles surface and minimizes their interactions with proteins (phenomenon called *opsonization*). In fact, the binding of plasma proteins is the mechanism by which the Reticuloendothelial System (RES) recognizes the circulating nanoparticles, causing a substantial loss of the injected drug dose (> 50%) within a few hours after administration. Macrophages, like Kupffer cells in

the liver, recognize opsonized nanoparticles by engulfing, making them no longer available for *in situ* therapeutic effect. Liver, spleen and bone marrow are the main RES organs for the clearance of nanoparticles (Fig.40). Therefore, PEGylation technology has been used to improve the pharmacokinetics of a large variety of nanoparticles. PEG-covered NPs are often referred to as "stealth" nanoparticles because of their capability to escape the immune system surveillance better than non-PEGylated (Li and Huang, 2010).

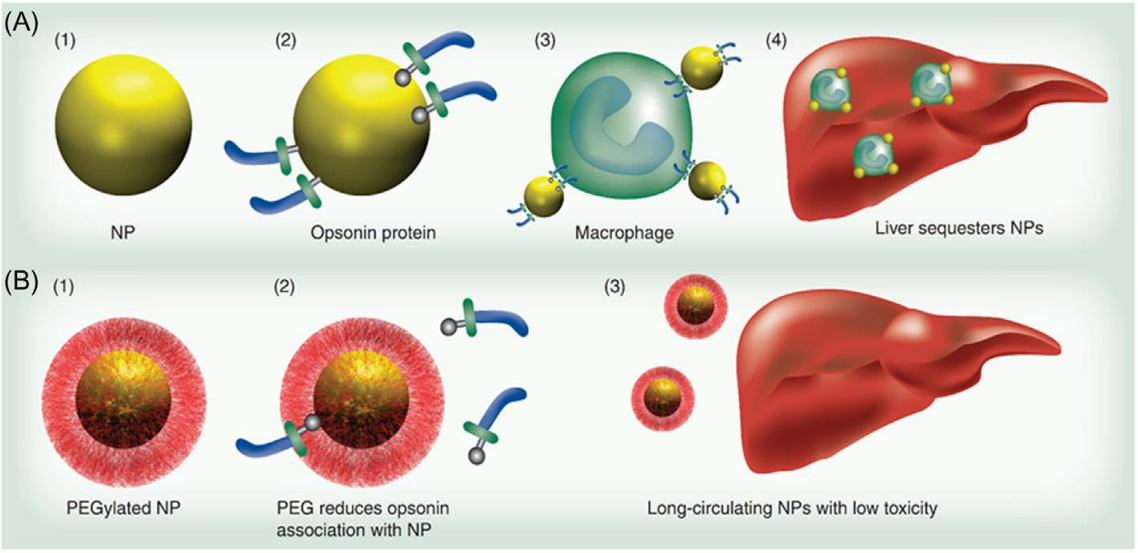

Fig. 40 Polyethylene glycol prevents uptake by the reticuloendothelial system. (A) Nanoparticles (NP) (A1) are coated with opsonin proteins (A2) and associate with macrophages (A3) for transit to the liver (A4). Macrophages stationary in the liver, known as Kupffer cells, also participate in nanoparticle scavenging. (B) Nanoparticles coated with PEG coating (B1) prevents this opsonization (B2), resulting in decreased liver accumulation (B3) and increased availability of the NP for imaging or therapy. NP: Nanoparticle; PEG: Polyethylene glycol (Hadjesfandiari and Parambath, 2018).

During the research several PEGylated particle strategies were found, with the aim of increasing the average circulation time and avoiding premature particles excretion.

Silva *et al.*, used two PEG chains with different polymerization degrees (N) (PEG350) and (PEG2000) to coat SPIONs. NPs proved to be non-toxic at a concentration of 100 µg/ml, furthermore the hydrophilic external functionalization discouraged the proteins adsorption by decreasing opsonization.

In another study (Liang *et al.*, 2016) compared the PEG stabilized SPIONs-Doxorubicin nanoparticles effects with simple free Doxorubicin (FD); the stability of NPs in blood environment is considerably greater for functionalized particles since first hours after injection (Fig.41). Therapeutic drug effects of were then studied, observing tumor

growth (Fig.42), in the first 24 hours the tumor treated with FD is three times larger than the mass treated with NPs, testifying the greater encapsulation drug ability of the PEGylated particles, therefore the greater release in situ by overcoming opsonization.

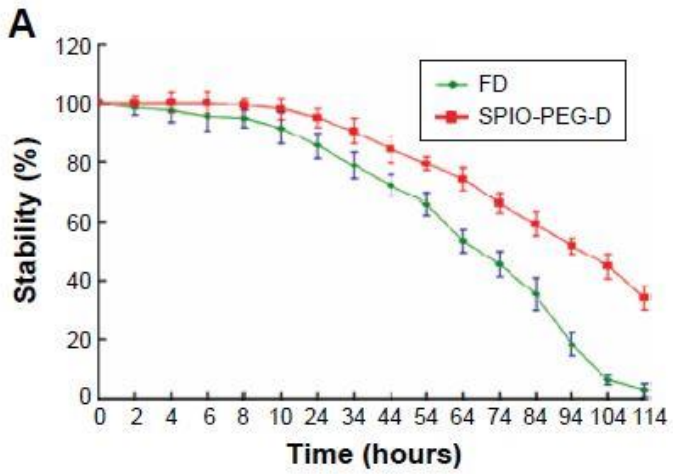

Fig. 41 Degradation curves of FD and SPIO-PEG-D over 114 hours (Liang *et al.*, 2016).

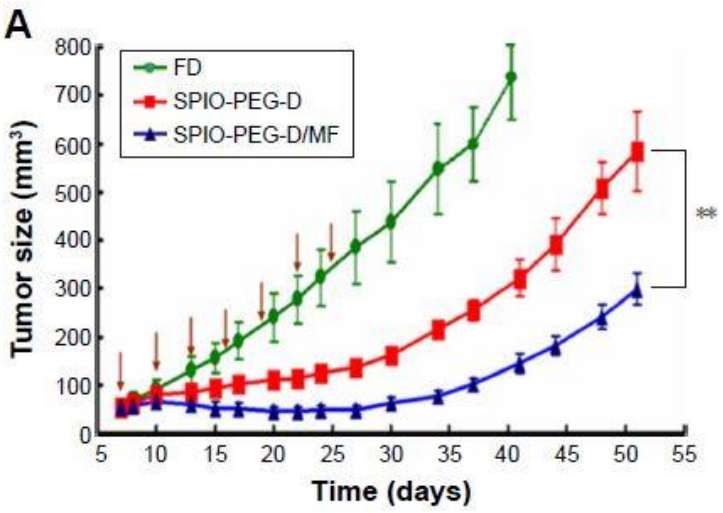

Fig. 42 Tumor growth inhibition, in vivo test (Liang *et al.*, 2016).

Substantially the investigated articles showed comparable results in terms of biocompatibility of the PEGylated particles, the following graph in Figure 43 shows that, on average, the particles with hydrophilic characteristics persist in the blood environment for much longer times if compared with naked NPs (Perry *et al.*, 2012).

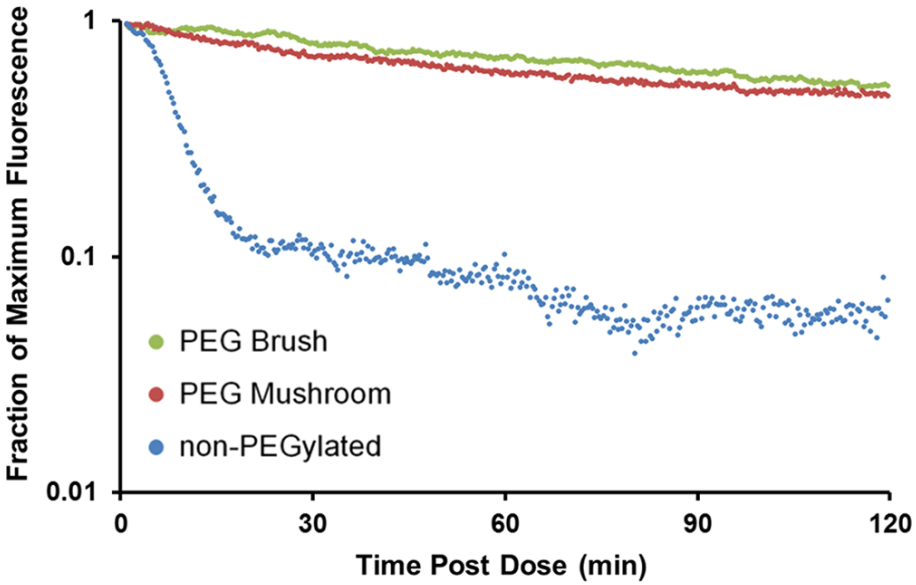

Fig. 43 Intravital microscopy circulation profiles based on fraction of maximum fluorescence remaining for non-PEGylated, PEG mushroom, and PEG brush nanoparticles. (Perry *et al.*, 2012).

However, other solutions for implementing anti-opsonization strategies have been found: polymers, biomolecules or phospholipid chains with biomimetic characteristics capable of increasing circulation time.

For example Poly(2-alkyl-2-oxazoline)s (POXs) are non-ionic polymers with polypeptide isomeric structures, their properties such as molecular weight, solubility, architecture and terminal functional groups can be optimized for applications and make them a promising alternative for PEG (Sedlacek *et al.*, 2012).

Polyvinylpyrrolidone (PVP) used in cosmetics could be a future candidate for the stealth strategy thanks to its approved biocompatibility and hydratability (Lee *et al.*, 2006). Still, Polyacrylamides has been shown to strongly decrease the surface adsorption of proteins increasing the average life of the coated nanoparticles. Furthermore, the presence of hydroxyl group promotes subsequent functionalisation (Sun *et al.*, 2006).

The materials mentioned above still need to be extensively studied, for this reason PEG and its functionalisation have been chosen for the nanoparticle design.

2.2.5 Active Targeting

The term "active targeting" defines the specific interaction between receptor expressed by the cell and the targeting ligand present on the theranostic platform with or without the use of cross-linking agents in the target site, exploiting different direct or indirect strategies.

These target molecules have a specific affinity for cell surface antigens (Receptors) and can discriminate between normal and tumor cells based on the receptor or antigen expression levels (Siegler, Kim and Wang, 2016). For example, using Herceptin targeted NPs helped to differentiate human epidermal growth factor receptor 2 (EGFR), human epidermal receptor-2 (HER2) positive and (HER2) negative breast cancer cells. Clearly, active targeting of HER2 receptors on cells overexpressed with NPs has been studied and confirmed (Vieira and Gamarra, 2016).

Unfortunately, the drug delivery system with active targeting has many uncertainties and limitations, in fact it is difficult to predict the effectiveness of the targeting molecule, its degradation and opsonization. Very poor penetration into the tumor site, the NPs complexity, and a lack of familiarity with the physiological and biological tumor structure, are variables that are highly regarded, as they can be the cause of early failure of the targeting strategy. However, this treatment has the main advantages of using targeted vascular NPs that can be used to treat or protect problems in the target drug release system (Riehemann *et al.*, 2009).

An interesting study conducted by Srinivasan *et al.*, investigated the internalization of PLGA nanoparticles loaded with doxorubicin (DOX) and functionalized with Human Epithelial Receptor-2 (HER-2). HER-2 antigen is an overexpressed molecule in many tumor phenotypes (colorectal, breast and ovarian cancer) and could be exploited as a targeting molecule. In the study just mentioned, in fact, the release of the drug (DOX) of the functionalized particles called AIDNPs was compared with the non-functionalized nanoparticles (IDNPs) and the free drug. The three platforms have been tested on three

different tumor phenotypes (SKOV-3, MES-SA, MES-SA / Dx5) among which only SKOV-3 has HER-2 overexpression (Fig.44). It can be seen that the amount of DOX released by AIDNPs has higher value in SKOV-3 cells (80%), while the other cell/control couplings reach lower values between 45 and 55%.

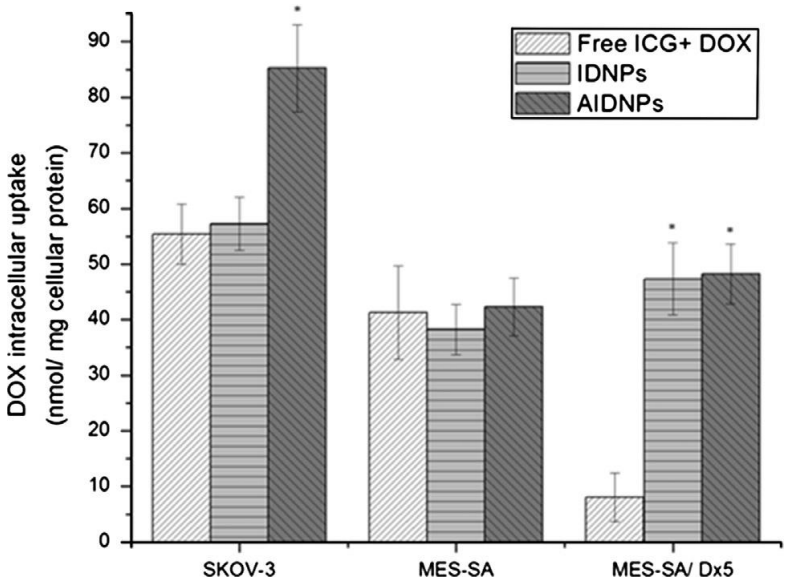

*Fig. 44 24 h intracellular DOX uptake data in SKOV-3, MES-SA, and Dx5 cells, n = 3 experiments, 3 wells per treatment. *P < 0.05 (by ANOVA) between free drug and NPs formulation for each cell line, indicating significant differences due to loading of DOX into PLGA NPs* (Srinivasan *et al.*, 2014).

More specific research was conducted by Wang *et al.*, on the treatment of lung carcinoma. The specific antibody was anti-EGFR, grafted onto PEG-SPIONs NPs. Initially the authors verified the NPs in vitro non-cytotoxicity, and subsequently applied localized thermal therapy with the parameters shown in the Table 6.

Table 6 Power, treatment time, and peak temperature of the four groups.

Groups/parameter	Negative control	Positive control	PEG-SPION	Anti-EGFR-PEG-SPIO
Power(W)	53.8 ± 2.8	75.8 ± 2.9	54.3 ± 2.5	32.0 ± 2.7
Treatment time(s)	24.2 ± 1.1	23.2 ± 1.2	24.0 ± 1.2	24.2 ± 1.0
Temperature(°C)	52.1 ± 1.8	72.4 ± 3.4	74.1 ± 2.9	75.2 ± 3.0

It must be said that such high powers and temperatures (54.3 W and 75.2 ^{o}C) are not applicable *in vivo* but provide an indicative figure for the feasibility of the platform.

The tumor size was assessed after the *in situ* NPs sedimentation (Fig.45) which shows a sharp decrease in the tumor volume when compared to the negative control. On the other hand, however, there are no substantial differences with the simple passive targeting therapy, this suggests that the power and temperature values used have produced tumor necrosis even with reduced quantities of NPs.

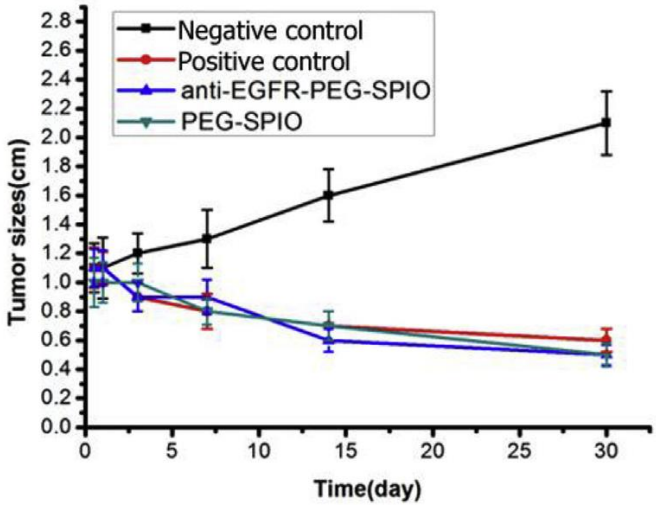

Fig. 45 tumor size change images before and after MRgFUS ablation of negative control (low power), positive control, PEGylated SPIO, and anti-EGFR-PEG-SPIO (Wang *et al.*, 2017).

Due to the low molecular weight, the relatively simple biochemical structure and the high tumor specificity, biotin has attracted great attention in the search for new active strategies for the release of drugs. To survive and multiply rapidly, cancer cells need more biotin than normal cells. Rapidly proliferating malignant cells overexpress biotin to compensate the body biotin. Biotin overexpression is observed in large types of tumors, including renal, lung, ovarian, astrocytoma and breast cancer cell lines (Shi *et al.*, 2014). This specific interaction of biotin and its receptors has been explored to develop various biotin-conjugated nanocarriers to increase the absorption of anticancer drugs by various cancer cells.

A different presented by Rompicharla *et al.*, which used 3D cultures of lung cancer tumor spheroids and poly(amidoamine) (PAMAM) dendrimers of generation 4 (G4) to deliver paclitaxel (PTX), NPs was coated with PEG and functionalized with biotin. Biotinylation of G4-PTX-PEG conjugate was performed by activating the carboxy group of biotin molecule using EDC/NHS activation. As seen in Figure 46-A, the therapeutic effect essentially due to the presence of Paclitaxel: all four tests in fact show regression of the tumor diameter. It is also interesting to note that the particles covered with PEG alone show better performances than the simple drug, proof of the greater biomimetic feture in the internalization phase of the hydrophilic polymer. The figure in Figure 46-B, detail shows that the greatest internalisation of the drug occurred by exploiting the biotin overexpression, tumor diameter remains approximately unchanged at a value of 500 μm.

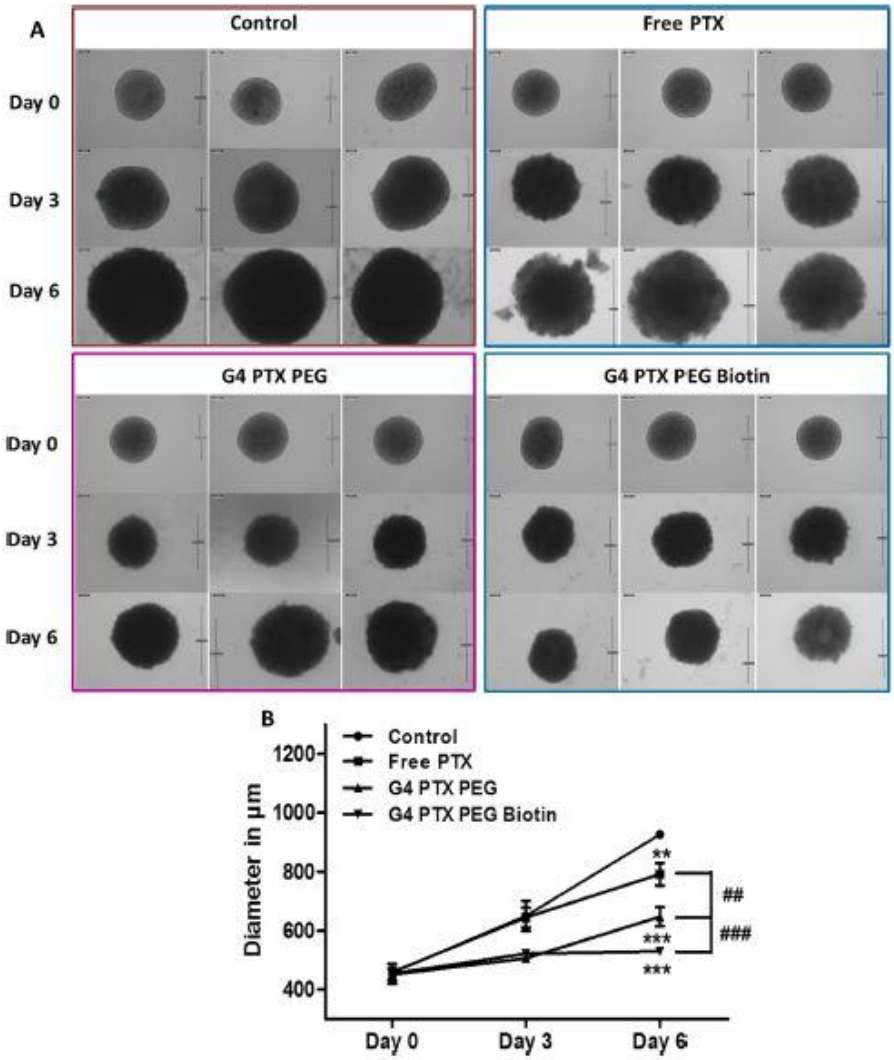

Fig. 46 (A) Brightfield images of tumor spheroids after different PTX treatments at the end of Day 0, Day 3, and Day 6 using bright field microscope. Magnification: 10X. (B) Line graph of spheroid diameters depicting growth inhibition. Data is represented as Mean of diameter in µm with SD; n=3 (Rompicharla *et al.*, 2019).

Finally, the use of HA for biomedical applications such as targeted drugs delivery through the receptor overexpression, CD44, has found great confirmation. PEGylated MNPs were synthesized and functionalized with HA to prolong the NPs circulation time.

Field Emission Scanning Electron Microscopy (FESEM) and the DLS have confirmed that the size of the synthesized nanoparticles is appropriate for targeted drugs delivery, about 200 nm. The MTX release from HA-MNP has been largely inhibited by starch bonds and the Fe_3O_4-DPA-PEG-HA-MTX NPs have been shown to be stable in physiological conditions even for 8 days, while protease enzymes and acidic conditions could accelerate the release amount of MTX. All experimental and computational methods

revealed that Fe_3O_4-DPA-PEG-HA-MTX NPs can bind to the receptor binding site and internalize into cancer cells, thus showing a significant impact on CD44 positive cell lines.

In light of what is reported in the literature, the possible strategies and target molecules to be applied in active targeting are manifold. Each tumor phenotype could overexpress unique ligands and different from patient to patient, therefore a more targeted and personalized approach would be needed for each individual case. The active technique is still very recent and will need to be investigated further. The proposed ligands are mostly indicative and have the purpose of showing how by grabbing different ligands it is possible to selectively target drug therapy in specific areas to be treated.

2.2.6 Drugs: Docetaxel and Paclitaxel

Paclitaxel and Docetaxel are chemotherapeutic agents belonging to the taxane class, which bind and stabilize the microtubules, causing the cell cycle arrest, the inhibition of mitosis and therefore apoptosis (Ganansia-Leymarie *et al.*, 2003). Taxanes have different action mechanism if compared to other anticancer drugs, ie the microtubules hyperstabilization (Fig.47). Structurally, docetaxel differs from paclitaxel both in the 3 'position on the side chain and in the 10' position on the baccatin ring (Fig.48). Their steric conformation inhibits the cytoplasmic tubulin polymerization by binding to the tubulin dimers. Taxanes target the subunit of tubulin heterodimer, the key component of cellular microtubules, critical in cell mitosis (Miller and Ojima, 2001). Although the action of paclitaxel and Docetaxel anticancer activity are comparable, but key differences exist. For example, docetaxel shows activity in patients with paclitaxel-resistant metastatic solid tumors (Verschraegen *et al.*, 2000).

Docetaxel was first approved in 1996 (followed by Paclitaxel) for the metastatic anthracycline-resistant breast cancer treatment 8-10, and subsequently for platinum refractory stage IIIB or IV lung cancer. Combined with corticosteroids it can increase survival in metastatic prostate cancer. In addition, docetaxel has been approved as an adjuvant therapy in patients with high-risk early breast cancer (Martin *et al.*, 2005).

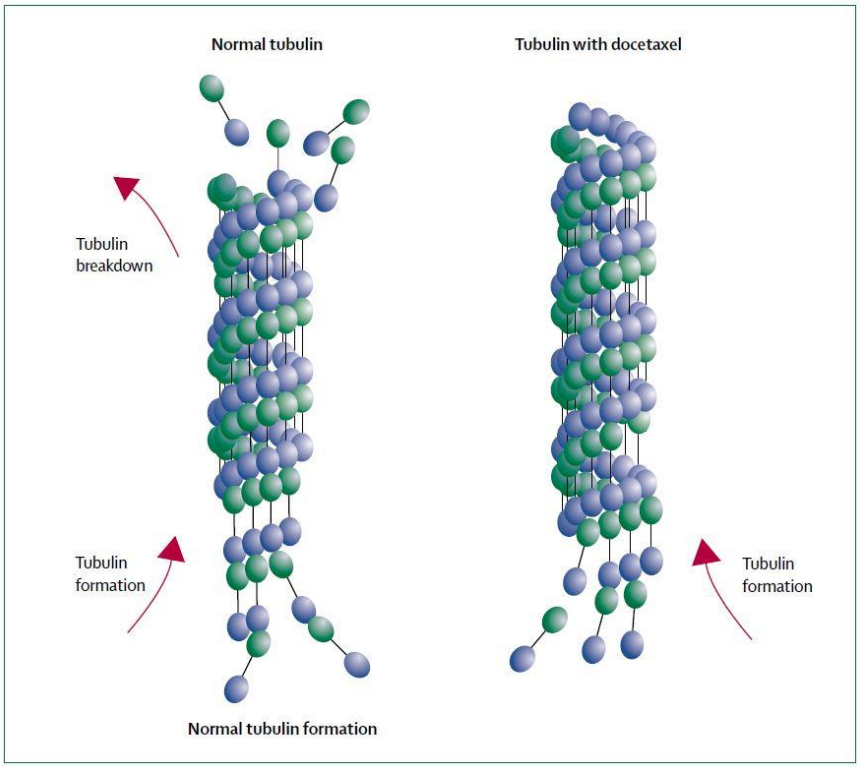

Fig. 47 Effect of docetaxel on microtubule function (Montero *et al.*, 2005).

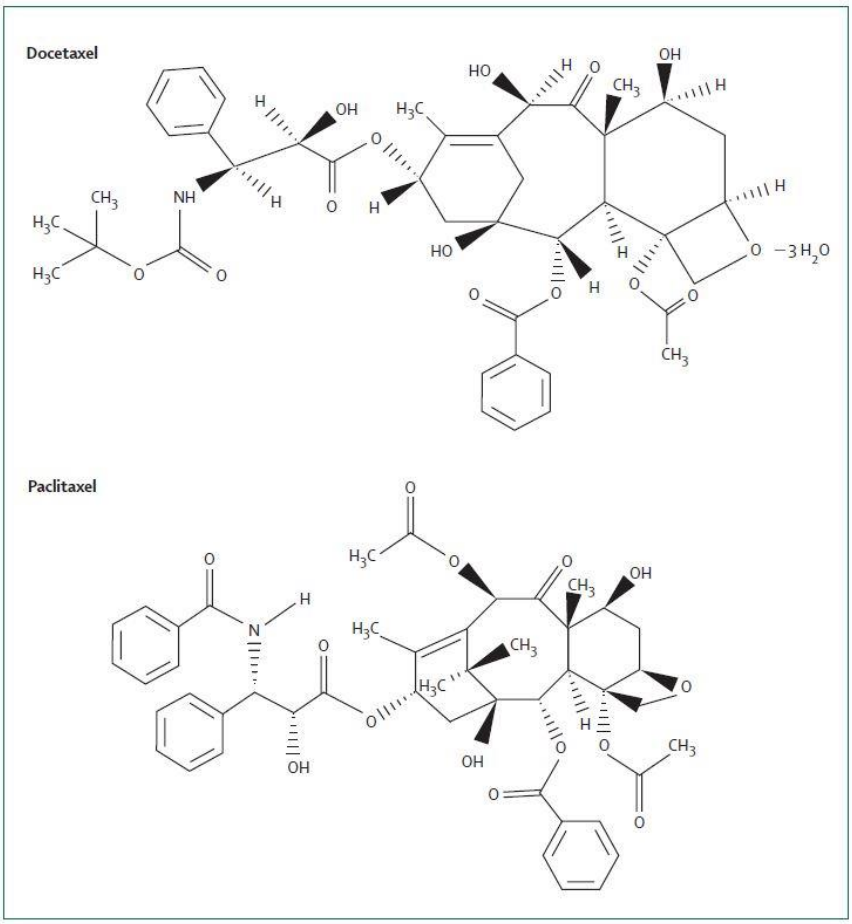

Fig. 48 Chemical structure of docetaxel and paclitaxel (Montero *et al.*, 2005).

Many different anticancer drugs have been implemented and many others are in development. Docetaxel and Paclitaxel have been chosen as drugs due to their versatility and broad range of efficacy in different types of cancer. The main purpose is to verify the presence in literature, of SPIONs based systems that have found positive *in vitro and in vivo* results. For this reason, the following example table is presented, with the aim of showing the potential applications of the drugs mentioned in more or less complex systems.

First, study 6 (Dadras *et al.*, 2017) showed that the surface charge of the SPIONs-PLGA nanoparticles does not change substantially when loaded with different concentrations of Docetaxel-Silane (from - 22.3 ± 1.1 at 28.6 ± 2.4 mV) suggesting the possibility to deposit by DTX simple adsorption on polyelectrolytes without altering their surface charge. Similar values are shown in study 9 (Lugert *et al.*, 2019) where at pH 4, surface

charge was 21.7 ± 1.9 / 23.0 ± 0.6 mV with and without incorporated Paclitaxel respectively.

Table 7 Examples of SPIONs based nanoparticles loaded with Docetaxel and Paclitaxel.

N°	Drug	Platform	Tumor-cell line	Reference
1	Docetaxel	PLGA-PEG-HER2 NPs	*In vitro* Lung cancer	(Koopaei *et al.*, 2011)
2	Docetaxel	PLA and PLGA-PEG NPs	N.R	(Rafiei and Haddadi, 2017)
3	Docetaxel	SPIONs-PSMA NPs	*In vivo* prostate cancer	(Nagesh *et al.*, 2016)
4	Docetaxel	PEO-PCL micelles	*In vitro* Prostate cancer Breast cancer	(Ostacolo *et al.*, 2010)
5	Docetaxel	SPIONs-CHI-FA SPIONs-PLGA-FA NPs	*In vitro* HeLa cells	(Shanavas *et al.*, 2017)
6	Docetaxel	SPIONs-PLGA NPs	*In vitro* Breast cancer (MCF-7 SKOV-3)	(Dadras *et al.*, 2017)
7	Paclitaxel	Cyclodextrin-SPION nano-assembly	*In vivo* Colon cancer cells (CT26) Breast carcinoma cells (MCF-7)	(Jeon *et al.*, 2016)
8	Paclitaxel	SPIONs-Palmitoyl-Chitosan NPs	*In vitro* Breast cancer (MCF-7)	(Mansouri *et al.*, 2017)
9	Paclitaxel	SPIONs-LA-HSA NPs	*In vitro* Human breast cancer cell lines	(Lugert *et al.*, 2019)
10	Paclitaxel	SPION-co-loaded PEG-PE NPs	*In vitro* Breast cancer (AT1) Melanoma (B16F10)	(Upponi *et al.*, 2018)
11	Paclitaxel	SPIONs-loaded micelles	*In vitro* Hepatocellular carcinoma (Bel-7402)	(Xiao *et al.*, 2020)

The variation of Paclitaxel release was instead assessed in article 11 (Xiao *et al.*, 2020), in fact at acid pH (Fig.49) the protonation of all diiminopyridine (DIP) group caused disassembly of the polymeric micelles allowing the realization of a pH-responsive NP.

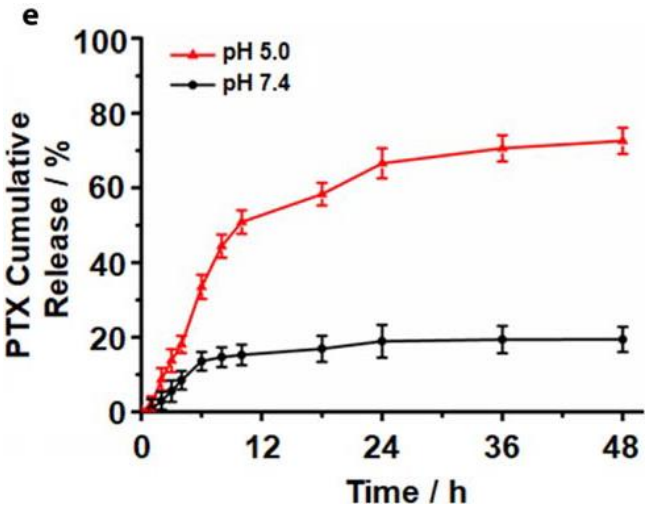

Fig. 49 PTX cumulative release of SPIONs / PTXPDPL micelles at pH 7.4 and 5.0 (Xiao *et al.*, 2020).

Finally two important considerations have been shown by studies 7 and 10. Figure 50 A-B *(Jeon* et al*., 2016)* shows the specific effect of Paclitaxel, tumor growth is substantially inhibited by the presence of the drug alone, while the particles of SPION and cyclodextrin show a trend of the tumor volume more similar to the control in PBS.

The staining in Figure 51 shows the section of two different tumor phenotypes, Breast (4T1) and melanoma (B16F10), after 48 h and treated with SPIONs covered by micelles, Paclitaxel as released drug (Upponi *et al.*, 2018). The simple micelles did not induce damage to the culture, maintaining an onset of apoptosis is visible in the second sample of PTX micelles. The most marked apoptosis, however, is noted for the more complex theranostic particles as the external magnetic field has resulted in an accumulation of SPIONs greater than 5% compared to the SPION free micelles.

It should be specified that all the studies mentioned are considered valid at the purpose of the research and that the techniques mentioned, applied to the whole proposed

study, have been designed to provide their best performances if applied synergistically. The design of the SPION based theranostic nanoparticle investigated therefore followed the logic of extrapolating the strengths of similar platforms critically, evaluating possible alternatives without losing sight of the practical feasibility. The bottom-up viability of the NP design strategy was therefore demonstrated, leaving further practical insights open.

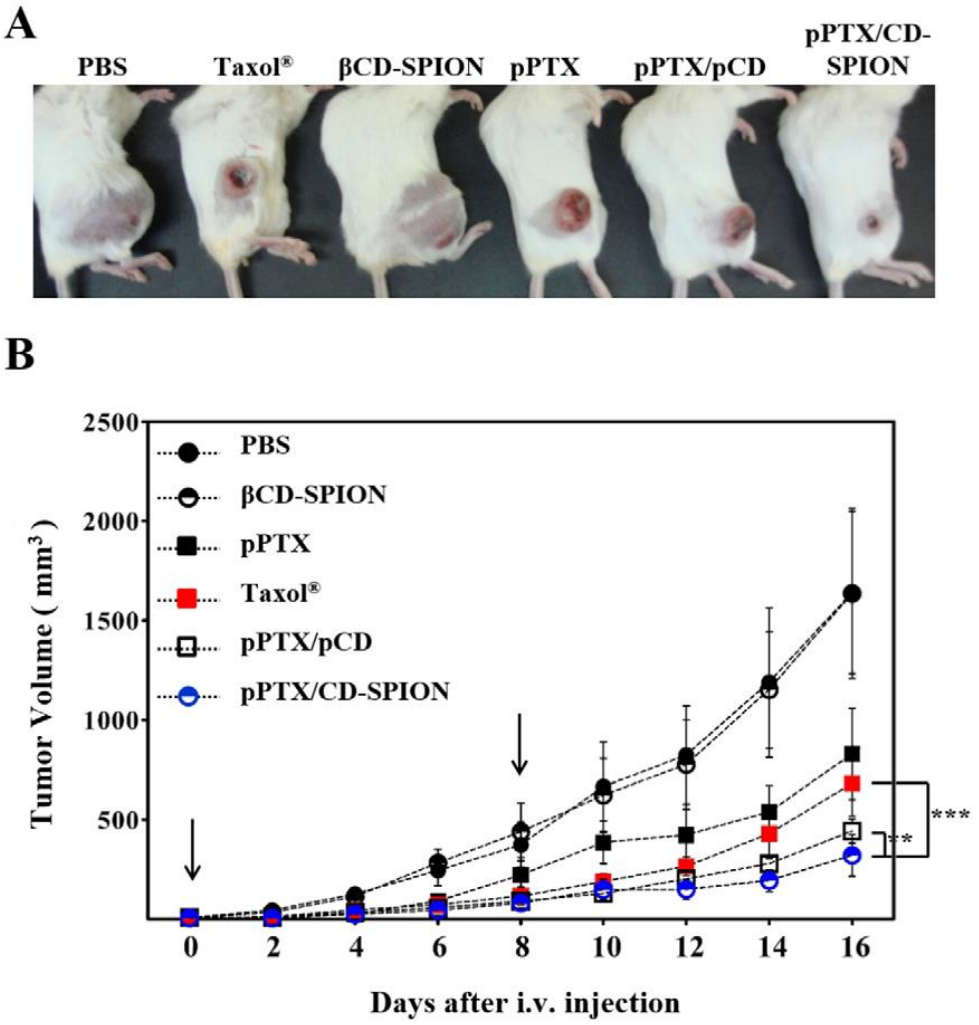

*Fig. 50 (A) Photo images of tumor-bearingmice on day 21 post inoculation. (B) CT26 tumor growth profile treatedwith PBS, βCD-SPION, pPTX, Taxol, pPTX/pCDand pPTX/CD-SPION. Data represent mean ± S.E.M. from n= 4 (*P < 0.05; **P < 0.01; ***P < 0.001). Each arrow represents the time of intravenous injection of samples* (Jeon *et al.*, 2016).

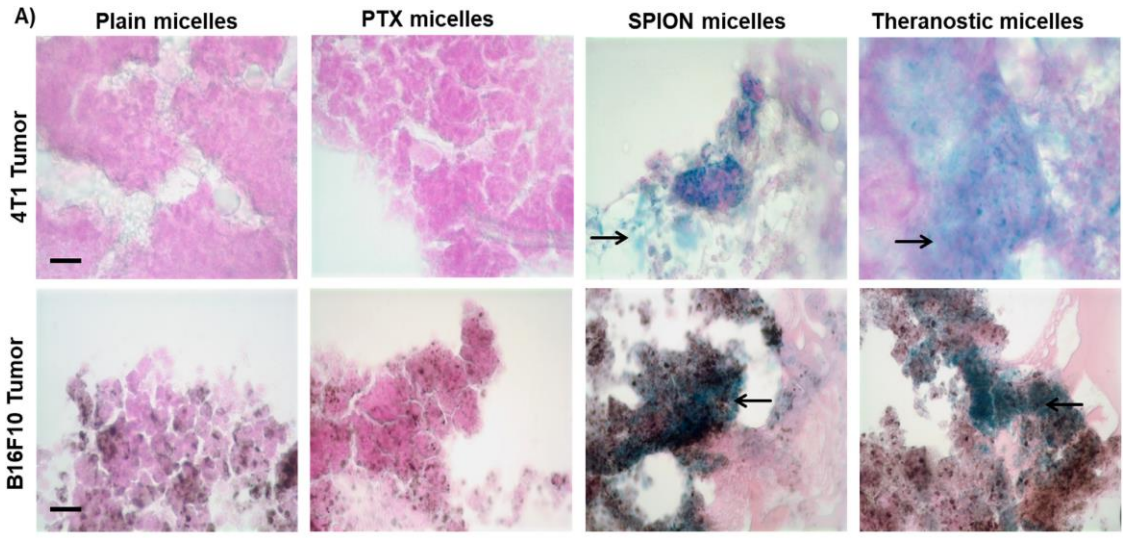

Fig. 51 Prussian blue staining of tumor cryosections: Breast (4T1) and melanoma (B16F10) tumor sections stained for SPIONs localized within the tumor interstitium at +48 h (Upponi et al.*, 2018).*

3 General Conclusions and Future Directions

Nanotheranostics is a strategy that aims to improve anticancer therapies, increase selectivity and treatment efficacy, reducing side effects that characterize traditional cancer therapies.

In this work the design of an innovative SPIONs based and LBL coated nanoparticle was designed, following critically among the most promising applications found in the literature. The bottom-up strategy was used to compose the NP, starting from the choice of SPIONs and LbL PEs deposition, up to the therapeutic characteristics of active and passive targeting, through superficial functionalizations.

The SPIONs core has proven to be among the most biocompatible and non-cytotoxic imaging tools (MRI), its small size (<20 nm) can provide a valid template on which to create complex particles, exploiting the net surface charge that can be implemented, both positive or negative. The lack of long-term in vivo studies suggests that biocompatibility and biodistribution should be widely evaluated, especially in the FDA phases III, IV, V. SPIONs' hyperthermia has proven to be a valid complementary therapy in vivo, but its human efficacy is still far from being approved.

Biomimetic skills, biocompatibility and encapsulation efficacy of chemotherapics (Paclitaxel/Docetaxel) were the leading characteristics to the PEs choice (Chitosan / Alginate and PSS/PAH). Among the challenges of nanomedicine, pH-responsive characteristics, Passive targeting (but also EPR Effect) and drug releases have proven essential in biodistribution and pharmacokinetics management. Other PEs have comparable properties, but the great tumor variability suggests that different materials are better suited to different contexts, solid or fluid tumors, biological barriers, proteins and signals expressed in vivo, can determine different choices and strategies.

In biodistribution the use of PEG functionalization has proven to be a good candidate for the purposes ("stealth" strategy, circulation times), however it must be said that other molecules such as human serum albumin or different RGD-based peptides could be valid substitutes for PEGylated NPs. However, only laboratory-specific studies can define which is the best chemical, physical and biological interaction between materials. All this design variability, however, in fact responds to one of the most important challenges of

recent years or personalized medicine. The NP was in fact designed to be versatile and easily modifiable according to the biological and engineering characteristics required. HER-2, antibody, EGFR, Biotin, HA, have been chosen as active targeting molecules because of their expression in the most common tumors (lung, liver, breast and prostate cancer). The furthest ambition is to adapt the NP to the individual patient's individual tumor characteristics. Finally, the first design of the NP specifications were provided with the intention of proposing a consistent and reproducible platform, in order to be optimized over time.

The intent of this study was therefore very preliminary, design protocols and feasibility should be carried out to verify and improve the global characteristics evaluated in the literature. Many studies and discoveries will be needed to make significant progress in medicine, for this reason the hope of this research is to have contributed with a small

References

Abdelhamid, A. S. *et al.* (2018) 'Layer-by-layer gelatin/chondroitin quantum dots-based nanotheranostics: Combined rapamycin/celecoxib delivery and cancer imaging', *Nanomedicine*. doi: 10.2217/nnm-2018-0028.

Agarwal, A. *et al.* (2008) 'Stable nanocolloids of poorly soluble drugs with high drug content prepared using the combination of sonication and layer-by-layer technology', *Journal of Controlled Release*. doi: 10.1016/j.jconrel.2008.03.017.

Aillon, K. L. *et al.* (2009) 'Effects of nanomaterial physicochemical properties on in vivo toxicity', *Advanced Drug Delivery Reviews*. doi: 10.1016/j.addr.2009.03.010.

Al-Nahain, A. *et al.* (2013) 'Target delivery and cell imaging using hyaluronic acid-functionalized graphene quantum dots', *Molecular Pharmaceutics*. doi: 10.1021/mp400219u.

Ali, L. M. A. *et al.* (2019) 'Polymer-coated superparamagnetic iron oxide nanoparticles as T2 contrast agent for MRI and their uptake in liver', *Future Science OA*. doi: 10.4155/fsoa-2017-0054.

American Cancer Society (2020) *The History of Cancer*. Available at: https://www.cancer.org/cancer/cancer-basics/history-of-cancer.html.

Arruebo, M. *et al.* (2011) 'Assessment of the evolution of cancer treatment therapies', *Cancers*. doi: 10.3390/cancers3033279.

Baskar, R. *et al.* (2012) 'Cancer and radiation therapy: Current advances and future directions', *International Journal of Medical Sciences*. doi: 10.7150/ijms.3635.

Baykal, A. *et al.* (2015) 'Preparation and characterization of SPION functionalized via caffeic acid', *Journal of Magnetism and Magnetic Materials*. doi: 10.1016/j.jmmm.2015.07.095.

Beckmann, N. *et al.* (2003) 'Macrophage labeling by SPIO as an early marker of allograft chronic rejection in a rat model of kidney transplantation', *Magnetic Resonance in Medicine*. doi: 10.1002/mrm.10387.

Berry, C. C. *et al.* (2003) 'Dextran and albumin derivatised iron oxide nanoparticles: Influence on fibroblasts in vitro', *Biomaterials*. doi: 10.1016/S0142-9612(03)00237-0.

Bidram, E. *et al.* (2019) 'A concise review on cancer treatment methods and delivery systems', *Journal of Drug Delivery Science and Technology*. doi: 10.1016/j.jddst.2019.101350.

Bobo, D. *et al.* (2016) 'Nanoparticle-Based Medicines: A Review of FDA-Approved Materials and Clinical Trials to Date', *Pharmaceutical Research*. doi: 10.1007/s11095-016-1958-5.

Bordat, C. *et al.* (2000) 'Distribution of iron oxide nanoparticles in rat lymph nodes studied using electron energy loss spectroscopy (EELS) and electron spectroscopic imaging (ESI)', *Journal of Magnetic Resonance Imaging*. doi: 10.1002/1522-2586(200009)12:3<505::AID-JMRI18>3.0.CO;2-A.

Bray, F. *et al.* (2012) 'Global cancer transitions according to the Human Development Index (2008-2030): A population-based study', *The Lancet Oncology*. doi: 10.1016/S1470-2045(12)70211-5.

Çağdaş, M., Sezer, A. D. and Bucak, S. (2014) 'Liposomes as Potential Drug Carrier Systems for Drug Delivery', in *Application of Nanotechnology in Drug Delivery*. doi: 10.5772/58459.

Cai, X. *et al.* (2016) 'PH-Sensitive ZnO Quantum Dots-Doxorubicin Nanoparticles for Lung Cancer Targeted Drug Delivery', *ACS Applied Materials and Interfaces*. doi: 10.1021/acsami.6b04933.

Carenza, E. *et al.* (2014) 'Rapid synthesis of water-dispersible superparamagnetic iron oxide nanoparticles by a microwave-assisted route for safe labeling of endothelial progenitor cells', *Acta Biomaterialia*. doi: 10.1016/j.actbio.2014.04.010.

Carregal-Romero, S. *et al.* (2015) 'Magnetically triggered release of molecular cargo from iron oxide nanoparticle loaded microcapsules', *Nanoscale*. doi: 10.1039/c4nr04055d.

Chaffer, C. L. and Weinberg, R. A. (2011) 'A perspective on cancer cell metastasis', *Science*. doi: 10.1126/science.1203543.

Chai, F. *et al.* (2017) 'Doxorubicin-loaded poly (lactic-co-glycolic acid) nanoparticles coated with chitosan/alginate by layer by layer technology for antitumor applications', *International Journal of Nanomedicine*, Volume 12, pp. 1791–1802. doi: 10.2147/IJN.S130404.

Chen, L. *et al.* (2018) 'Using PEGylated magnetic nanoparticles to describe the EPR effect in tumor for predicting therapeutic efficacy of micelle drugs', *Nanoscale*. doi: 10.1039/c7nr08319j.

Chin, A. B. and Yaacob, I. I. (2007) 'Synthesis and characterization of magnetic iron oxide nanoparticles via w/o microemulsion and Massart's procedure', *Journal of Materials Processing Technology*, 191(1–3), pp. 235–237. doi: 10.1016/j.jmatprotec.2007.03.011.

Choi, J. H. *et al.* (2019) 'Poly(D,L-lactic-co-glycolic acid) (PLGA) hollow fiber with segmental switchability of its chains sensitive to NIR light for synergistic cancer therapy', *Colloids and Surfaces B: Biointerfaces*. doi: 10.1016/j.colsurfb.2018.09.081.

Choi, K. Y. *et al.* (2012) 'Theranostic nanoplatforms for simultaneous cancer imaging and therapy: Current approaches and future perspectives', *Nanoscale*. doi: 10.1039/c1nr11277e.

Choi, Y. W. *et al.* (2015) 'Colloidal stability of iron oxide nanoparticles with multivalent polymer surfactants', *Journal of Colloid and Interface Science*. doi: 10.1016/j.jcis.2014.11.068.

Di Corato, R. *et al.* (2015) 'Combining magnetic hyperthermia and photodynamic therapy for tumor

ablation with photoresponsive magnetic liposomes', *ACS Nano*. doi: 10.1021/nn506949t.

Corot, C. *et al.* (2006) 'Recent advances in iron oxide nanocrystal technology for medical imaging', *Advanced Drug Delivery Reviews*. doi: 10.1016/j.addr.2006.09.013.

Cui, J. *et al.* (2014) 'Emerging methods for the fabrication of polymer capsules', *Advances in Colloid and Interface Science*. doi: 10.1016/j.cis.2013.10.012.

Dadras, P. *et al.* (2017) 'Formulation and evaluation of targeted nanoparticles for breast cancer theranostic system', *European Journal of Pharmaceutical Sciences*. doi: 10.1016/j.ejps.2016.11.005.

Dai, Y. *et al.* (2017) 'Nanoparticle design strategies for enhanced anticancer therapy by exploiting the tumour microenvironment', *Chemical Society Reviews*. doi: 10.1039/c6cs00592f.

Danhier, F., Feron, O. and Préat, V. (2010) 'To exploit the tumor microenvironment: Passive and active tumor targeting of nanocarriers for anti-cancer drug delivery', *Journal of Controlled Release*. doi: 10.1016/j.jconrel.2010.08.027.

Deatsch, A. E. and Evans, B. A. (2014) 'Heating efficiency in magnetic nanoparticle hyperthermia', *Journal of Magnetism and Magnetic Materials*. doi: 10.1016/j.jmmm.2013.11.006.

Deng, Z. J. *et al.* (2013) 'Layer-by-layer nanoparticles for systemic codelivery of an anticancer drug and siRNA for potential triple-negative breast cancer treatment', *ACS Nano*. doi: 10.1021/nn4047925.

DeSantis, C. E. *et al.* (2014) 'Cancer treatment and survivorship statistics, 2014', *CA: A Cancer Journal for Clinicians*. doi: 10.3322/caac.21235.

Diamantis, N. and Banerji, U. (2016) 'Antibody-drug conjugates - An emerging class of cancer treatment', *British Journal of Cancer*. doi: 10.1038/bjc.2015.435.

Dierendonck, M. *et al.* (2014) 'Just spray it-LbL assembly enters a new age', *Soft Matter*. doi: 10.1039/c3sm52202d.

Dimasi, J. A. *et al.* (2010) 'Trends in risks associated with new drug development: Success rates for investigational drugs', *Clinical Pharmacology and Therapeutics*. doi: 10.1038/clpt.2009.295.

Dolores, R., Raquel, S. and Adianez, G. L. (2015) 'Sonochemical synthesis of iron oxide nanoparticles loaded with folate and cisplatin: Effect of ultrasonic frequency', *Ultrasonics Sonochemistry*. doi: 10.1016/j.ultsonch.2014.08.005.

Dreaden, E. C. *et al.* (2014) 'Bimodal tumor-targeting from microenvironment responsive hyaluronan layer-by-layer (LbL) nanoparticles', *ACS Nano*. doi: 10.1021/nn502861t.

Du, J. *et al.* (2019) 'Carbon Dots for In Vivo Bioimaging and Theranostics', *Small*. doi: 10.1002/smll.201805087.

Elani, Y. (2016) ‘Construction of membrane-bound artificial cells using microfluidics: A new frontier in bottom-up synthetic biology’, *Biochemical Society Transactions*. doi: 10.1042/BST20160052.

Espinosa, A. *et al.* (2016) ‘Duality of Iron Oxide Nanoparticles in Cancer Therapy: Amplification of Heating Efficiency by Magnetic Hyperthermia and Photothermal Bimodal Treatment’, *ACS Nano*. doi: 10.1021/acsnano.5b07249.

Flavahan, W. A., Gaskell, E. and Bernstein, B. E. (2017) ‘Epigenetic plasticity and the hallmarks of cancer’, *Science*. doi: 10.1126/science.aal2380.

Foo, J. and Michor, F. (2014) ‘Evolution of acquired resistance to anti-cancer therapy’, *Journal of Theoretical Biology*. doi: 10.1016/j.jtbi.2014.02.025.

Gai, M. *et al.* (2018) ‘Micro-Patterned Polystyrene Sheets as Templates for Interlinked 3D Polyelectrolyte Multilayer Microstructures’, *BioNanoScience*. doi: 10.1007/s12668-017-0403-5.

Ganansia-Leymarie, V. *et al.* (2003) ‘Signal Transduction Pathways of Taxanes-Induced Apoptosis’, *Current Medicinal Chemistry-Anti-Cancer Agents*, 3(4), pp. 291–306. doi: 10.2174/1568011033482422.

Golub, T. R. *et al.* (1999) ‘Molecular classification of cancer: Class discovery and class prediction by gene expression monitoring’, *Science*. doi: 10.1126/science.286.5439.531.

Grillone, A. *et al.* (2015) ‘Active Targeting of Sorafenib: Preparation, Characterization, and In Vitro Testing of Drug-Loaded Magnetic Solid Lipid Nanoparticles’, *Advanced Healthcare Materials*. doi: 10.1002/adhm.201500235.

Gutiérrez, L. *et al.* (2015) ‘Synthesis methods to prepare single- and multi-core iron oxide nanoparticles for biomedical applications’, *Dalton Transactions*. doi: 10.1039/c4dt03013c.

Habibi, N. *et al.* (2017) ‘Polyelectrolyte multilayers and capsules: S-layer functionalization for improving stability and biocompatibility’, *Journal of Drug Delivery Science and Technology*. doi: 10.1016/j.jddst.2016.12.004.

Hadjesfandiari, N. and Parambath, A. (2018) ‘Stealth coatings for nanoparticles: Polyethylene glycol alternatives’, in *Engineering of Biomaterials for Drug Delivery Systems: Beyond Polyethylene Glycol*. doi: 10.1016/B978-0-08-101750-0.00013-1.

Hafner, A. *et al.* (2014) ‘Nanotherapeutics in the EU: An overview on current state and future directions’, *International Journal of Nanomedicine*. doi: 10.2147/IJN.S55359.

Hamid Akash, M. S., Rehman, K. and Chen, S. (2015) ‘Natural and synthetic polymers as drug carriers for delivery of therapeutic proteins’, *Polymer Reviews*. doi: 10.1080/15583724.2014.995806.

Hanahan, D. and Weinberg, R. A. (2000) ‘The hallmarks of cancer’, *Cell*. doi: 10.1016/S0092-8674(00)81683-9.

Hanahan, D. and Weinberg, R. A. (2011) 'Hallmarks of cancer: The next generation', *Cell*. doi: 10.1016/j.cell.2011.02.013.

Ho, D., Sun, X. and Sun, S. (2011) 'Monodisperse magnetic nanoparticles for theranostic applications', *Accounts of Chemical Research*. doi: 10.1021/ar200090c.

Javanbakht, T. *et al.* (2016) 'Relating the Surface Properties of Superparamagnetic Iron Oxide Nanoparticles (SPIONs) to Their Bactericidal Effect towards a Biofilm of Streptococcus mutans', *PLoS ONE*. doi: 10.1371/journal.pone.0154445.

Jeon, H. *et al.* (2016) 'Poly-paclitaxel/cyclodextrin-SPION nano-assembly for magnetically guided drug delivery system', *Journal of Controlled Release*. doi: 10.1016/j.jconrel.2016.01.006.

Jhaveri, A. *et al.* (2018) 'Transferrin-targeted, resveratrol-loaded liposomes for the treatment of glioblastoma', *Journal of Controlled Release*. doi: 10.1016/j.jconrel.2018.03.006.

Jia, N. *et al.* (2007) 'Intracellular delivery of quantum dots tagged antisense oligodeoxynucleotides by functionalized multiwalled carbon nanotubes', *Nano Letters*. doi: 10.1021/nl071114c.

Jia, Y. P. *et al.* (2017) 'The in vitro and in vivo toxicity of gold nanoparticles', *Chinese Chemical Letters*. doi: 10.1016/j.cclet.2017.01.021.

Jordan, A. *et al.* (2001) 'Presentation of a new magnetic field therapy system for the treatment of human solid tumors with magnetic fluid hyperthermia', *Journal of Magnetism and Magnetic Materials*. doi: 10.1016/S0304-8853(00)01239-7.

Kalber, T. L. *et al.* (2016) 'Hyperthermia treatment of tumors by mesenchymal stem cell-delivered superparamagnetic iron oxide nanoparticles', *International Journal of Nanomedicine*. doi: 10.2147/IJN.S94255.

Kita, E. *et al.* (2010) 'Ferromagnetic nanoparticles for magnetic hyperthermia and thermoablation therapy', *Journal of Physics D: Applied Physics*. doi: 10.1088/0022-3727/43/47/474011.

Koopaei, M. N. *et al.* (2011) 'Docetaxel immunonanocarriers as targeted delivery systems for HER 2-positive tumor cells: preparation, characterization, and cytotoxicity studies.', *International journal of nanomedicine*. doi: 10.2147/ijn.s23211.

Kumar, C. S. S. R. and Mohammad, F. (2011) 'Magnetic nanomaterials for hyperthermia-based therapy and controlled drug delivery', *Advanced Drug Delivery Reviews*. doi: 10.1016/j.addr.2011.03.008.

Laconte, L., Nitin, N. and Bao, G. (2005) 'Magnetic nanoparticle probes', *Materials Today*. doi: 10.1016/S1369-7021(05)00893-X.

Lammers, T *et al.* (2011) 'GUEST EDITORIAL Theranostic Nanomedicine', *Acc Chem Res*.

Lammers, Twan *et al.* (2011) 'Theranostic nanomedicine', *Accounts of Chemical Research*. doi: 10.1021/ar200019c.

Laurent, S. *et al.* (2008) 'Magnetic iron oxide nanoparticles: Synthesis, stabilization, vectorization, physicochemical characterizations and biological applications', *Chemical Reviews*. doi: 10.1021/cr068445e.

Lee, H. Y. *et al.* (2006) 'Preparation and magnetic resonance imaging effect of polyvinylpyrrolidone-coated iron oxide nanoparticles', *Journal of Biomedical Materials Research - Part B Applied Biomaterials*. doi: 10.1002/jbm.b.30524.

Leung, K. C. F., Xuan, S. and Wang, Y. J. (2010) 'From micro to nano magnetic spheres: Size-controllable synthesis, multilayer coatings, and biomedical applications', in *Nanotechnology 2010: Advanced Materials, CNTs, Particles, Films and Composites - Technical Proceedings of the 2010 NSTI Nanotechnology Conference and Expo, NSTI-Nanotech 2010*.

Li, Q. *et al.* (2017) 'Correlation between particle size/domain structure and magnetic properties of highly crystalline Fe3O4 nanoparticles', *Scientific Reports*. doi: 10.1038/s41598-017-09897-5.

Li, S. D. and Huang, L. (2010) 'Stealth nanoparticles: High density but sheddable PEG is a key for tumor targeting', *Journal of Controlled Release*. doi: 10.1016/j.jconrel.2010.03.016.

Li, X. *et al.* (2015) 'Effects of physicochemical properties of nanomaterials on their toxicity', *Journal of Biomedical Materials Research - Part A*. doi: 10.1002/jbm.a.35384.

Li, Xiankai *et al.* (2018) 'Biomimetic engineering of spider silk fibres with graphene for electric devices with humidity and motion sensitivity', *Journal of Materials Chemistry C*. doi: 10.1039/c8tc00265g.

Li, Xiaomin *et al.* (2018) 'The systematic evaluation of size-dependent toxicity and multi-time biodistribution of gold nanoparticles', *Colloids and Surfaces B: Biointerfaces*. doi: 10.1016/j.colsurfb.2018.04.005.

Liang, P. C. *et al.* (2016) 'Doxorubicin-modified magnetic nanoparticles as a drug delivery system for magnetic resonance imaging-monitoring magnet-enhancing tumor chemotherapy', *International Journal of Nanomedicine*. doi: 10.2147/IJN.S94139.

Lim, C. *et al.* (2017) 'A stable nanoplatform for antitumor activity using PEG-PLL-PLA triblock co-polyelectrolyte', *Colloids and Surfaces B: Biointerfaces*. doi: 10.1016/j.colsurfb.2017.01.027.

Lin, W. *et al.* (2017) 'Doxorubicin-Loaded Unimolecular Micelle-Stabilized Gold Nanoparticles as a Theranostic Nanoplatform for Tumor-Targeted Chemotherapy and Computed Tomography Imaging', *Biomacromolecules*. doi: 10.1021/acs.biomac.7b00810.

Liu, X. Q. and Picart, C. (2016) 'Layer-by-Layer Assemblies for Cancer Treatment and Diagnosis',

Advanced Materials. doi: 10.1002/adma.201502660.

Lugert, S. *et al.* (2019) 'Cellular effects of paclitaxel-loaded iron oxide nanoparticles on breast cancer using different 2D and 3D cell culture models', *International Journal of Nanomedicine*. doi: 10.2147/IJN.S187886.

Lvov, Y. M. *et al.* (2011) 'Converting poorly soluble materials into stable aqueous nanocolloids', *Langmuir*. doi: 10.1021/la1041635.

Macdonald, M. L. *et al.* (2011) 'Tissue integration of growth factor-eluting layer-by-layer polyelectrolyte multilayer coated implants', *Biomaterials*. doi: 10.1016/j.biomaterials.2010.10.052.

Maeda, H., Bharate, G. Y. and Daruwalla, J. (2009) 'Polymeric drugs for efficient tumor-targeted drug delivery based on EPR-effect', *European Journal of Pharmaceutics and Biopharmaceutics*. doi: 10.1016/j.ejpb.2008.11.010.

Mansouri, M. *et al.* (2017) 'Magnetic responsive of paclitaxel delivery system based on SPION and palmitoyl chitosan', *Journal of Magnetism and Magnetic Materials*. doi: 10.1016/j.jmmm.2016.07.066.

Martin, M. *et al.* (2005) 'Adjuvant docetaxel for node-positive breast cancer', *New England Journal of Medicine*. doi: 10.1056/NEJMoa043681.

Masood, F. (2016) 'Polymeric nanoparticles for targeted drug delivery system for cancer therapy', *Materials Science and Engineering C*. doi: 10.1016/j.msec.2015.11.067.

Mattu, C. *et al.* (2018) 'Alternating block copolymer-based nanoparticles as tools to modulate the loading of multiple chemotherapeutics and imaging probes', *Acta Biomaterialia*. doi: 10.1016/j.actbio.2018.09.021.

Mendes, M. *et al.* (2018) 'Targeted theranostic nanoparticles for brain tumor treatment', *Pharmaceutics*. doi: 10.3390/pharmaceutics10040181.

Merbach, A., Helm, L. and Tóth, É. (2013) *The Chemistry of Contrast Agents in Medical Magnetic Resonance Imaging: Second Edition*, *The Chemistry of Contrast Agents in Medical Magnetic Resonance Imaging: Second Edition*. doi: 10.1002/9781118503652.

Miller, M. L. and Ojima, I. (2001) 'Chemistry and chemical biology of taxane anticancer agents', *Chemical Records*. doi: 10.1002/tcr.1008.

Mirsadeghi, S. *et al.* (2016) 'Effect of PEGylated superparamagnetic iron oxide nanoparticles (SPIONs) under magnetic field on amyloid beta fibrillation process', *Materials Science and Engineering C*. doi: 10.1016/j.msec.2015.10.026.

Mohs, R. C. and Greig, N. H. (2017) 'Drug discovery and development: Role of basic biological research', *Alzheimer's and Dementia: Translational Research and Clinical Interventions*. doi:

10.1016/j.trci.2017.10.005.

Montero, A. *et al.* (2005) 'Docetaxel for treatment of solid tumours: A systematic review of clinical data', *Lancet Oncology*. doi: 10.1016/S1470-2045(05)70094-2.

Mornet, S., Portier, J. and Duguet, E. (2005) 'A method for synthesis and functionalization of ultrasmall superparamagnetic covalent carriers based on maghemite and dextran', in *Journal of Magnetism and Magnetic Materials*. doi: 10.1016/j.jmmm.2005.01.053.

Nagesh, P. K. B. *et al.* (2016) 'PSMA targeted docetaxel-loaded superparamagnetic iron oxide nanoparticles for prostate cancer', *Colloids and Surfaces B: Biointerfaces*. doi: 10.1016/j.colsurfb.2016.03.071.

Naumov, A. A. *et al.* (2018) 'A Study of the Cytotoxic Effect of Microcapsules and Their Constituent Polymers on Macrophages and Tumor Cells', *Bulletin of Experimental Biology and Medicine*. doi: 10.1007/s10517-018-4291-7.

Nenclares, P. and Harrington, K. J. (2020) 'The biology of cancer', *Medicine (United Kingdom)*. doi: 10.1016/j.mpmed.2019.11.001.

Okoli, C. *et al.* (2011) 'Application of magnetic iron oxide nanoparticles prepared from microemulsions for protein purification', *Journal of Chemical Technology and Biotechnology*. doi: 10.1002/jctb.2704.

Ortega, R. A. and Giorgio, T. D. (2012) 'A mathematical model of superparamagnetic iron oxide nanoparticle magnetic behavior to guide the design of novel nanomaterials', *Journal of Nanoparticle Research*. doi: 10.1007/s11051-012-1282-x.

Ostacolo, L. *et al.* (2010) 'In vitro anticancer activity of docetaxel-loaded micelles based on poly(ethylene oxide)-poly(epsilon-caprolactone) block copolymers: Do nanocarrier properties have a role?', *Journal of Controlled Release*. doi: 10.1016/j.jconrel.2010.08.006.

Pandey, A. P. *et al.* (2015) 'Sonication-Assisted drug encapsulation in layer-by-layer self-Assembled gelatin-poly (styrenesulfonate) polyelectrolyte nanocapsules: Process optimization', *Artificial Cells, Nanomedicine and Biotechnology*. doi: 10.3109/21691401.2014.898646.

Pascu, O. *et al.* (2012) 'Surface reactivity of iron oxide nanoparticles by microwave-assisted synthesis; Comparison with the thermal decomposition route', *Journal of Physical Chemistry C*. doi: 10.1021/jp303204d.

Pearce, A. K. and O'Reilly, R. K. (2019) 'Insights into Active Targeting of Nanoparticles in Drug Delivery: Advances in Clinical Studies and Design Considerations for Cancer Nanomedicine', *Bioconjugate Chemistry*, 30(9), pp. 2300–2311. doi: 10.1021/acs.bioconjchem.9b00456.

Perry, J. L. *et al.* (2012) 'PEGylated PRINT nanoparticles: The impact of PEG density on protein binding,

macrophage association, biodistribution, and pharmacokinetics', *Nano Letters*. doi: 10.1021/nl302638g.

Poon, Z. *et al.* (2011) 'Layer-by-layer nanoparticles with a pH-sheddable layer for in vivo targeting of tumor hypoxia', *ACS Nano*. doi: 10.1021/nn200876f.

Qing, Y. E. *et al.* (2002) 'In vivo detection of acute rat renal allograft rejection by MRI with USPIO particles', in *Kidney International*. doi: 10.1046/j.1523-1755.2002.00195.x.

Rafiei, P. and Haddadi, A. (2017) 'Docetaxel-loaded PLGA and PLGA-PEG nanoparticles for intravenous application: Pharmacokinetics and biodistribution profile', *International Journal of Nanomedicine*. doi: 10.2147/IJN.S121881.

Rahman, I. A. and Padavettan, V. (2012) 'Synthesis of Silica nanoparticles by Sol-Gel: Size-dependent properties, surface modification, and applications in silica-polymer nanocompositesa review', *Journal of Nanomaterials*. doi: 10.1155/2012/132424.

Rai, M. and Jamil, B. (eds) (2019) *Nanotheranostics*. Cham: Springer International Publishing. doi: 10.1007/978-3-030-29768-8.

Rai, P. and Morris, S. A. (2019) *Nanotheranostics for Cancer Applications*. 1st edn. Edited by P. Rai and S. A. Morris. Cham: Springer International Publishing (Bioanalysis). doi: 10.1007/978-3-030-01775-0.

Reddy, L. H. *et al.* (2012) 'Magnetic nanoparticles: Design and characterization, toxicity and biocompatibility, pharmaceutical and biomedical applications', *Chemical Reviews*. doi: 10.1021/cr300068p.

Revia, R. A. and Zhang, M. (2016) 'Magnetite nanoparticles for cancer diagnosis, treatment, and treatment monitoring: Recent advances', *Materials Today*. doi: 10.1016/j.mattod.2015.08.022.

Richardson, J. J. *et al.* (2016) 'Innovation in Layer-by-Layer Assembly', *Chemical Reviews*. doi: 10.1021/acs.chemrev.6b00627.

Richardson, J. J., Björnmalm, M. and Caruso, F. (2015) 'Technology-driven layer-by-layer assembly of nanofilms', *Science*. doi: 10.1126/science.aaa2491.

Riehemann, K. *et al.* (2009) 'Nanomedicine - Challenge and perspectives', *Angewandte Chemie - International Edition*. doi: 10.1002/anie.200802585.

Rizzo, L. Y. *et al.* (2013) 'Recent progress in nanomedicine: Therapeutic, diagnostic and theranostic applications', *Current Opinion in Biotechnology*. doi: 10.1016/j.copbio.2013.02.020.

Rompicharla, S. V. K. *et al.* (2019) 'Biotin functionalized PEGylated poly(amidoamine) dendrimer conjugate for active targeting of paclitaxel in cancer', *International Journal of Pharmaceutics*. doi: 10.1016/j.ijpharm.2018.12.069.

Rui, H. *et al.* (2010) 'Synthesis, functionalization, and biomedical applications of multifunctional magnetic nanoparticles', *Advanced Materials*. doi: 10.1002/adma.201000260.

Santos, A. C. *et al.* (2015) 'Sonication-Assisted Layer-by-Layer Assembly for Low Solubility Drug Nanoformulation', *ACS Applied Materials and Interfaces*. doi: 10.1021/acsami.5b02002.

Santos, A. C. *et al.* (2018) 'Layer-by-Layer coated drug-core nanoparticles as versatile delivery platforms', in *Design and Development of New Nanocarriers*. doi: 10.1016/b978-0-12-813627-0.00016-8.

Sanz, B. *et al.* (2017) 'Magnetic hyperthermia enhances cell toxicity with respect to exogenous heating', *Biomaterials*. doi: 10.1016/j.biomaterials.2016.11.008.

Saqib, J. and Aljundi, I. H. (2016) 'Membrane fouling and modification using surface treatment and layer-by-layer assembly of polyelectrolytes: State-of-the-art review', *Journal of Water Process Engineering*. doi: 10.1016/j.jwpe.2016.03.009.

Scientific and Clinical Applications of Magnetic Carriers (1997) *Scientific and Clinical Applications of Magnetic Carriers*. doi: 10.1007/978-1-4757-6482-6.

Scott, A. M., Wolchok, J. D. and Old, L. J. (2012) 'Antibody therapy of cancer', *Nature Reviews Cancer*. doi: 10.1038/nrc3236.

Sedlacek, O. *et al.* (2012) 'Poly(2-Oxazoline)s - Are They More Advantageous for Biomedical Applications Than Other Polymers?', *Macromolecular Rapid Communications*, 33(19), pp. 1648–1662. doi: 10.1002/marc.201200453.

Shanavas, A. *et al.* (2017) 'Magnetic core-shell hybrid nanoparticles for receptor targeted anti-cancer therapy and magnetic resonance imaging', *Journal of Colloid and Interface Science*. doi: 10.1016/j.jcis.2016.09.060.

Shapin, S. (2010) *Cancer World: The making of a modern disease*, *The New Yorker*.

Shefet-Carasso, L. and Benhar, I. (2015) 'Antibody-targeted drugs and drug resistance - Challenges and solutions', *Drug Resistance Updates*. doi: 10.1016/j.drup.2014.11.001.

Shen, S. *et al.* (2015) 'Magnetic nanoparticle clusters for photothermal therapy with near-infrared irradiation', *Biomaterials*. doi: 10.1016/j.biomaterials.2014.10.064.

Shi, C. *et al.* (2018) 'Active-targeting docetaxel-loaded mixed micelles for enhancing antitumor efficacy', *Journal of Molecular Liquids*. doi: 10.1016/j.molliq.2018.05.039.

Shi, J. F. *et al.* (2014) 'Synthesis and tumor cell growth inhibitory activity of biotinylated annonaceous acetogenins', *European Journal of Medicinal Chemistry*. doi: 10.1016/j.ejmech.2013.11.012.

Shutava, T. G. *et al.* (2012) 'Architectural layer-by-layer assembly of drug nanocapsules with PEGylated

polyelectrolytes', *Soft Matter*. doi: 10.1039/c2sm25683e.

Siegler, E. L., Kim, Y. J. and Wang, P. (2016) 'Nanomedicine targeting the tumor microenvironment: Therapeutic strategies to inhibit angiogenesis, remodel matrix, and modulate immune responses', *Journal of Cellular Immunotherapy*. doi: 10.1016/j.jocit.2016.08.002.

Silva, A. H. *et al.* (2016) 'Superparamagnetic iron-oxide nanoparticles mPEG350- and mPEG2000-coated: Cell uptake and biocompatibility evaluation', *Nanomedicine: Nanotechnology, Biology, and Medicine*. doi: 10.1016/j.nano.2015.12.371.

Singh, N. *et al.* (2010) 'Potential toxicity of superparamagnetic iron oxide nanoparticles (SPION)', *Nano Reviews*. doi: 10.3402/nano.v1i0.5358.

Singh, S. K. *et al.* (2015) 'Development of docetaxel nanocapsules for improving in vitro cytotoxicity and cellular uptake in MCF-7 cells', *Drug Development and Industrial Pharmacy*. doi: 10.3109/03639045.2014.1003220.

Soares, P. I. P. *et al.* (2015) 'Thermal and magnetic properties of iron oxide colloids: Influence of surfactants', *Nanotechnology*. doi: 10.1088/0957-4484/26/42/425704.

Srinivasan, S. *et al.* (2014) 'Targeted nanoparticles for simultaneous delivery of chemotherapeutic and hyperthermia agents - An in vitro study', *Journal of Photochemistry and Photobiology B: Biology*. doi: 10.1016/j.jphotobiol.2014.04.012.

Sumer, B. and Gao, J. (2008) 'Theranostic nanomedicine for cancer', *Nanomedicine*. doi: 10.2217/17435889.3.2.137.

Sun, H. *et al.* (2006) 'Novel core-shell structure polyacrylamide-coated magnetic nanoparticles synthesized via photochemical polymerization', *Surface and Coatings Technology*. doi: 10.1016/j.surfcoat.2005.11.112.

Sun, J. *et al.* (2007) 'Synthesis and characterization of biocompatible Fe3O4 nanoparticles', *Journal of Biomedical Materials Research - Part A*. doi: 10.1002/jbm.a.30909.

Tanimoto, A. *et al.* (1994) 'Effects of spatial distribution on proton relaxation enhancement by particulate iron oxide', *Journal of Magnetic Resonance Imaging*. doi: 10.1002/jmri.1880040506.

Tartaj, P. *et al.* (2003) 'The preparation of magnetic nanoparticles for applications in biomedicine', *Journal of Physics D: Applied Physics*. doi: 10.1088/0022-3727/36/13/202.

Teja, A. S. and Koh, P. Y. (2009) 'Synthesis, properties, and applications of magnetic iron oxide nanoparticles', *Progress in Crystal Growth and Characterization of Materials*. doi: 10.1016/j.pcrysgrow.2008.08.003.

Tsoulfas, G. (2012) 'The impact of the European financial crisis on clinical research within the European

union or “when life gives you lemons, make lemonade”’, *Hippokratia*.

Turcheniuk, K. *et al.* (2013) ‘Recent advances in surface chemistry strategies for the fabrication of functional iron oxide based magnetic nanoparticles’, *Nanoscale*. doi: 10.1039/c3nr04131j.

Uchegbu, I. F. *et al.* (eds) (2013) *Fundamentals of Pharmaceutical Nanoscience*. New York, NY: Springer New York. doi: 10.1007/978-1-4614-9164-4.

Upponi, J. R. *et al.* (2018) ‘Polymeric micelles: Theranostic co-delivery system for poorly water-soluble drugs and contrast agents’, *Biomaterials*. doi: 10.1016/j.biomaterials.2018.03.054.

Urhahn, R. *et al.* (1996) ‘Superparamagnetic iron particles: Value of the T 1 effect in MR diagnosis of focal liver lesions’, *RoFo Fortschritte auf dem Gebiete der Rontgenstrahlen und der Neuen Bildgebenden Verfahren*.

Verschraegen, C. F. *et al.* (2000) ‘Docetaxel for patients with paclitaxel-resistant mullerian carcinoma’, *Journal of Clinical Oncology*. doi: 10.1200/JCO.2000.18.14.2733.

Vieira, D. B. and Gamarra, L. F. (2016) ‘Advances in the use of nanocarriers for cancer diagnosis and treatment’, *Einstein (Sao Paulo, Brazil)*. doi: 10.1590/S1679-45082016RB3475.

Volodkin, D. V. *et al.* (2004) ‘Matrix Polyelectrolyte Microcapsules: New System for Macromolecule Encapsulation’, *Langmuir*. doi: 10.1021/la036177z.

Vozar, S. *et al.* (2009) ‘Automated spin-assisted layer-by-layer assembly of nanocomposites’, *Review of Scientific Instruments*. doi: 10.1063/1.3078009.

Wan, X. *et al.* (2016) ‘The preliminary study of immune superparamagnetic iron oxide nanoparticles for the detection of lung cancer in magnetic resonance imaging’, *Carbohydrate Research*. doi: 10.1016/j.carres.2015.11.003.

Wang, S. *et al.* (2020) ‘Zwitterionic-to-cationic charge conversion polyprodrug nanomedicine for enhanced drug delivery’, *Theranostics*. doi: 10.7150/thno.47849.

Wang, X. *et al.* (2018) ‘Fluorescent magnetic PEI-PLGA nanoparticles loaded with paclitaxel for concurrent cell imaging, enhanced apoptosis and autophagy in human brain cancer’, *Colloids and Surfaces B: Biointerfaces*. doi: 10.1016/j.colsurfb.2018.09.033.

Wang, Z. *et al.* (2017) ‘Active targeting theranostic iron oxide nanoparticles for MRI and magnetic resonance-guided focused ultrasound ablation of lung cancer’, *Biomaterials*. doi: 10.1016/j.biomaterials.2017.02.037.

Wegner, K. D. and Hildebrandt, N. (2015) ‘Quantum dots: Bright and versatile in vitro and in vivo fluorescence imaging biosensors’, *Chemical Society Reviews*. doi: 10.1039/c4cs00532e.

Wei, Y. *et al.* (2012) 'Synthesis of Fe3O4 nanoparticles and their magnetic properties', in *Procedia Engineering*. doi: 10.1016/j.proeng.2011.12.498.

Weiner, G. J. (2015) 'Building better monoclonal antibody-based therapeutics', *Nature Reviews Cancer*. doi: 10.1038/nrc3930.

Xiao, F. X. *et al.* (2016) 'Layer-by-layer assembly of versatile nanoarchitectures with diverse dimensionality: A new perspective for rational construction of multilayer assemblies', *Chemical Society Reviews*. doi: 10.1039/c5cs00781j.

Xiao, H. *et al.* (2020) 'Intracellular pH-responsive polymeric micelle for simultaneous chemotherapy and MR imaging of hepatocellular carcinoma', *Journal of Nanoparticle Research*. doi: 10.1007/s11051-020-04821-x.

Xiao, K. *et al.* (2011) 'The effect of surface charge on in vivo biodistribution of PEG-oligocholic acid based micellar nanoparticles', *Biomaterials*. doi: 10.1016/j.biomaterials.2011.01.021.

Xue, R. *et al.* (2016) 'Cancer cell aggregate hypoxia visualized in vitro via biocompatible fiber sensors', *Biomaterials*. doi: 10.1016/j.biomaterials.2015.10.055.

Yu, X. and Pishko, M. V. (2011) 'Nanoparticle-based biocompatible and targeted drug delivery: Characterization and in vitro studies', *Biomacromolecules*. doi: 10.1021/bm200681m.

Zahr, A. S., De Villiers, M. and Pishko, M. V. (2005) 'Encapsulation of drug nanoparticles in self-assembled macromolecular nanoshells', *Langmuir*. doi: 10.1021/la0478595.

Zarepour, A., Zarrabi, A. and Khosravi, A. (2017) *SPIONs as Nano-Theranostics Agents*. Singapore: Springer Singapore (SpringerBriefs in Applied Sciences and Technology). doi: 10.1007/978-981-10-3563-0.

Zheng, Z. *et al.* (2010) 'Sonication-assisted synthesis of polyelectrolyte-coated curcumin nanoparticles', *Langmuir*. doi: 10.1021/la101246a.

Zhou, J. *et al.* (2010) 'Layer by layer chitosan/alginate coatings on poly(lactide-co-glycolide) nanoparticles for antifouling protection and Folic acid binding to achieve selective cell targeting', *Journal of Colloid and Interface Science*. doi: 10.1016/j.jcis.2010.02.004.